

ROLE OF RAF FAMILY MEMBERS IN MOUSE DEVELOPMENT

Dissertation

For completion of the Doctorate degree in Natural Sciences at the
Bayerische Julius-Maximilians-Universität Würzburg



Oleg Tyrsin

from Moscow, Russia

Würzburg 2003

The hereby submitted thesis was completed from May 1999 until August 2003 at the Institut für Medizinische Strahlenkunde und Zellforschung, Bayerische Julius-Maximilians Universität, Würzburg under the supervision of **Professor Dr. U. R. Rapp** (Faculty of Medicine) and **Professor Dr. R. Benavente** (Faculty of Biology).

Submitted on:

Members of the thesis committee:

Chairman: Prof. Dr. U. Scheer

Examiner: Prof. Dr. U. R. Rapp

Examiner: Prof. Dr. R. Benavente

Date of oral exam:

Certificate issued on:

ACKNOWLEDGEMENTS

First of all I would like to express my gratefulness to Prof. Dr. Ulf. R. Rapp for inviting me to the MSZ and for giving me the chance to express myself as a young scientist doing my research. Thank you for giving me the important lessons in conducting an independent and fruitful research and for the strong scientific guidance. Also I greatly appreciate the international atmosphere in our institute that help all people to stay deeper in touch and know more about different cultures (these wonderful scientific-ski-retreats each year are unforgettable). I would also thank Prof. R. Benavente for accepting me to the faculty of biology and his support during my doctorate degree.

I would like to thank to members of our group for the superb climate and support me during four and half years. A very special thank to Lev for guiding me through the obscure labyrinths of mouse genetics, to *mi niña preciosa Lupitina* for the excellent and expressive lessons of mouse neurobiology and Spanish language, to our “Russian mafia” members : Alla and Nikolaj for their wonderful technical assistance, to *unsere Mauskönigin* Hilde for her help in understanding mouse language and culture. I would also like to express my thanks to Bruce (nevertheless his strong London accent compared to Russian one) for his readiness to help every time and for his indispensable aid in thesis preparation. Many thanks to Roland and Rudolf for their help in German translations, clever scientific discussions and interest of my work, to Ralf for his help to resolve the perpetual Mac/PC conflicts and sense of humour, to my lab mates Fatih, Sveta, Chaomei for the easiness in communication.

I am very grateful to Renate and Ludmilla for their support in protein chemistry and cloning. Thanks a lot to ex-MSZ people: Anke, Andris, Bernd, Britta, Carrine, Christina, Daniel, Dennis, Dima, Dragomir, Enrico, Friedrich, Gordon, Irute, Jakob, Jannic, Jiang, Jörg, Lena, Manikkam, Nikola, Vadim, Veronique, Walter, and the present-MSZ-lers: Anaid, Andreas, Barbara, Carolin, Gunter, Kallal, Ludmila, Michael, Renate, Reinhold, Stefan, Suzanna, Tamara, Uli and Wolf.

Thanks a lot to Fr.Krämmer for supporting us with clean supplies and for excellent hygiene and to our animal caretakers: Galina, Jaklin, Markus, Viktor for keeping our mice healthy and happy.

I’m very grateful to Rosemarie Röder and Regine Blättler for their patience in helping me in so many things concerning paper work. Special thanks to Evald Lipp and Silvia Pfränger.

It is difficult to express in a few sentences the gratitude for my family, for their love and support.

The greatest acknowledgement I reserve for my wife Julia, supporting me every time either mentally or in reality, to whom I dedicate this dissertation.

Table of Contents

ZUSAMMENFASSUNG	1
SUMMARY.....	2
1. INTRODUCTION.....	3
1-2.1 Localization and structure of Raf family members.....	3
<i>Expression pattern and chromosome localization.....</i>	<i>3</i>
<i>Structure of Raf proteins.....</i>	<i>4</i>
1-2.2 Activation and function.....	5
1-2.2.1 Small GTP-ases.....	6
<i>GEF and adaptor proteins, Ras activation.....</i>	<i>6</i>
<i>Ras family proteins, differential Raf activation.....</i>	<i>6</i>
<i>Raf signalling in PC12 cells.....</i>	<i>7</i>
1-2.2.2 14-3-3 proteins	8
<i>14-3-3 binding and regulation of C-Raf activity.....</i>	<i>8</i>
1-2.2.3 Phosphorylation/dephosphorylation events and C-Raf activation.....	9
1-2.2.4 Activation of MEK/ERK by different Rafs.....	12
1-2.2.5 Regulators of Raf/MEK/ERK module.....	13
<i>MP1 (MEK-1 Partner 1).....</i>	<i>13</i>
<i>KSR (Kinase Suppressor of Ras).....</i>	<i>14</i>
<i>RKIP (C-Raf Kinase Inhibitor Protein).....</i>	<i>15</i>
<i>Spred protein.....</i>	<i>15</i>
<i>Hsp90, Hsp70 and BAG-1.....</i>	<i>16</i>
1-2.3 Raf isozymes specific interaction partners.....	16
1-2.3.1 B-Raf interaction partners.....	16
<i>PA28a subunit.....</i>	<i>16</i>
1-2.3.2 C-Raf specific partners.....	17
<i>Bcl-2.....</i>	<i>17</i>
<i>VDAC (voltage-dependent anion channel).....</i>	<i>17</i>
<i>ASK1 (apoptosis signal-regulating kinase 1).....</i>	<i>18</i>
<i>Grb10.....</i>	<i>18</i>
<i>MEKK1.....</i>	<i>18</i>
1-2.3.3 A-Raf specific partners.....	19

<i>CK2β, regulatory subunit of protein kinase CK2</i>	19
<i>Pyruvate kinase type M2 (M2-PK)</i>	19
<i>hTOM and hTIM</i>	19
1-2.4 Raf knock-out experiments	20
<i>A-Raf deficient mice</i>	20
<i>B-Raf null mice</i>	20
<i>C-Raf knock-out and knock-in mice</i>	21
<i>C-Raf and B-Raf double deficient mice</i>	21
1-2.5 Experimental design and aim of the project	22
2. RESULTS	23
2-1. Design and cloning of B-Raf targeting constructs	23
2-2. Vector electroporation and positive clone selection	25
2-3. Confirmation of chimeric protein expression in ES cells	26
2-4. Injection of targeted ES cell clones into mouse blastocyst and generation of chimeric and F1 heterozygous mice	26
2-5. Genotyping of F2 embryos. Analysis of B-Raf expression in embryos	29
2-6. Comparison of B-Raf KO and KIN embryo phenotype and life span depending on genetic background	30
<i>E12.5d, 129Sv/B16 KO and KIN embryos</i>	32
<i>E15.5d, 129Sv/B16, only KIN embryos are alive</i>	32
<i>E12.5d-13.5d (129Sv/B16/CD-1=37.5/37.5/25) and E16.5d (129Sv/B16/CD-1=1/1/2) living KIN embryos</i>	33
2-7. Obtaining adult KIN mouse, and its biochemical characterization	33
2-8. Histochemical and immunochemical analysis of E12.5d embryos	35
2-9. Histochemical and immunochemical characterization of E13.5d embryos	37
2-10. Histochemical and immunochemical comparison of E16.5d embryos	39
2-11. Comparison of adult p20 tissues	42
2-12. Characterization of neurogenesis in p20 adult +/KIN and KIN mouse brain using cell lineage specific markers	44
2-13. Establishment of primary mouse embryonic fibroblasts (MEF) culture and characterization of proliferative capacity	48
2-14. Different survival of MEFs after induction of apoptosis	49
2-15. The kinetic of ERK activation is delayed in KIN fibroblasts	50
2-16. Akt pathway is disturbed in KIN MEFs	51

2-17. Chimeric A-Raf possesses moderate kinase activity compared to B-Raf.....	52
3. DISCUSSION.....	54
3-1. A-Raf rescues B-Raf KO embryonic lethality with a low incidence.....	54
3-2. KIN embryo phenotype.....	56
<i>Fraction of KIN embryos displays phenotype similar to B-Raf KO.....</i>	<i>56</i>
<i>Some 12.5d KIN embryos are normal but reduced in size, neurological defects are observed.....</i>	<i>59</i>
<i>Increased apoptosis in tissues of E13.5d KIN embryo.....</i>	<i>60</i>
<i>Normal phenotype of E16.5d embryo.....</i>	<i>60</i>
3-3. Phenotype of adult KIN mouse.....	61
<i>Hematopoietic defects.....</i>	<i>61</i>
<i>The apoptosis is not increased in adult KIN tissues.....</i>	<i>62</i>
<i>Analysis of neurogenesis in adult KIN brain.....</i>	<i>62</i>
3-4. Cell culture experiments on KIN MEFs.....	65
<i>KIN fibroblasts display reduced proliferation and are more susceptible to apoptotic stimuli.....</i>	<i>65</i>
<i>ERK and Akt signaling pathways are disturbed in KIN MEFs.....</i>	<i>66</i>
4. MATERIALS AND METHODS.....	69
4-1. Materials.....	69
4-1.1. Instruments.....	69
4-1.2. Chemical reagents and general materials.....	70
4-1.3. Cell culture and embryo manipulation materials.....	71
4-1.4. Antibodies used for Western blot.....	72
4-1.5. Enzymes.....	73
4-1.6. Kits.....	73
4-1.7. Plasmid DNA.....	74
4-1.8. Oligonucleotides.....	74
4-1.9. Cell lines, mouse lines and bacterial strains.....	76
4-2. Solutions and buffers.....	76
4-2.1. Bacterial medium and DNA isolation buffers.....	76
4-2.2. RNA buffers.....	77

4-2.3. DNA buffers.....	77
4-2.4. Protein analysis buffers.....	79
4-2.5. Immunochemical buffers.....	80
4-3. Methods.....	80
4-3.1. Bacterial manipulation.....	80
4-3.1.1. Preparation of competent cells (CaCl ₂ method).....	80
4-3.1.2. Transformation of competent bacteria.....	81
4-3.2. DNA methods.....	81
4-3.2.1. Electrophoresis of DNA on agarose gel.....	81
4-3.2.2. Isolation of plasmid DNA from agarose (QIAEX II agarose gel extraction protocol).....	82
4-3.2.3. Purification of plasmid DNA (QIAquick PCR purification kit).....	82
4-3.2.4. Ligation of DNA fragments.....	83
4-3.2.5. Cohesive-end ligation.....	83
4-3.2.6. Mini-preparation of plasmid DNA.....	83
4-3.2.7. Maxi-preparation of plasmid DNA.....	83
4-3.2.8. Measurement of DNA concentration.....	84
4-3.2.9. DNA Sequencing (Sanger Dideoxy Method).....	84
4-3.2.10. Isolation of genomic DNA from cell and tissue.....	86
4-3.2.11. Southern blot.....	86
4-3.3. Extracting and handling RNA.....	86
4-3.3.1. Isolation of RNA from cell and tissue.....	86
4-3.3.2. Running RNA samples on denaturing gels.....	87
4-3.3.3. RT PCR.....	87
4-3.4. Protein methodologies.....	87
4-3.4.1. Immunoprecipitation.....	87
4-3.4.2. In vitro kinase assay.....	88
4-3.4.3. Measurement of Protein concentration (Bio-Rad protein assay).....	88
4-3.4.4. Sodium dodecyl sulfate polyacrylamide gel electrophoresis (SDS PAGE)..	88
4-3.4.5. Immunoblotting.....	89

4-3.4.6. Immunoblot stripping.....	90
4-3.5. Cell culture techniques.....	90
4-3.5.1. Cell maintenance	90
4-3.5.2. Isolation of primary of MEFs.....	91
4-3.5.3. ES cell transfection and positive clone selection.....	91
4-3.5.4. Independent clone isolation.....	91
4-3.5.5. Cell proliferation assay.....	92
4-3.5.6. Cell survival assay.....	92
4-3.5.7. ES cell injection and production of chimeras.....	92
4-3.6. Immunohistochemical methods.....	93
4-3.6.1. Embedding in paraffin.....	93
4-3.6.2 Hematoxylin/eosin staining.....	93
4-3.6.3. TUNEL assay.....	93
4-3.6.4 Immunohistochemistry.....	93
5. BIBLIOGRAPHY.....	95
APPENDIX.....	105
CURRICULUM VITAE.....	109

Zusammenfassung

Raf Proteine sind Serin/Threonin Kinasen, die als zentrale Elemente des Ras, Raf, Mek, Map Kinase Wegs, an der Weiterleitung von extrazellulären Signalen von der Zellmembran zu nukleären Effektoren beteiligt sind. Auf diese Weise kontrollieren sie elementare Prozesse wie Proliferation, Differenzierung und das Überleben von Zellen.

In Säugetieren wurden drei funktionelle Gene (A-, B- and C-raf) beschrieben. Aus biochemischen Untersuchungen ergibt sich, dass die Isozyme überlappende aber auch differentielle Funktionen übernehmen. Allerdings wurde ein differenziertes Verständnis der jeweiligen spezifischen Rolle dadurch erschwert, dass in den meisten Zelltypen verschiedene Raf-Isozyme exprimiert werden und dass wegen der Vielzahl der Aktivatoren und Effektoren eine eindeutige Isoform-Zuordnung schwer möglich war. Aufgrund der Beteiligung an verschiedenen Krankheitsbildern, insbesondere der Tumorentstehung und -progression, ist jedoch die Aufklärung der Isozym-spezifischen Funktionen von vorrangiger wissenschaftlicher Bedeutung.

B-Raf hat unter den Raf Kinasen die höchste Kinaseaktivität und zeigt antiapoptotische Eigenschaften. B-Raf knockout Mäuse zeigen eine allgemeine Wachstumsverzögerung und sterben zwischen E10,5 und E12,5 aufgrund fehlentwickelter Gefäße in Folge massiver Apoptose differenzierter Endothelzellen. [1]. Um die Lethalität des B-Raf^{-/-} (KO) Phänotyps zu überkommen und um die Redundanz der B-Raf Proteine weiter zu untersuchen, wurden Mäuse generiert, die unter der Kontrolle des B-Raf Promoters statt B-Raf eine A-Raf cDNA exprimieren. Nur in einem Fall entwickelte sich eine ausgewachsene p20 Maus ohne sichtbare Entwicklungsdefekte oder Verhaltensauffälligkeiten. Darüber hinaus wurden lebende Embryonen mit normaler Entwicklung aber reduzierter Grösse mit niedriger Inzidenz zwischen E12,5d und E16,5d beobachtet. In allen diesen Fällen fanden wir ein intaktes Gefäßsystem. Andererseits waren Neurogenese und die Bewegung der neuronalen Vorläuferzellen in den überlebenden Embryonen gestört, was in einigen Fällen zu unterentwickelten Hirnregionen führte.

Mittels TUNEL bzw. PCNA Assay konnten wir zeigen, dass mehr apoptotische und weniger proliferierende Zellen in ventrikulärer und subventrikulärer Zone der Hirn Ventrikel und im Striatum der KIN Embryonen zu finden sind. Außerdem wurden in einer Reihe von Geweben von E13,5d und in den Lungen von E16,5d Embryonen, vermehrt apoptotische Zellen beobachtet. Dies war in der einen ausgewachsenen KIN Maus nicht der Fall. Diese zeigte einen reduzierten Anteil an neuronalen Vorläuferzellen in der subgranulären Zone des Hippocampus und an reifen Neuronen im Riechkolben. Ansonsten waren aber keine Störungen der Neurogenese in der ausgewachsenen KIN Maus detektierbar. Fibroblasten die aus KIN Embryonen etabliert wurden, zeigten im Vergleich zu Wildtypzellen reduzierte Fähigkeit zur Proliferation und erhöhte Sensibilität gegenüber Apoptoseauslösern. Die erhöhte Apoptosetendenz spiegelte sich auf molekularer Ebene in einer Reduktion an antiapoptotischen Molekülen wieder. Aktive ERK und Akt Kinase sind erniedrigt. Außerdem war von dem bekannten Raf Substrat BAD, weniger an der inaktiven phosphorylierten Form zu beobachten, wodurch bei gleicher Menge Gesamtprotein auf ein Mehr an proapoptotischem unphosphoryliertem BAD geschlossen werden kann.

Zusammengefasst zeigen diese Daten, dass die Substitution von B-Raf durch die weniger aktive A-Raf Kinase zwar die endotheliale Apoptose verhindern kann, die die Ursache für das frühe Absterben der B-Raf^{-/-} (KO) Mäuse ist, dass aber die normale Entwicklung dennoch entscheidend gestört ist.

SUMMARY

Cellular proliferation, differentiation and survival in response to extracellular signals are controlled by the signal transduction pathway of Ras, Raf and MAP kinase. The Raf proteins are serine/threonine kinases with essential function in growth/differentiation/survival - related signal transduction events. In mammals, three functional (A-, B-, and C-Raf) genes were described. Biochemical studies suggest overlapping and differential utilization of Raf isozymes. However, the frequent co-expression of Raf isozymes and their multiple activators and effectors impedes the full understanding of their specific roles. The elucidation of these roles is important due to the involvement of the Ras/Raf/MEK/MAP kinase cascade in human disorders especially in tumor development and progression.

B-Raf was shown to possess the strongest kinase activity among Raf kinases and display antiapoptotic properties. Mice deficient in B-Raf show overall growth retardation and die between E10.5 and E12.5 of vascular defects caused by excessive death of differentiated endothelial cells [1]. To elucidate the redundancy of Raf isozymes during embryonic development and to rescue B-Raf^{-/-} (KO) phenotype, B-Raf alleles were disrupted by introducing A-Raf cDNA under the control of endogenous B-Raf promoter. The resulting B-Raf^{A-Raf/A-Raf} (KIN) phenotype depends on genetic background. The living embryos displaying normal development but size reduction were found with low incidence at E12.5d-16.5d. All of them displayed the rescue of vascular system. One adult p20 mouse without any visible defects in development and behavior was obtained. On the other hand, the processes of neurogenesis and neural precursors migration in survived embryos were disturbed which led in some cases to underdevelopment of different brain compartments. TUNEL and cell proliferation (PCNA staining) assays revealed more apoptotic (E13.5d) and less proliferating (E12.5d) cells within ventricular and sub-ventricular zones of brain ventricles and in striatum of KIN embryos. In addition, more apoptotic cells were detected in many other tissues of E13.5d and in lung of E16.5d KIN embryos but not in adult KIN mouse. p20 KIN mouse demonstrated reduced fraction of neural precursor cells in sub-granular zone of hippocampus and mature neurons in olfactory bulb. The other processes of neurogenesis were not disturbed in adult KIN animal. Fibroblasts obtained from KIN embryos demonstrated less proliferative ability and were more susceptible to apoptotic stimuli compared to WT. This was accompanied by the reduction of active ERK and Akt required for survival, and with decrease of inactive phosphorylated BAD. The kinetic of both ERK and Akt phosphorylation upon serum stimulation was delayed. All these data indicate that moderate A-Raf kinase activity can prevent the endothelial apoptosis but is not enough to completely rescue the other developmental consequences.

1. INTRODUCTION

The Ras/Raf/MEK/MAP kinase cascade is an essential component of intracellular signaling pathways from activated cell-surface receptors to transcription factors in the nucleus. Upon activation, Raf phosphorylates mitogen-activated protein kinase kinase (MEK), which in turn activates mitogen-activated protein kinase (MAPK/ERK), leading to the propagation of the signals. Depending on the specific stimuli and cellular environment, Ras/Raf/MEK/MAPK cascade regulates diverse cellular processes such as proliferation, differentiation and apoptosis [2] [3] (Fig.1-1).

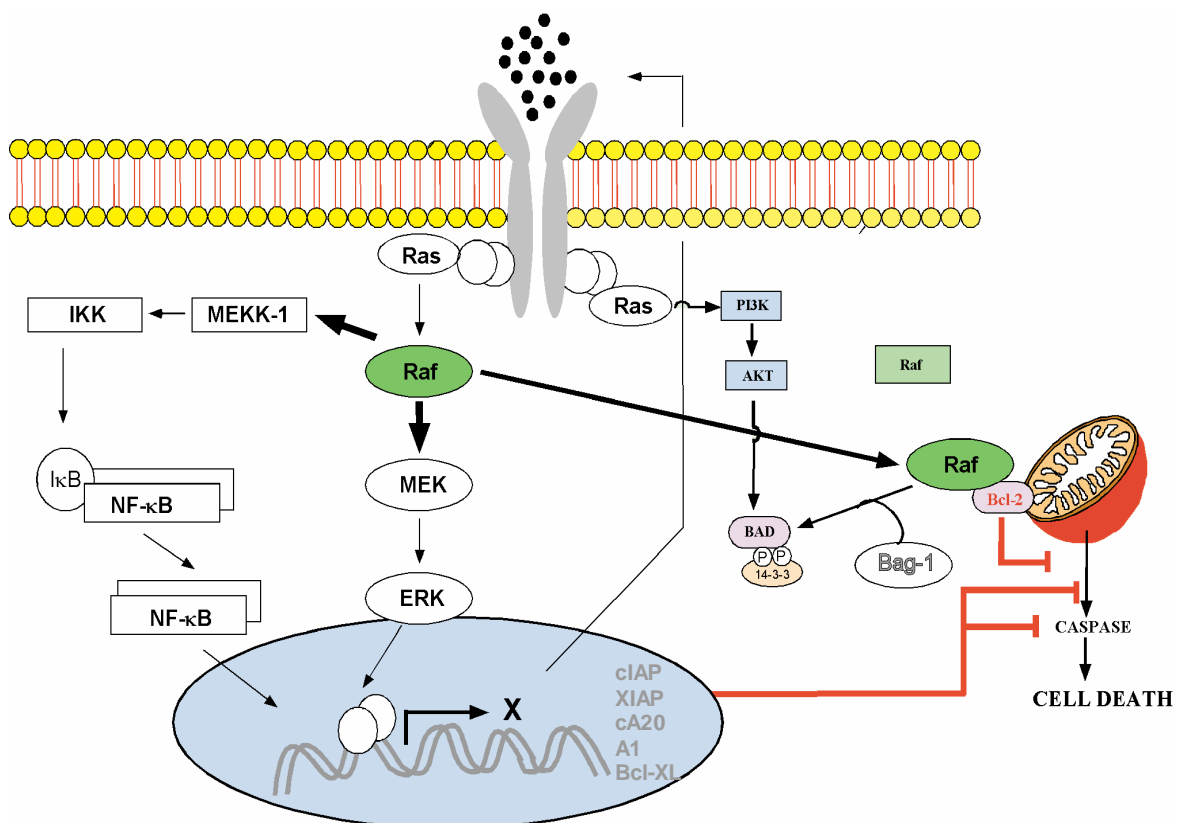


Fig. 1-1 The main pathways of Raf action.

1-2.1 Localization and structure of Raf family members.

Expression pattern and chromosome localization.

Raf genes are evolutionarily highly conserved and encode protein serine/threonine kinases. Raf genes are found in higher and lower eukaryotes including *C. elegans*, *Drosophila melanogaster*, *Xenopus laevis*, chicken, mouse, rat and humans. In mammals three functional (A-, B-, and C-Raf) and several pseudo genes have been described. In all other eukaryotes,

only one *raf* homologue is detected and these are more closely related to mammalian *B-raf* in nucleotide sequence than either *A-raf* or *C-raf*. *Raf* homologues have not been detected in *Saccharomyces cerevisiae* or *Schizosaccharomyces pombe*, although other MEKKs have been detected in these species [4]. In humans *C-raf* gene is located on chromosome 3p25, *B-raf* on chromosome 7p34, and *A-raf* on the X chromosome at position Xp11.2.

The 3.4 kb C-Raf transcript is ubiquitously expressed in the mouse, with highest expression levels in striated muscle, cerebellum, and fetal brain. It encodes a 74 kD protein [2], [3].

B-Raf exhibits the highest expression level in neural tissues, testes, and fetal membrane. While the B-Raf protein is barely detectable in many tissues, mRNA transcripts are clearly present. The number and size of *B-raf* transcripts, ranging between 2.6 and 12 kb, depend on the tissue analyzed. All of them contain Ras-binding and catalytic domains [5, 6]. It was established that *B-raf* gene carries two alternatively spliced exons: 8b and 10 as well as alternative translation initiation resulting in isoforms ranging in size from 67 to 99 kD. The long forms of B-Raf contain additional 115 amino acids encoded by exons 1, 2 and part of exon 3 [6]. It is not clear whether these different termini arise by the use of different promoters, by the use of different translation initiation start sites but the same promoters or by differential splicing. The presence of exons 8b and 10 modulates both MEK activating activity and oncogenicity of B-Raf [7]. A striking example is the sequence encoded by exon 10 which is found only in B-Raf isoforms from neural tissues [6, 8] and which enhances the affinity for MEK, the basal kinase activity, as well as the mitogenic and transforming properties of B-Raf [7].

The 2.6 kb A-Raf transcript is preferentially expressed in urogenital tissue but it is detectable in many other tissues and cell lines [9, 10]. It gives rise to the 68 kD protein, the smallest of the family [3].

Structure of Raf proteins.

The three Raf-family proteins share a comparable structure. They possess three conserved regions (CR1, CR2, and CR3) embedded in variable sequences. In C-Raf, CR1 encompasses residues 61-194 and contains two domains that bind to Ras-GTP; the Ras binding domain (RBD) which spans residues 51-131, and the cysteine-rich domain (CRD) which spans residues 139-184 [11]. CR2 encompasses residues 254-269 of C-Raf and is rich in Ser and Thr amino acids, some of which are regulatory phosphorylation sites (Fig. 1-2). The CR1 and CR2 domains are part of the regulatory N-terminal half of the Raf proteins, whereas CR3

(residues 254-269 of C-Raf) represents the C-terminal kinase domain that is the most homologous between Raf proteins (Fig. 1-2). Deletion of the regulatory half of all three Raf kinases leads to constitutively active forms [2]. CR3 domain is separated into N-terminal and C-terminal lobes and the ATP binding site is located at the interface of the two lobes. The N-terminal lobe contains the glycine loop that is important for localizing the phosphates of ATP, whereas the C-terminal lobe contains the substrate recognition sequence (Fig. 1-2).

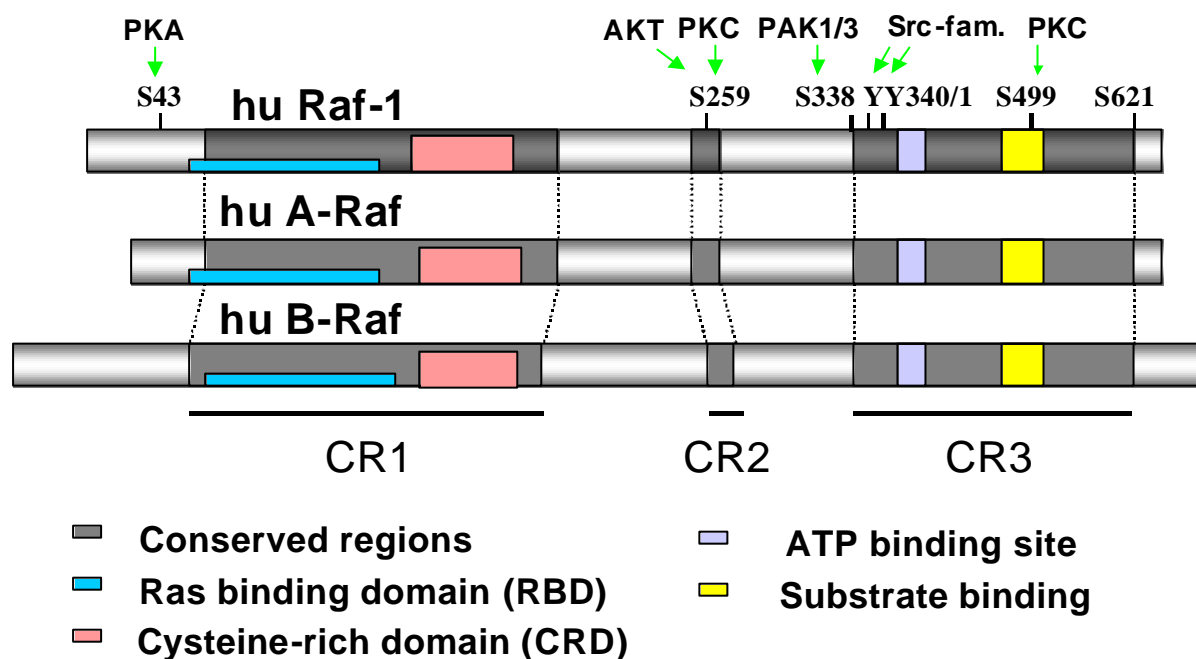


Fig. 1-2 The structure of mammalian Raf family members. Arrows indicate known phosphorylation sites.

1-2.2 Activation and function.

Biochemical studies suggest overlapping and differential utilization of Raf isozymes [12], [13]. However, the frequent co-expression of Raf isozymes and their multiple activators and effectors impedes the full understanding of their specific roles. The elucidation of these roles is important due to the involvement of the Ras/Raf/MEK/MAP kinase cascade in human disorders especially in tumor development and progression. Mutations of the Raf activator Ras are present in 30% of human cancers and their transforming potential is dependent on Raf [14] [15]. Recently *BRAF* somatic missense mutations in 66% of malignant melanomas and at lower frequency in a wide range of human cancers were demonstrated [16]. All mutations are within the kinase domain, with a single substitution (Val599Glu) accounting for 80%.

Mutated B-Raf proteins displayed elevated kinase activity and were transforming in NIH3T3 cells. Furthermore, RAS function was not required for the growth of cancer cell lines with the Val599Glu mutation [16].

1-2.2.1 Small GTP-ases.

GEF and adaptor proteins, Ras activation.

The common upstream activator of all three Rafs is a small G protein, Ras, which in its GTP-bound activated form binds first to the Raf-RBD and recruits the inactive cytoplasmic Raf to the plasma membrane for activation. The second contact is mediated by the Raf-CRD, which forms a zinc finger motif [17] (Fig.1-2). Since the CRD negatively controls the catalytic activity, probably by directly interacting with the kinase domain [18], its binding to Ras will relieve the repression of the kinase domain. Activation of Ras requires guanine nucleotide exchange factors (GEFs), which induce the dissociation of GDP to allow association of the more abundant GTP, and deactivation requires GTPase-activating proteins (GAPs), which bind to the GTP-bound form and enhance the rate of intrinsic GTPase activity.

Son-of-sevenless (Sos) 1 and Sos2 are widely expressed mammalian Ras GEFs [19]. They are normally localized to the cell cytosol but, in response to growth-factor stimulation, they are recruited to the plasma membrane. Ras is localized to the inner leaflet of the plasma membrane - this localization is necessary for it to signal - targeting Sos to this membrane efficiently regulates Ras activation. Sos is recruited to the plasma membrane in complexes with the adaptor proteins growth-factor receptor bound protein 2 (Grb2) and Src-homology-2 domain containing (SHC), which bind to phosphotyrosine-binding domains.

Ras family proteins, differential Raf activation.

There are three essential Ras isoforms: H-Ras, N-Ras, and K-Ras4A or 4B with different ability to activate the Raf isoforms. For example K-Ras is a more effective C-Raf activator than N-Ras, and N-Ras is more effective than H-Ras [20]. These differences could be due in part to distinct membrane microlocalizations. Thus, K-Ras is localized predominantly to the disordered plasma membrane, whereas H-Ras exists in a GTP-regulated equilibrium between disordered plasma membrane, caveolae and cholesterol-rich lipid rafts [21]. In addition, other GTPases of the Ras superfamily, including R-Ras, M-Ras, TC21 and Rheb have been shown to interact with Raf proteins [22] but their role as physiological activators of the ERK pathway remains to be established.

It was shown that the binding activity of the isolated A-Raf-RBD for H-Ras, TC21, and Rap1A were markedly diminished compared to those of C-Raf and B-Raf-RBD. The interacting amino acids in the Ras/Raf interface are identical for C-Raf and B-Raf, but there is a change from Arg to Lys in A-Raf-RBD corresponding to position 59 in C-Raf [23]. This opens the question as to whether Ras represents the physiological activator for A-Raf, or whether an alternative activator exists for A-Raf.

It has been recently reported that maximal activation of B-Raf can be achieved by GTP-loaded Ras alone, whereas both A-Raf and C-Raf require co-stimulatory tyrosine kinases, e.g. Src [13]. It could be that Ser338 and Tyr341 phosphorylation is necessary for C-Raf activation. The maximal C-Raf activation can be achieved only when both oncogenic Ras and activated Src are present. A-Raf harbors the analogous Ser and Tyr. In contrast, B-Raf has negatively charged aspartic acid residues (Asp/Asp 447/448) equivalent to Tyr340 and 341 in C-Raf. Ser445 in B-Raf which is equivalent to Ser338 of C-Raf, is phosphorylated constitutively and not stimulated by oncogenic Ras [24]. These pSer445 and Asp448 are thought to contribute to the high basal kinase activity of B-Raf being 15-20 times that of C-Raf [24].

TC21 is another member of the family of small G proteins, which binds and activates B-Raf and at least binds the cysteine-rich region of C-Raf [25] [26]. Since overexpression of TC21 in PC12 cells induces their differentiation, it is possible that this response is mediated via B-Raf. A-Raf activity is not affected by TC21 at all [26].

Raf signaling in PC12 cells.

PC12 cells proliferate under EGF stimulation but differentiate into a neuron-like phenotype after treatment with NGF. Both growth factors are able to activate Raf proteins. In PC12 cells, where all three Rafs are expressed, an initial activation of all three isoforms was detected, but only A- and B-Raf showed sustained activation by NGF, whereas EGF treatment caused only transient activation. C-Raf demonstrated highest degree of initial activation but was rapidly inactivated. The expression of oncogenic versions of the three Rafs, mimicking a sustained activation, led to constitutive ERK activation and differentiation of PC12 cells [27]. The initial C-Raf activation requires Ras, but the following sustained activity of B-Raf is mediated by another small G protein, Rap1 [28]. The cAMP-dependent protein kinase PKA is able to phosphorylate Ser43 and thereby inhibit C-Raf [29]. In addition Rap1 interacts with the RBD and the cysteine-rich region of C-Raf in competition with Ras binding, and antagonizes the C-Raf activation by Ras [30]. In PC12 cells cAMP activated PKA blocks the C-Raf activity by

the inhibiting phosphorylation, and is able to phosphorylate Rap1, which in turn binds B-Raf, resulting in sustained activation of this kinase and differentiation of PC12 cells [31], [28]. This regulatory system also has implications for differential responses of cell types in the brain to elevation of cAMP level. In PC12 cells and hippocampal neurons, depolarization-mediated calcium influx activates calmodulin. Ca²⁺-calmodulin dependent adenylatecyclase then elevates the level of cAMP that finally leads to the Erk activation [32]. Given the fact that both Rap1 and B-Raf are highly expressed in the central nervous system, this signaling pathway may regulate a number of activity-dependent neuronal functions.

1-2.2.2 14-3-3 proteins.

One family of proteins that interact with Raf kinases are the 14-3-3 adaptor-scaffold proteins. These are highly conserved acidic proteins with molecular masses of ≈ 30 kDa that bind to a large number and variety of target proteins and regulate cell-cycle checkpoints, proliferation, differentiation and apoptosis [33-36]. In many cases 14-3-3 inactivates the target protein by changing its subcellular localization or protein associations [37]. The binding of 14-3-3 to client proteins occurs through short peptide motifs. For some peptides, binding occurs only if a specific serine within the motif is phosphorylated, but binding to other motifs is phosphorylation independent [38-40].

14-3-3 binding and regulation of C-Raf activity.

The role that 14-3-3 binding plays in regulating C-Raf is controversial. Many studies suggest that 14-3-3 binding is essential for kinase activity [41-44], while others suggest that it is not [45-47]. In part, the confusion stems from the fact that there are two 14-3-3 binding sites on C-Raf that appear to play opposing roles. Both sites conform to the consensus sequence RSXpSXP (pS, phosphorylated serine; X, any amino acid) with binding being dependent on phosphorylation of the central serine [38, 40]. One motif is in CR2, and requires phosphorylation of Ser259. The other is in CR3, at the C-terminal end of the kinase domain and requires phosphorylation of Ser621 (Fig. 1-2). Binding of 14-3-3 to CR2 appears to suppress C-Raf activity. Thus, since 14-3-3 proteins are dimeric and can simultaneously bind to two peptides [39, 40], one model suggests that one 14-3-3 dimer binds to both CR2 and CR3 to keep C-Raf in a closed, inactive conformation [48, 49]. Activation requires release of

CR2, and 14-3-3 can then bind to a third, unidentified site to maintain the active conformation (Fig. 1-3) [50].

Recent studies have shown that protein kinase B can suppress C-Raf activity by directly phosphorylating Ser259 [51, 52], and it has also been suggested that protein phosphatase 1 (PP1) and 2A (PP2A) mediate Ser259 dephosphorylation as a prerequisite for C-Raf activation in growth factor-stimulated cells (Fig. 1-3) [53, 54]. Treatment of cells with concentrations of okadaic acid that specifically inhibit PP2A prevents C-Raf activation and results in the accumulation of inactive C-Raf/14-3-3 complexes at the plasma membrane [53]. These studies are supported by genetic data from *Drosophila* and *Caenorhabditis elegans* which reveal a positive role for PP2A in C-Raf function [55, 56]. It has also been demonstrated that 14-3-3 dimers bridge C-Raf to substrates or to other signaling molecules. For example the interaction between C-Raf and Bcr serine/threonine kinase that occurs preferentially at the cell membrane where C-Raf is activated [57].

There also appears to be competition between Ras and 14-3-3 for binding to C-Raf. Both Ras and 14-3-3 have secondary binding sites within the cysteine-rich domain (CRD), which is also in CR1 and C terminal to the RBD [46, 58, 59]. The role of 14-3-3 binding to CR3 for C-Raf activation is contradictory. Some data suggest that 14-3-3 is completely displaced from active C-Raf, and in some experimental conditions, this appears to be the case [43]. However, a number of other studies argue that binding of 14-3-3 to CR3 is essential for activity, with the strongest evidence coming from peptide displacement studies. Active C-Raf can be inactivated by phosphopeptides that displace 14-3-3; C-Raf is reactivated by subsequent addition of recombinant 14-3-3 [49, 60, 61]. Importantly, this approach also works with the isolated kinase domain, supporting binding to CR3 as being essential for activity [44]. Furthermore, it has been shown that 14-3-3 binding to CR3 protects S621 from dephosphorylation to maintain C-Raf activity [61], and also that 14-3-3 protects active C-Raf from PP1 and PP2A-mediated inactivation [62].

1-2.2.3 Phosphorylation/ dephosphorylation events and C-Raf activation.

During C-Raf activation, a poorly understood sequence of events follows Ras binding whereby the catalytic function of the protein is unmasked via the dissociation of the regulatory domain from the kinase domain [18]. This sequence involves complex changes in phosphorylation, protein-protein interactions, and protein-lipid interactions. The examination

of phosphorylation has revealed multiple layers of regulation. In resting cells C-Raf is phosphorylated on serines 43, 259, and 621 [63] (Fig. 1-2, 3). Mitogen stimulation results in phosphorylation of other sites in the kinase domain including Ser338 [64] and Tyr341 [65] just upstream of the kinase domain, Thr491 and Ser494 within the activation loop [66], and possibly Ser621 within the C-terminal portion of the protein [61] (Fig. 1-2, 3).

The most intensely studied sites are Ser338 and Tyr341 [50, 67]. They synergize to activate C-Raf, while the mutation of either site almost completely obliterates kinase activation by mitogens [24]. Replacing Tyr341 by a phosphomimetic aspartate results in strong activation [65]. A similar change of Ser338 causes only modest activation [64]. Monitoring Ser338 phosphorylation with phosphospecific antibodies shows that it is induced by growth factors, integrins, and Ras, and closely parallels the kinetics of kinase activation [50, 67]. p21 activated kinases PAK3 and PAK1 were described as Ser338 kinases which act in a phosphatidylinositol 3-kinase (PI3K)-dependent manner [64, 68]. However, the identity of the physiological Ser338 kinase was recently disputed [69], and the existence of more than one Ser338 kinase is likely. It was demonstrated that different survival factors promote differential C-Raf phosphorylation and its subsequent redirecting to specific intracellular compartments. In endothelial cell culture it was shown that bFGF signalling activated C-Raf via PAK1 phosphorylation of Ser338 and 339, resulting in C-Raf mitochondrial translocation and protection from intrinsic apoptosis, independent of MEK/ERK signalling. In contrast, VEGF activated C-Raf via Src kinase, leading to phosphorylation of Tyr340 and 341 and MEK/ERK dependent protection from extrinsic-mediated apoptosis [70].

Evidence for the important role of Tyr341 mainly stems from studies with C-Raf mutants. Although Tyr341 readily becomes phosphorylated when Src family tyrosine kinases are co-overexpressed [24], phosphorylation in response to physiological mitogens has not yet been conclusively demonstrated. The only exception may be hematopoietic cells, where erythropoietin was reported to induce C-Raf activation and Tyr341 phosphorylation [71]. Curiously, Raf TyrTyr340/341PhePhe mutants can hardly be activated by mitogens, but retain potent transforming properties when combined with the deletion of the regulatory domain [65]. This seemingly contradictory result can be reconciled by the observation that a major role of Tyr341 phosphorylation is to relieve the kinase domain from the repressive effect of the regulatory domain [18].

The knock-in of a C-Raf TyrTyr340/341PhePhe mutant also can fully rescue the embryonic lethal phenotype of C-Raf knock-out mice [72]. This suggests that the residual kinase activity of this mutant is sufficient to fulfil its biological functions. Alternatively, the physiological functions of C-Raf may be independent of its ability to phosphorylate MEK1/2, but for instance proapoptotic BAD [73]. C-Raf's main function could also be that of a scaffolding protein, or it may have substrates other than MEK1/2, whose phosphorylation is not compromised by the TyrTyr340/341PhePhe mutations.

Recently, Thr491 and Ser494 in the activation loop were reported to be phosphorylated in a mitogen-induced manner and contribute to C-Raf activation [66]. Substitution of both sites with acidic amino acids could further enhance the activity of C-Raf proteins already containing acidic substitutions of Ser338 and Tyr341 [66]. Activation loop phosphorylation on Ser499 has previously been implicated in the PKC-mediated activation of C-Raf (Fig. 1-2) [74]. Curiously, the mutation of Ser499 to alanine abolished C-Raf autophosphorylation and the phosphorylation of artificial peptide substrates [74], but did not interfere with the activation of MEK1/2 [75]. The reason for this discrepancy is unresolved, and its potential significance will depend on whether a role for C-Raf autophosphorylation

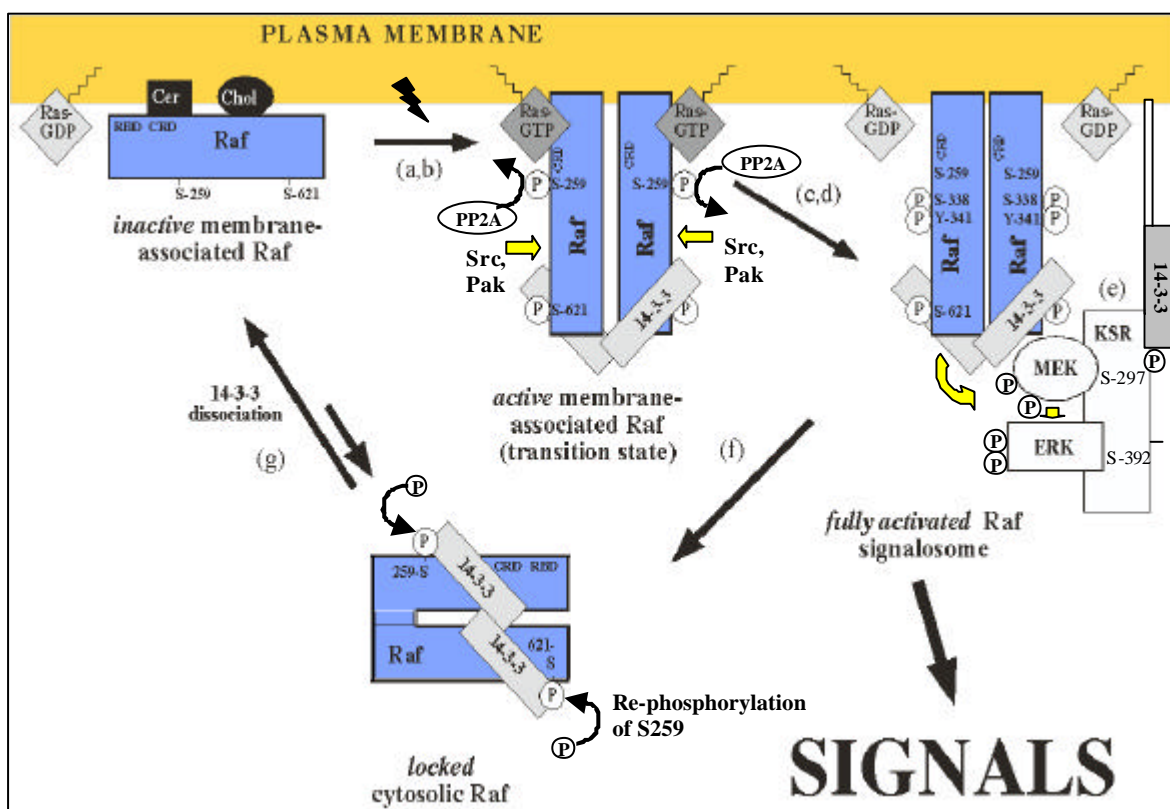


Fig. 1-3 Proposed model for C-Raf activation.

can be demonstrated.

The current understanding of C-Raf phosphorylation predicts that C-Raf activity can be finely tuned via the cooperation between activating phosphorylation sites and further that C-Raf molecules with different levels of activities may be generated in response to different mitogens. This could serve as a combinatorial mechanism to achieve the exact level and compartmentalization of C-Raf activity that ensures the fidelity of the biological response. Recent studies also indicate that dephosphorylation, particularly on Ser259, plays an important role in C-Raf activation. This site has been identified as a target for inhibitory phosphorylation by Akt [52] and cAMP activated protein kinase (PKA) [76], and needs to be dephosphorylated to allow mitogenic activation [77] (Fig.1-3).

The role of Ser621 phosphorylation is controversial, with claims made that it is an activating or inhibitory site. The former hypothesis is mainly based on the observation that its mutation leads to a loss of catalytic activity [61] and the latter that its phosphorylation correlates with the ability of PKA to inhibit the catalytic domain of C-Raf [78]. Both views may be true if 14-3-3 binding to phosphoserine 621 could convert inhibition into activation, for instance by preventing phosphoserine 621 from engaging in inhibitory interactions within the catalytic domain (Fig. 1-3). This hypothesis has been recently discussed in more detail [67].

The major *in vitro* autophosphorylation site on C-Raf is Thr268 [79]. The adjacent Thr269 has been reported to mediate the activation of C-Raf by the ceramide-activated protein kinase and KSR [80]. The physiological significance of this phosphorylation is doubtful as KSR has been shown to regulate C-Raf signaling independent of its kinase activity [81].

1-2.2.4 Activation of MEK/ERK by different Rafs.

MEK is so far the only one of two *in vivo* substrates common for all Raf proteins. The other is proapoptotic BAD protein, a member of Bcl-2 family (our unpublished data). Two isoforms are known: MEK1 (44 kD) and MEK2 (45 kD), but in many cell lines MEK1 was described as the main Raf-activated MAPKK [82-84]. MEK1 is activated by phosphorylation of two serine residues at positions 218 and 222 present in activation loop [85-87]. MEK1 and 2 contain a proline-rich sequence that is thought to be required for recognition and activation by Raf proteins [88]. This sequence is not present in other MAPKKs.

The three Raf proteins are not equal in their ability to activate MEK. A-Raf, the least well-characterized member of the family, appears to be a poor MEK activator, its activity being difficult to measure [89]. B-Raf has been identified as the major MEK activator, not only in the neuronal tissues where it is expressed at the highest levels, but also in cells where its expression was barely detectable [72, 90-93]. Consistently, B-Raf displays higher affinity for MEK-1 and MEK-2 than C-Raf [7, 94] and is more efficient in phosphorylating MEKs [7, 13, 89]. The usage of estradiol inducible oncogenic forms of Raf isoforms demonstrated that Δ B-Raf:ER phosphorylated MEK1 around 10 times more efficiently than Δ C-Raf:ER and at least 500 times more efficiently than Δ A-Raf:ER [89]. B-Raf also has a higher binding affinity for MEK1 and 2 compared to C-Raf [7].

Targeted disruption of *raf* genes in mouse showed that B-Raf is the major ERK activator *in vivo* but acts in cooperative manner with C-Raf [72, 93, 95-97]. Indeed, no defect in G1-S transition, and ERK activation by serum and EGF has been observed in mouse embryonic fibroblasts derived from knock-outs of the *C-Raf* gene [98], [72, 93]. In this case the compensatory B-Raf up-regulation rescued ERK activity in C-Raf deficient MEFs [93]. On the other hand EGF failed to stimulate ERK in B-Raf null fibroblasts, where C-Raf could not compensate B-Raf function. Immunoprecipitation experiments demonstrated that both C-Raf and B-Raf are required for ERK activation by EGF [96]. A-Raf deficient mouse embryonic fibroblasts and embryonic stem cells were normal in proliferation, differentiation, resistance to apoptosis and ERK activation, despite the high level of A-Raf expression in both normal cell types [97]. This implies either that A-Raf plays no role in MEK/ERK activation, that its function is fully compensated by other Raf members or that its role in MEK/ERK activation is highly tissue-specific.

Therefore, B-Raf, which is more closely related to D-Raf than are A-Raf and C-Raf, is likely to be the functional homologue of ancestral Raf proteins in *Caenorhabditis elegans* and *Drosophila melanogaster*, whereas A-Raf and C-Raf have diversified in their regulation.

1-2.2.5 Regulators of Raf/MEK/ERK module.

MP1 (MEK-1 Partner 1).

MP-1 is a small protein displaying no sequence homology with known proteins. MP1 selectively interacts with ERK1 and MEK1 but fails to bind to ERK2 and MEK2 [99]. Although MP1 exhibits properties of a scaffolding protein, it was not found to interact with Raf. *In vitro*, MP1 enhances the activation of MEK by C-Raf, and when overexpressed in

cells, MP1 can selectively induce the activation of ERK1 but not that of ERK2, suggesting that MP1 could help to discriminate between two closely related MAPKs in the same module [82] (Fig. 1-4).

KSR (Kinase Suppressor of Ras).

KSR is an evolutionary conserved component of the Ras/MAPK pathway. Two mammalian homologues, called mKsr-1 and hKsr-1, have been isolated in mouse and human respectively [100]. The kinase domain of mKsr-1 is 35.1 % and 33.7 % identical to those of B-Raf and C-Raf respectively. In addition, KSR shares other structural similarities with Rafs including a serine/threonine-rich sequence (CA4) that resembles the CR2 of Raf proteins and a cysteine-rich motif (CA3) which is present in the CR1 domain of Raf (Fig. 1-2).

Biochemical studies have shown that kinase domain of KSR interacts strongly with MEK1 and MEK2, but mKsr-1 failed to phosphorylate either MEKs [101, 102]. MEK is not the only partner identified for KSR, since mKsr-1 also binds to ERK via the CA4 domain [103] and to C-Raf, via the CA5 kinase domain [104, 105]. The only substrate so far proposed for KSR is C-Raf itself, which was found activated upon phosphorylation at threonine 269 by mKsr-1 [106, 107]. Although this observation is very attractive with respect to the function of KSR, it has not been so far reproduced by several independent groups [101, 102, 108, 109]. While the interaction with MEK appears constitutive, the ability of KSR to interact with C-Raf and ERK is induced by treating the cells with growth factors [103]. Under these conditions, ERK phosphorylates mKsr-1 on three residues, but the functional significance of this remains unclear since mutation of these phosphorylation sites does not impair the biological properties of KSR [103]. In addition, KSR is cytosolic in resting cells but a fraction is translocated to the membrane upon treatment with growth factors [105, 108, 110]. A possible explanation for this is suggested by a recent study showing that the CA3 domain of mKsr-1 binds to G-protein beta/gamma subunits [111]. Studies in both *Drosophila* and vertebrates cells have demonstrated that the effects of KSR on the ERK pathway strongly depend on level of KSR expression. At low levels, KSR cooperates with Ras to activate the pathway [103, 104] and the kinase activity of KSR does not appear to be required [108, 110]. Upon overexpression, however, KSR inhibits Ras-induced cell proliferation and transformation [101, 102] and beta/gamma-induced ERK activation [111]. Moreover, the isolated CA5 kinase domain is sufficient to inhibit the pathway, whatever its level of expression [103, 112]. These observations are consistent with a model, where formation of

scaffold–kinase complexes can be used to regulate the specificity, efficiency, and amplitude of signal propagation with a concentration value optimal for signal amplitude [113] (Fig. 1-4).

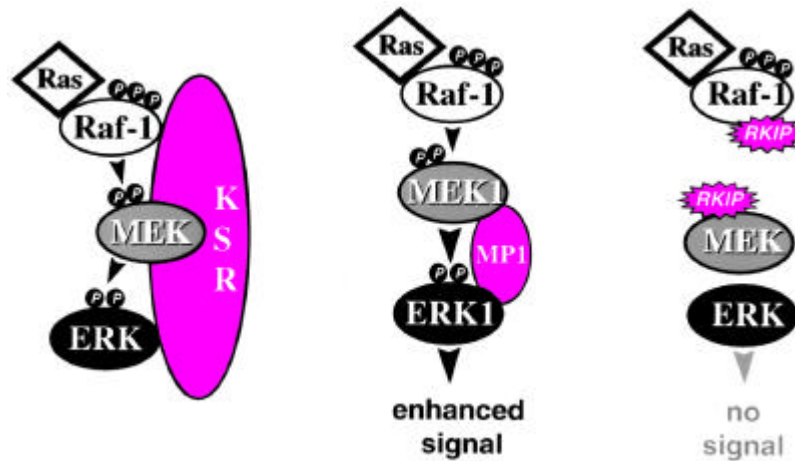


Fig. 1-4 Different functions of KSR, MP1 and RKIP [67].

RKIP (C-Raf Kinase Inhibitor Protein).

RKIP belongs to the family of phosphatidylethanol-binding proteins, which are widely expressed and evolutionarily conserved [114]. RKIP was also found to bind MEK and this interaction is exclusive since the binding sites for Raf and MEK in RKIP overlap [115]. Consequently, overexpression of RKIP can disrupt the physical interaction between C-Raf and MEK, thereby impairing MEK phosphorylation by Raf, without affecting that of ERK by MEK. Cell treatment with growth factors provokes the release of RKIP from C-Raf, allowing phosphorylation and activation of MEK. Thus, RKIP represents the unique case of an accessory molecule with a physiological role unequivocally devoted to a negative regulation of the pathway by blocking propagation of the signal between Raf and MEK (Fig. 1-4). It will be of interest to determine whether RKIP is also able to bind A-Raf and B-Raf.

Spred protein.

More recently, another Ras interacting protein, Spred, was identified as suppressor of EGF-mediated stimulation of the Ras-ERK pathway. Spred is related to the Sprouty family of receptor tyrosine kinase signaling antagonists which were discovered in *Drosophila*. Spred did not affect Ras activation or translocation of Raf to the membrane. Despite enhancing the

Ras-Raf interaction, ERK1/2 activation was suppressed due to the prevention of C-Raf Ser338 phosphorylation [116].

Hsp90, Hsp70, and BAG-1.

Hsp90 is an ubiquitous chaperone that appears to have an important role in assisting and maintaining the folding of many signaling proteins including C-Raf. Drugs, such as geldanamycin and derivatives, that prevent the interaction of Hsp90 with client proteins lead to the ubiquitination and degradation of C-Raf and other signaling proteins [117].

BAG-1, originally isolated as Bcl-2 binding partner, is a co-chaperone for Hsp70, but can also bind to and activate C-Raf [118]. The mechanism of activation is unknown, but requires physical interaction. However, no C-Raf/BAG/Bcl-2 ternary complex has been observed so far. Recently, a simple mechanism has been described to elucidate how Hsp70 orchestrates the cellular stress response and the regulation of the ERK1/2 pathway. Cell stress increases Hsp70 expression. As a consequence BAG-1 is diverted away from C-Raf to Hsp70, resulting in the down-regulation of C-Raf activity and DNA synthesis. BAG-1 mutants that did not interact with Hsp70, but retained C-Raf binding, constitutively activated the ERK1/2 pathway [119].

1-2.3 Raf isozymes specific interaction partners.

1-2.3.1 B-Raf interaction partners

PA28a subunit.

The PA28 α subunit of the 11S regulator of proteasomes was identified as a new B-Raf interacting protein. It binds to the N-terminal variable domain of B-Raf [120]. Both A- and C-Raf lack this domain, which is highly conserved among B-Raf vertebrate species [3]. In PA28 α the B-Raf interacting region overlaps with the region important for its proteasomal-activating function [121].

It was known that proteasomal degradation machinery increases the diversity of antigenic peptides presented at the cell surface by MHC class I molecules [122]. In Ras-transformed cells and some human tumor cells a suppression of the antigenic presentation machine was observed. This correlated with downregulation of MHC class I expression, of the peptide transporters TAP1, 2 and of proteasomal subunits LMP2,7 [123]. The binding of the Ras effector B-Raf to a region in PA28 α , which is essential for proteasome activation may

indicate an additional pathway for downregulation of antigen presentation in Ras-transformed cells by decreasing proteasomal activity.

The results from knockout experiments also suggest a role for B-Raf as a survival factor [1]. The connection between proteasomal activity and apoptosis has been described. Dependent on the cellular background programmed cell death (PCD) was induced or inhibited by the proteasomal inhibitor lactacystin [124-126]. The interaction of B-Raf with PA28 α may therefore be involved in this process.

1-2.3.2 C-Raf specific partners.

Bcl-2

C-Raf was shown to cooperate with Bcl-2 and act as an apoptosis suppressor. After recruitment by Bcl-2 to the mitochondrial membrane, C-Raf may become activated by BAG-1 and in turn phosphorylates and inactivates BAD [118, 127, 128] (Fig. 1-1). BAD is proapoptotic relative of Bcl-2 that can be neutralized by phosphorylation-induced 14-3-3 binding and sequestration into the cytosol [129]. Examination of BAD phosphorylation by purified Raf kinases revealed that B-Raf, like PAK1 kinase, target Ser112 and 136, whereas C-Raf was restricted to Ser112 [73]. However, recently, the independent role of C-Raf and Bcl-2 in suppression of apoptosis was shown. In these studies mitochondrion targeted C-Raf protected Bcl-2^{-/-} fibroblasts against apoptosis as well as Bcl-2 overexpression did so in C-Raf^{-/-} cells [130]. In promyeloid 32D cell line mitochondrion targeted constitutively active C-Raf-BxB significantly decreased IL-3 deprivation induced mitochondrial membrane depolarization, cytochrome c release and procaspases 3 and 9 activation. Overexpression of Bcl-2 enhanced the survival effect of C-Raf [131]. Thus, Bcl-2 can target C-Raf to the mitochondria where it executes its antiapoptotic function.

VDAC (voltage-dependent anion channel)

VDAC, which is the most abundant protein of the outer mitochondrial membrane, provides a major channel for the movement of ions, ADP/ATP and metabolites in and out of mitochondria. It is a core component of the permeability transition pore (PTP) [132]. Opening of the PTP causes mitochondrial membrane potential disruption and release of cytochrome c, most likely through VDAC/Bax channels [133-135]. Bcl-2 induces closure of these channels, thereby inhibiting cytochrome c release and membrane potential loss. C-Raf binds to VDAC independently of Bcl-2 and this interaction leads to a reduced reconstitution of VDAC proteins into the outer mitochondrial membrane, thereby limiting the flow of metabolites in

and out of mitochondria [131]. C-Raf kinase activity is not required for this interaction but rather negatively charged phospho-TyrTyr340/341 and multiple autophosphorylated Ser/Thr sites may bind to and induce conformational changes of the VDAC [131]. C-Raf and Bcl-2 could cooperate to directly block the VDAC protein and thereby inhibit VDAC induced depolarization and PTP formation during apoptosis.

ASK1 (apoptosis signal-regulating kinase 1)

Recently it was shown that C-Raf interacts with the proapoptotic, stress activated protein kinase ASK1. This interaction allows C-Raf to act independently of the MEK-ERK pathway to inhibit apoptosis [136]. Furthermore, catalytically inactive forms of C-Raf can mimic the wild type effect, raising the possibility of a kinase independent function of C-Raf [136]. Such a kinase-independent mechanism to counteract apoptosis could explain why the non-mitogen responsive C-RafFF mutant can rescue C-Raf knockout mice [72].

Grb10

Mitochondrion located C-Raf interacts with Grb10, an adaptor protein interacting with a variety of signaling molecules (IGF-1, insulin, EGF), Eph family and growth hormone receptors, and kinases (Bcr-Abl and JAK2) [137]. It was shown that apoptosis protection by insulin-like growth factor (IGF-1) is mediated by three pathways, all of which culminate in BAD phosphorylation [138]. One pathway induces the mitochondrial translocation of C-Raf and Nedd4. Nedd4 is a target of caspases in apoptosis and also interacts with Grb10. Since Nedd4 is also a ubiquitin ligase, it was suggested that C-Raf mediated translocation of BAD away from mitochondria may stimulate ubiquitination and consequent degradation of BAD by the proteasome [139].

MEKK1

C-Raf transforming and survival abilities are not only linked with ERK activation and mitochondrial localization, but also with NF- κ B induction. The NF- κ B/Rel transcription factor family members are involved in cell proliferation, differentiation and protection from apoptosis. They also mediate immune, inflammatory or stress responses as well as cell adhesion and tumorigenesis [140, 141], [142]. It was shown that active C-Raf synergizes with membrane shuttle kinase MEKK1 in order to activate I κ B-kinase complex, which in turn phosphorylates NF- κ B inhibitor protein, I κ B. This leads to NF- κ B/ I κ B complex dissociation and NF- κ B activation [143] (Fig. 1-1).

1-2.3.3 A-Raf specific partners.

CK2b , regulatory subunit of protein kinase CK2.

It was shown that A-Raf specifically interacts with regulatory subunit of protein kinase CK2, CK2 β [144]. CK2 kinase is a ubiquitously expressed and highly conserved pleiotropic Ser/Thr kinase. Its level and activity is increased in proliferating cells. It was shown that CK2 β binding to A-Raf resulted in A-Raf activation, possibly through its conformational alterations [144]. Proliferating tissue-culture cells and human kidney-tumor cells express β subunits of CK2 in excess compared to α subunits [145]. At the same time A-Raf shows highest expression level in urogenital tissues [3]. Therefore CK2 β -mediated A-Raf activation could be involved in formation of these tumors.

Pyruvate kinase type M2 (M2-PK).

The other A-Raf interacting protein, M2-PK [146] binds to the very C-terminal variable domain of A-Raf. Pyruvate kinase is a key enzyme of glycolysis catalyzing the transition of phosphoenolpyruvate to pyruvate with concomitant formation of ATP. M2PK is the embryonic form of pyruvate kinases and replaces the other isoforms in proliferating and tumor cells [147]. A-Raf directly binds to M2-PK and induces its transition from the dimeric to the tetrameric active form. It was shown, that after co-expression in NH3T3 cells, A-Raf and M2-PK interaction leads to M2-PK activation by phosphorylation and cell transformation. In transformed cells, a strong correlation between lactate and alanine production was found [148]. It is a consistent feature of solid tumors and is a consequence of the increase of both glycolysis and glutaminolysis [149]. The increase in the glycolytic flux capacity has the potential to provide tumor cells with a growth/survival advantages under hypoxic conditions.

hTOM and hTIM

Two other human mitochondrial proteins, which interact specifically with N-terminal part of A-Raf, were recently discovered [150]. These proteins, referred to as hTOM and hTIM, are similar to components of mitochondrial outer and inner membrane protein-import receptors from lower organisms, implicating their involvement in the mitochondrial transport of A-Raf. hTOM contains multiple tetratricopeptide repeat (TPR) domains, which function in protein-protein interactions. TPR domains are frequently present in proteins involved in cellular transport systems. It was shown that A-Raf is imported into mitochondria via a system for

isoform-specific uptake [150]. This fact implies the existence of a novel mode for cell regulation of mitochondrial activities by phosphorylation or interaction with mitochondrial proteins

1-2.4 Raf knockout experiments.

To elucidate the specific roles of mammalian Raf isozymes mouse strains with disrupted Raf genes were generated.

A-Raf deficient mice.

The phenotype of A-Raf mutants depends on genetic background-specific modifiers: on a C57Bl/6 genetic background mice die between 7 and 21 days post partum displaying gastrointestinal and neurological defects including megacolon, abnormal movements, abnormal proprioception and excessive agitation. In contrast, on a 129/OLA background they survive to adulthood, and only develop a subset of the neurological defects [95].

B-Raf null mice.

Mice deficient in B-Raf show overall growth retardation and die between E10.5 and E12.5 of vascular defects caused by excessive death of differentiated endothelial cells. They also display some neurological abnormalities namely disturbed growth and differentiation of the neuroepithelium [1]. Sensory and motoneurons from B-Raf deficient mice do not respond to neurotrophic factors for their survival. However, these primary neurons can be rescued by transfection of a B-Raf expression plasmid. In contrast, C-Raf deficient neurons survive in response to neurotrophic factors, similarly to wild type neurons [151]. Thus, the actions of B-Raf and C-Raf are not overlapping in primary neurons and it points to an essential and specific function of B-Raf in mediating survival of sensory and motoneurons during development [151]. It seems that B-Raf survival effect is not related with activation of MAPK pathway because B-Raf cannot activate MAPK in the absence of functional C-Raf protein [96]. Moreover, the inhibition of MAPK pathway has only limited effects in inhibiting NGF-mediated survival of sympathetic neurons in cell culture [152, 153]. Based on observations that B-Raf overexpression can inhibit caspase activation in extracts of rat-1 fibroblasts after addition of cytochrome-c [154], B-Raf is likely essential in the upregulation of IAP proteins, downstream regulators of neuronal survival in response to neurotrophic factors [155].

C-Raf knock-out and knock-in mice.

C-Raf deficiency results in general growth retardation and defects of the placenta, lungs, skin and liver. In an inbred background targeted mice die between E10.5 and E12.5 while in an outbred one they develop to term, are born, and die within hours after birth, because their lungs fail to inflate [98], [72, 93]. C-Raf fetal livers are hypocellular and contain numerous apoptotic cells. Fibroblasts derived from C-Raf deficient embryos exhibit poor proliferation and are more sensitive than wild type cells to specific apoptotic stimuli. Since ERK activation is normal in these cells, possibly compensated by B-Raf (B-Raf activity was up-regulated in C-Raf deficient MEFs), and G1-S transition is unaffected, it is likely that the essential function of C-Raf during embryonic development is to counteract apoptosis rather than promote proliferation [98], [93], [72].

Huser and colleagues also obtained C-Raf^{FF} knock-in mice [72]. C-Raf^{FF} is a point mutant which, at least in cell culture, cannot be efficiently activated by mitogens owing to the mutation of Tyr^{340/341} to PhePhe. The phenotype of these mice is normal - they survive to adulthood, are fertile and display none of the abnormalities associated with the complete C-Raf knock-outs. However, C-Raf^{FF} mutant retains a low level of kinase activity and still could signal through MEK (data from U.R. Rapp lab), and a conclusive answer has to await the knock-in of a true kinase negative C-Raf mutant.

C-Raf and B-Raf double deficient mice.

Since mouse embryo mutants for each of the Raf genes exhibit no developmental defects before mid-gestation, it is possible that Raf isoforms could compensate each other before this period. To elucidate this possibility the double mutant *C-Raf/B-Raf* embryos were obtained and analyzed. It was shown that the loss of one additional Raf allele (C-Raf^{-/-}/B-Raf^{+/-} or C-Raf^{+/-}/B-Raf^{-/-}) increased dramatically the extent of abnormalities and led to the death of 90% of the embryos before E10.5. At the same time the disruption of all four copies of B-Raf and C-Raf abrogated the differentiation of most embryonic lineages, but had no effect on cell proliferation and implantation of the embryo [96]. It has been reported that injections of oncogenic C-Raf expressing vector prevented two-cell stage block induced by Ras pathway inhibition in mouse embryo. However, Raf signaling was dispensable for subsequent development to morula and blastocyst [156]. In double allele knock-out embryos this two-cell stage block could be overcome by A-Raf signaling or other ERK activators as Mos, Tpl2, and MEKK. The evidence of such early developmental cooperation between B-Raf and C-Raf is

supported by the observation that both enzymes are required for the activation of MAP kinase [96]. The molecular basis of this interaction between C-Raf and B-Raf can be enzymatically active heterodimer formation with subsequent MAP kinase activation in response to growth factors [157] (Fig. 1-3).

1-2.5 Experimental design and aim of the project.

The phenotypical differences among the Raf-deficient mutants suggested the existence of the exclusive roles for the individual Raf isozyms in mammalian development. Knock-out experiments point to an important role of C-Raf in apoptosis suppression and suggest that this function could be still performed when its MEK kinase activity is reduced [72]. The presence of numerous other partners besides MEK, some of which are implicated in the control of apoptosis [67] and genetic experiments [96], [72, 93] raise the possibility that modulation of C-Raf kinase activity in survival depends on cooperation with different interaction partners.

Since B-Raf is the more important MEK activator in many cell types and tissues [4], and B-Raf deficient mice display severe phenotype and die at mid-gestation from massive endothelial apoptosis [1], it would be of great interest to rescue such early lethality and define the critical role of B-Raf in further developmental processes. This was successfully performed in knock-in experiments, where isomorphic/hypomorphic mice expressing chimeric A-Raf protein under control of endogenous B-Raf promoter were obtained. The weak kinase activity of A-Raf could help to overcome the critical time period at mid-gestation where most of lethality occurred in B-Raf null mice. The phenotype of obtained B-Raf /A-Raf knock-in mice and mechanisms leading to survival will be described in the following chapters.

2. RESULTS

2-1. Design and cloning of B-Raf targeting constructs.

Gene targeting is defined as the genetic modification of an endogenous DNA sequence by homologous recombination with a DNA segment introduced into genomic DNA. The key tools for this are embryonic stem (ES) cells and the targeting vector. The vector must contain sequences homologous to the chromosomal locus to be disrupted, together with a positive, and ideally a negative selection marker.

Mice deficient in B-Raf on C57Bl6 genetic background show overall growth retardation and die between E10.5 and E12.5 of vascular defects caused by excessive death of differentiated endothelial cells [1]. To elucidate the redundancy of Raf isozymes during mouse embryonic development and possibly to rescue B-Raf null phenotype it would be interesting to knock-in B-Raf gene by disrupting the wild type B-Raf alleles and introducing one of the other Raf family members: A-Raf or c-Raf-1 under the control of endogenous B-Raf promoter. Since B-Raf has the unique N-terminal part encoded by first three exons and possibly executing antiapoptotic functions it would be reasonable to create kind of chimeric hypomorphic B-Raf protein with its own N-part fused with either A-Raf or c-Raf-1 (Fig. 2). Taking into consideration that basal B-Raf kinase activity is the highest among Raf proteins, it will allow us to understand the specific role of the unique N-part e.g. in C-Raf heterodimerization and C-Raf activation or its own kinase activity in midgestational survival and further development. To achieve this, a set of knock-in constructs in pKS TK*neo*LoxP vector, containing positive (neo) and negative (HSV-tk) selection markers was created both for human A-Raf and c-Raf-1. Each set includes wild type version of human cDNA and two mutants: with constitutive kinase activity (DD 340/341 for c-Raf-1 and DD 301/302 for A-Raf) and without kinase activity (K375W for c-Raf-1 and K338M for A-Raf). The HA tag was introduced in all these constructs to detect the resulting proteins. Since B-Raf gene has many splice variants and exon 3 is present in all of them, the 8-kb BamHI genomic fragment subcloned in pBluescript KS vector and containing exon 3 was used as a backbone for all constructs [1]. The HA tag, and the polyA signal from human growth hormone (hGH) were introduced in each cDNA of human A-Raf and c-Raf-1. The PstI restriction site compatible with NsiI in exon 3 of B-Raf was introduced in cDNAs by PCR at the beginning of Ras Binding Domain (RBD). Thus, cDNA was introduced in frame with the third exon of B-Raf at the beginning of its own RBD (Fig. 2). After electroporation and homologous recombination in ES cells chimeric proteins carrying first three exons of B-Raf and the remainder of A-Raf or c-Raf-1 will be expressed under control of endogenous B-Raf promoter.

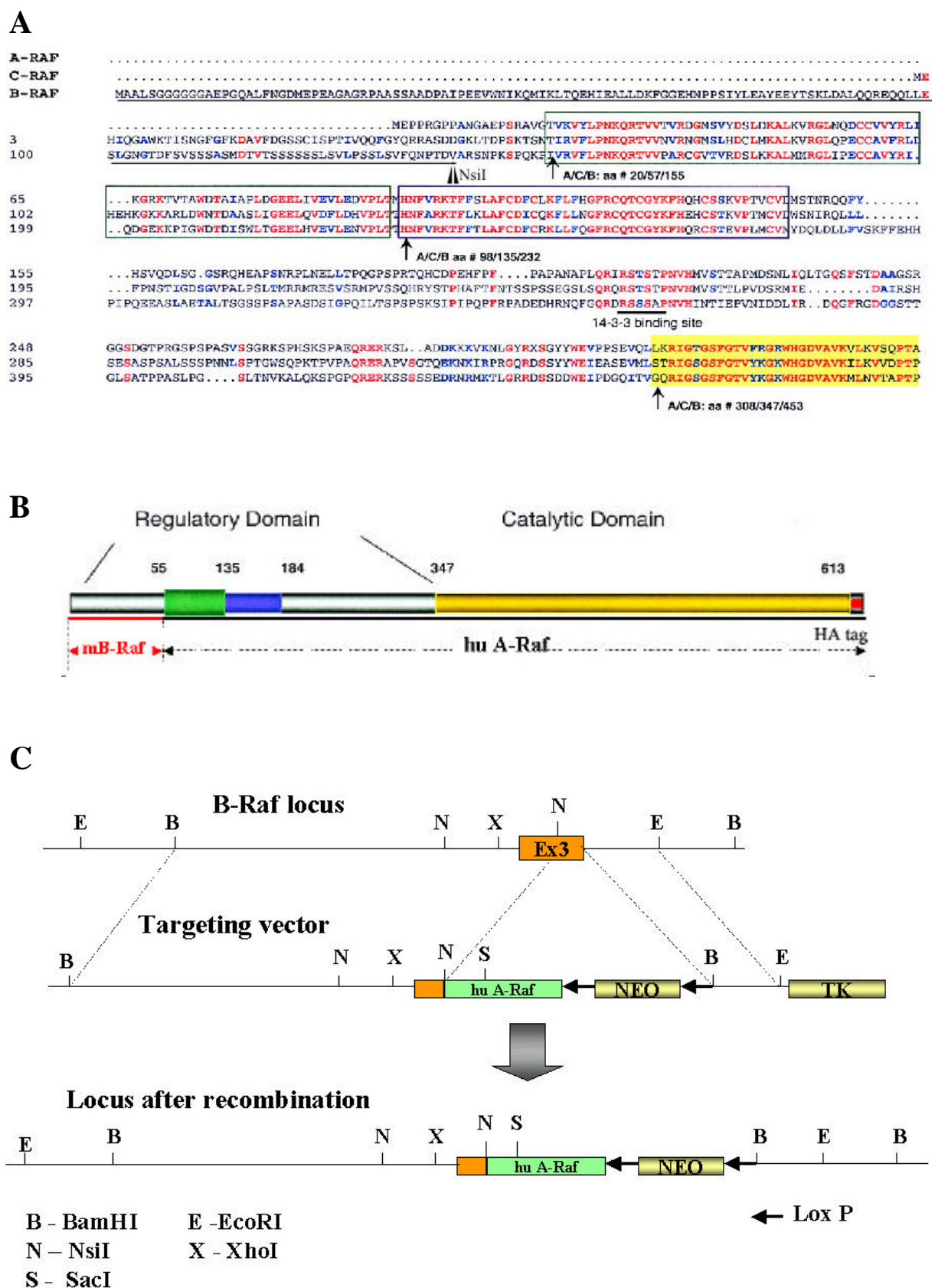


Fig. 2-1 A. Alignment of regulatory domains of three human Raf proteins. The unique N-terminal part of B-Raf is underlined. NsiI restriction site is indicated by arrow. **B.** Expected chimeric protein harbors N-terminal part of mouse B-Raf until NsiI site in exon 3 and the remainder of A-Raf or c-Raf-1. **C.** Targeting strategy of B-Raf locus. NEO cassette is flanked by LoxP sites to do not interfere with expression of chimeric protein.

2-2. Vector electroporation and positive clone selection.

One of these targeting vectors containing WT version of human A-Raf, possessing the weakest kinase activity among Raf isozymes, was linearized at the unique NotI site and electroporated into CJ7 ES cells (129Sv genetic background, passage 11) and survived colonies were isolated following G418 and gancyclovir selection.

Targeted clones (7 out of 420) were identified first by PCR using one sense primer corresponding to the neomycin cassette sequence and the other antisense to the genomic sequence outside the vector (Fig. 2-2 A). All PCR confirmed clones were then verified by Southern hybridization for homologous recombination probing with both 3' end 1.3 kb EcoRI/BamHI and 5' end 1.6 kb EcoRI/BamHI fragments. In all cases the homologous recombination of both arms was confirmed (Fig. 2-2. B, C).

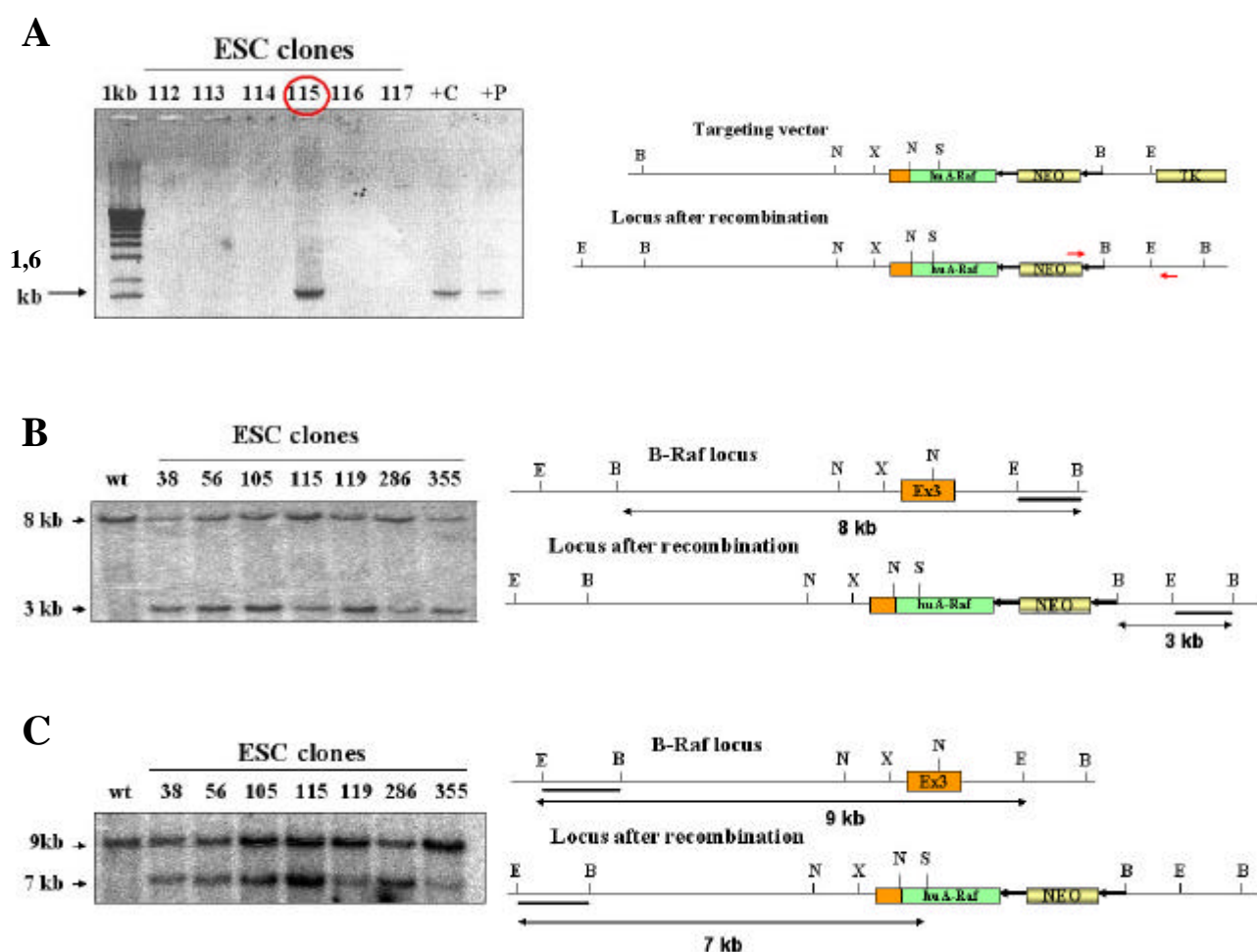


Fig. 2-2 A. PCR screening for homologous recombination of 3' arm. The expected fragment size is 1,6 kb. +C-control positive clone, +P-control positive plasmid. Red arrows indicate primers used for PCR. **B.** Homologous recombination of 3' arm confirmed by Southern hybridization. After BamHI restriction an additional band at 3 kb appears where homologous recombination has occurred. **C.** Homologous recombination of 5' arm confirmed by Southern hybridization. After EcoRI/SacI restriction an additional band at 7 kb appears where homologous recombination has occurred. Black bars indicate fragments used as the probes for hybridization. B-BamHI, E-EcoRI, S-SacI

2-3. Confirmation of chimeric protein expression in ES cells.

To be sure that targeted ES cells express the mRNA of the resulting chimeric protein the RT PCR with two sense primers corresponding to exon2 and 3 of B-Raf respectively and one antisense primer for N-terminal part of A-Raf was performed. In all tested clones the expression of chimeric mRNA was observed (Fig. 2-3 A). The expression of protein was confirmed by Western blot using the mouse monoclonal a-HA-tag antibodies. The size of the fusion protein corresponds to the predicted 87 kD (Fig. 2-3 B).

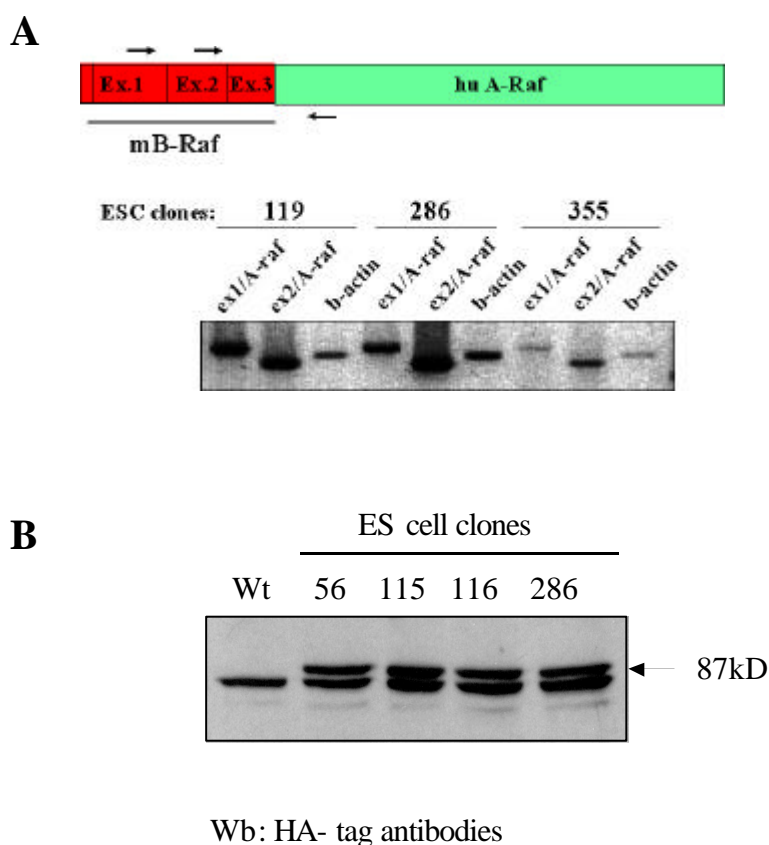


Fig. 2-3 A. RT PCR confirms the expression of resultant chimeric mRNA in targeted ES cell clones. **B.** Western blot with a-HA-tag antibodies demonstrates the expression of predicted 87 kD chimeric protein in targeted ES cell clones. The lower band can be the result of nonspecific interaction of the first monoclonal mouse a-HA-tag antibodies.

2-4. Injection of targeted ES cell clones into mouse blastocyst and generation of chimeric and F1 heterozygous mice.

Four of seven targeted ES cell clones with good morphology (round shaped sharp edge colonies) were taken for injection experiments. Using micromanipulator and dissecting microscope ES cells were injected into WT (C57Bl6) 3.5 day-old blastocyst, 12-15 cells/blastocyst. After injection chimeric blastocyst was implanted into the uterus of a

pseudopregnant mother, 15 injected blastocysts/mouse. The most significant factor in this experiment is the contribution of the targeted ES cells to the germ-line cells (Fig. 2-4 A). Twelve chimeric males with more than 40% of ES cell component in coat color were obtained and two of them have the germ line transmission detected by agouti color of F1 offspring after mating with C57Bl6 WT females (Table 2-4, Fig. 2-4 B).

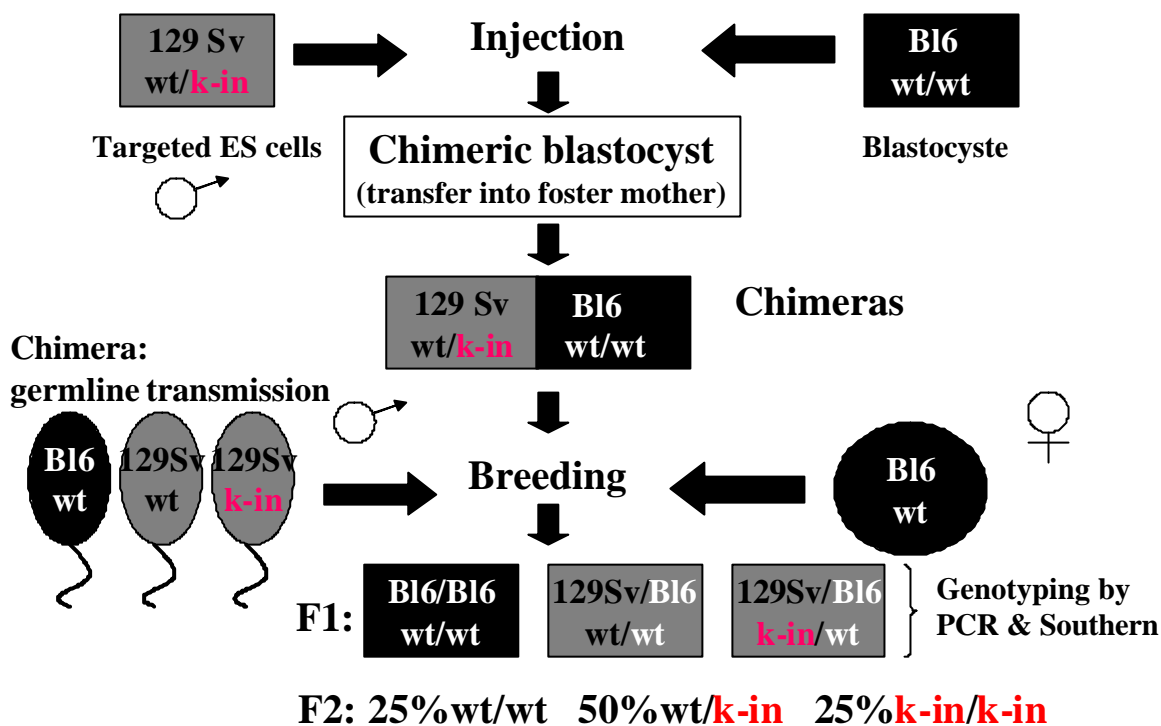


Fig. 2-4 A. Scheme of chimeric mice production and further breedings to obtain knock-in mice. After ES cell injection and obtaining chimeric males with high percent of ES cell component, they were crossed with C57Bl6 WT females. The germ line transmission in offspring can be recognized by dominant 129Sv (background of ES cells) agouti coat color.

Nr of chimera	ES cell impact (%)	Notes
127	60	no tm
130	70	no tm
131	85	germ line tm
132	95	sterile
4423	85	no tm
4424	85	no tm
4422	50-60	no tm
164	99	germ line tm
165	45	sterile
166	95	tail branching
65	90	sterile
168	70	no tm
169	85	sterile

Interestingly, due to somatic mutation in some fraction of ES cells during culturing and manipulation and/or improper colonization in host blastocyst the chimeric male Nr.166 displays dichotomic tail branching (Fig. 2-4 B). This abnormality is not transmitted to offspring. Two germ line

Table 2-4 Summary of totally obtained chimeric mice.

transmitting males gave 4 litters with 15 pups. Most of pups (12 out of 15) had agouti colored coat suggesting high ES cells colonization in germ lineage (Fig. 2-4 B)

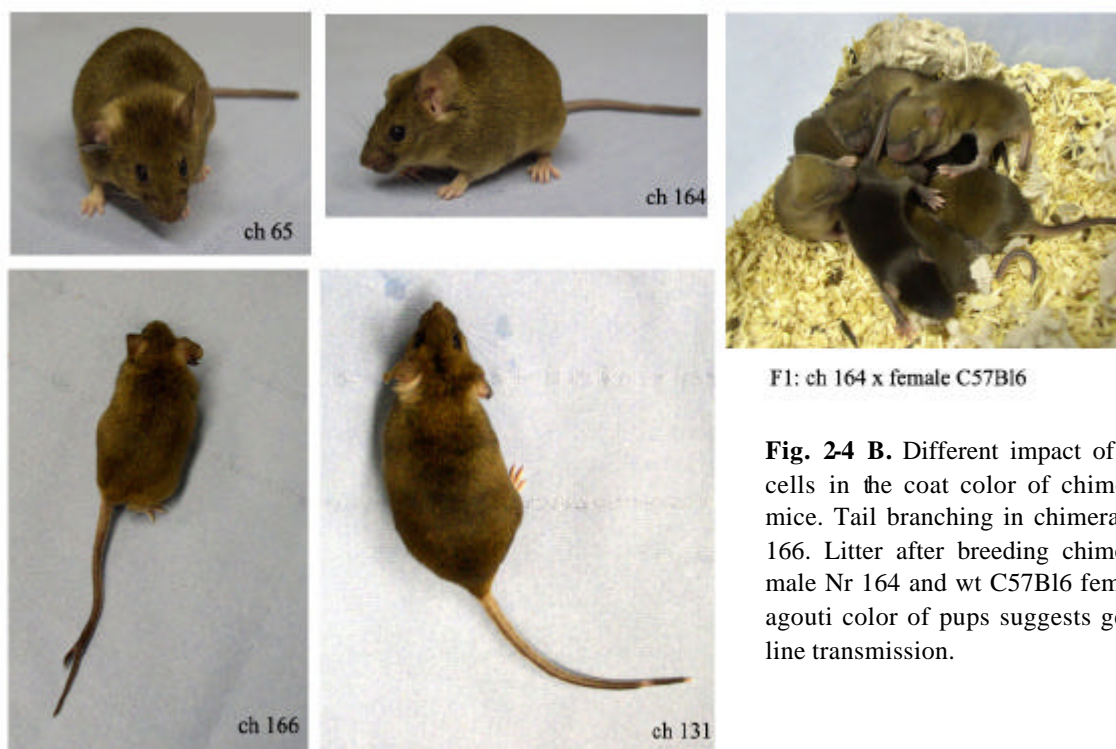
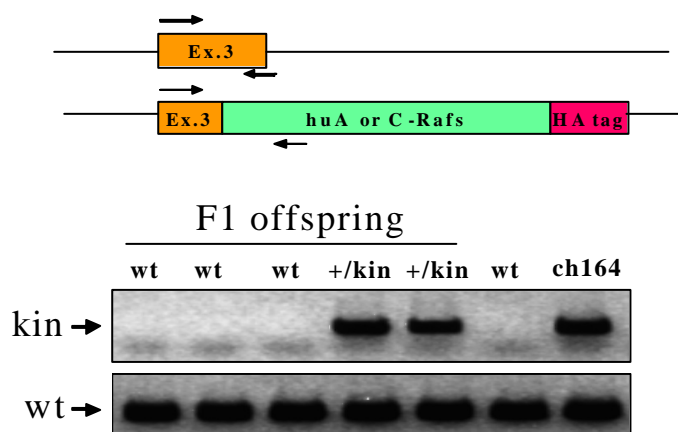


Fig. 2-4 B. Different impact of ES cells in the coat color of chimeric mice. Tail branching in chimera Nr 166. Litter after breeding chimeric male Nr 164 and wt C57B16 female, agouti color of pups suggests germ line transmission.

The F1 offspring was genotyped first by PCR. To detect wild type allele one sense primer corresponding to the 5' sequence of exon 3 of B-Raf and the other antisense to the 3' sequence which is absent in knock-in allele were used. For KIN allele the sense primer was the same as for WT allele and the antisense corresponded to the 5' sequence of human A-Raf (Fig. 2-4 C). PCR genotyped offspring was then verified by Southern hybridization probing with 3'end 1.3 kb EcoRI/BamHI fragment used as a probe for ES cells (see the chapter 2-2) (Fig. 2-4 D). Four out of fifteen analyzed F1 mice were heterozygous (+/KIN). They did not display any abnormalities during 9 months observation period, and were fertile.

C



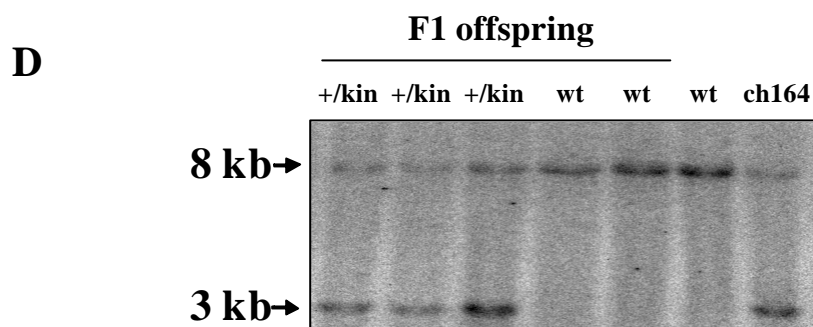


Fig. 2-4 C. PCR detection of heterozygous F1 offspring. 450 bp band corresponds to KIN allele, 250 bp to WT. **D.** Southern blot confirms heterozygous F1 offspring. After BamHI restriction and probing the bands at 8 kb and 3 kb appear corresponding to WT and KIN alleles respectively.

2-5. Genotyping of F2 embryos. Analysis of B-Raf expression in embryos.

The embryos at different stages of development were genotyped by PCR from yolk sack or tail lysates using the same primers as for genotyping F1 heterozygous mice (Fig. 2-5 A). The KIN founders were confirmed by Southern hybridization probing with 3' end 1.3 kb EcoRI/BamHI fragment (Fig. 2-5 B). The absence of endogenous B-Raf expression in KIN embryos was confirmed by Western blot using a-B-Raf antibodies (Fig. 2-5 C).

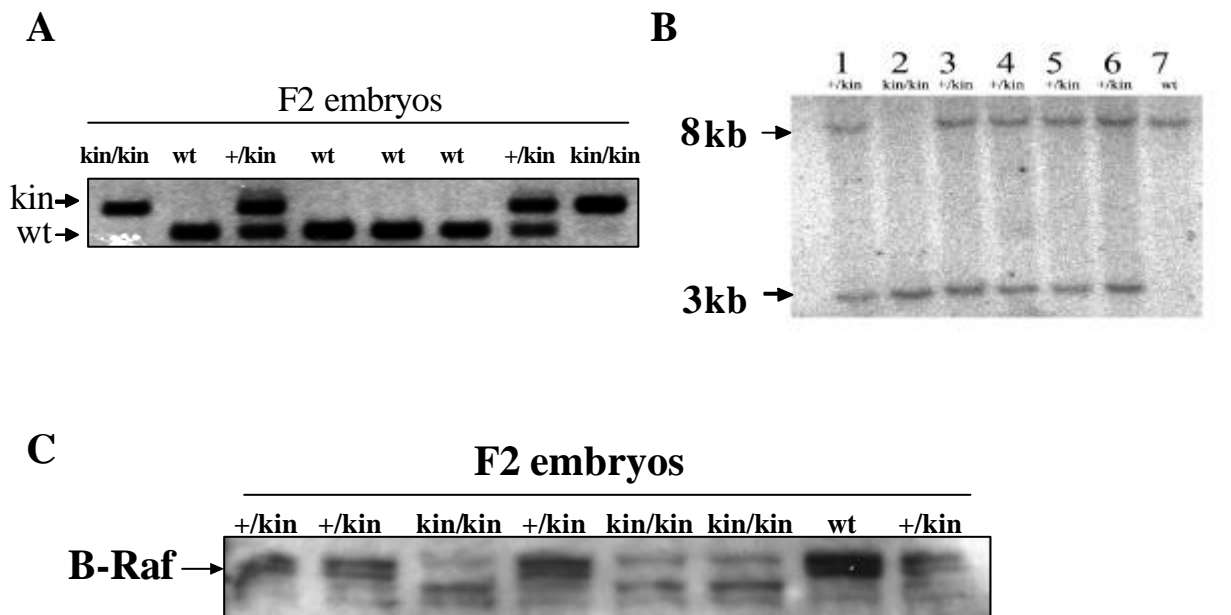


Fig. 2-5 A. Example of PCR genotyping of F2 E10.5d embryos. 450 bp band corresponds to KIN allele, 250 bp to WT. **B.** Southern blot confirms the presence of homozygous KIN embryo Nr2 in litter. After BamHI restriction and probing the bands at 8 kb and 3 kb appear corresponding to WT and KIN alleles respectively. **C.** Western blot using a-B-Raf antibodies detects no expression of B-Raf in KIN homozygous embryos in contrast to heterozygous and WT. The specific band corresponding to endogenous B-Raf is indicated by arrow.

2-6. Comparison of B-Raf KO and KIN embryo phenotype and life span depending on genetic background.

Since F1 KIN offspring has mixed genetic background (129Sv/B16) the first F2 after intercross of F1 was on 129Sv/B16 background (Fig. 2-4 A). To adequately compare the phenotypes of KO and KIN embryos, the same genetic background was obtained for KO. The viability of embryos was detected by observing the beat heart after isolation. Figure 2-6 A shows that at E10.5d 100% of analyzed embryos of both KO and KIN genotypes were alive.

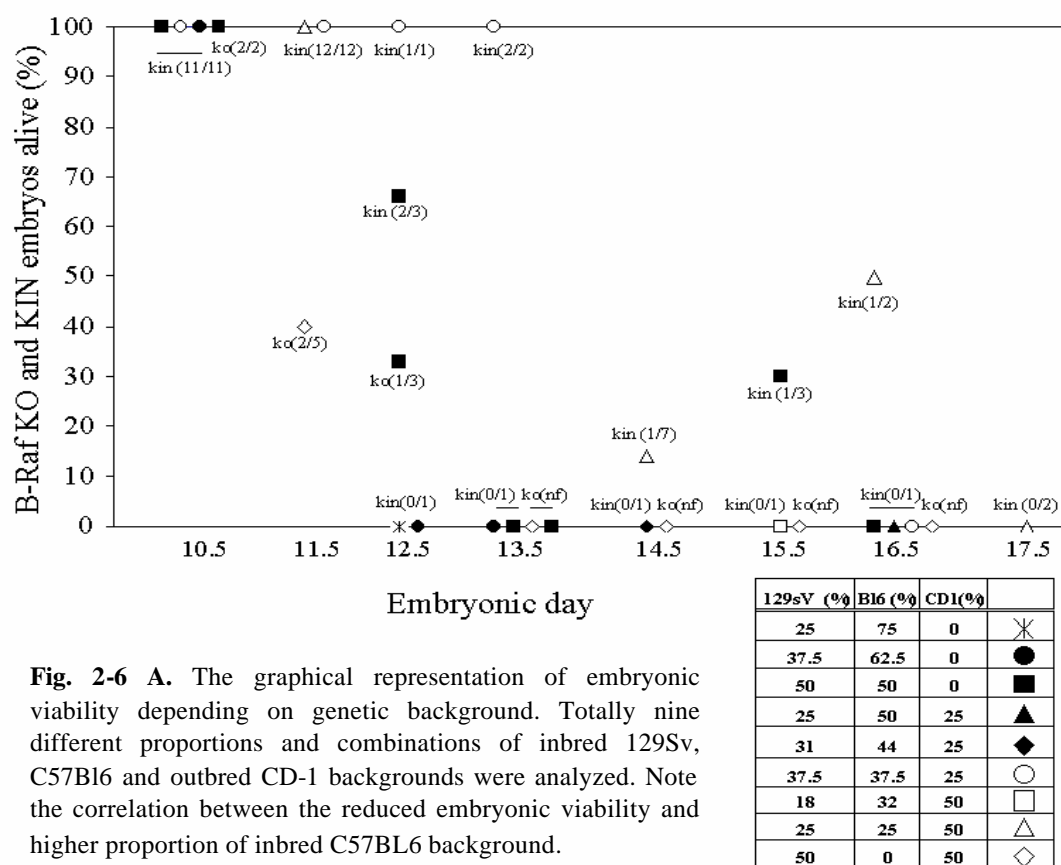


Fig. 2-6 A. The graphical representation of embryonic viability depending on genetic background. Totally nine different proportions and combinations of inbred 129Sv, C57Bl6 and outbred CD-1 backgrounds were analyzed. Note the correlation between the reduced embryonic viability and higher proportion of inbred C57BL6 background.

Some of KIN and KO embryos displayed hemorrhages in body cavity and retarded head development. Many KO embryos were pale, probably because of extravasated blood. Nearly all of both KINs and KOs had the reduced body size, usually KO embryos were smaller than KIN. Null embryos demonstrated more pronounced defects in overall development than KIN suggesting the compensatory role of A-Raf protein in early development (Fig 2-6 B).

According to the literature, in B-Raf KO embryos the blood extravasation is caused by massive apoptosis in endothelial cells lining blood vessels [1]. To define which processes are involved in hemorrhages observed in some KIN embryos, the whole embryo displaying

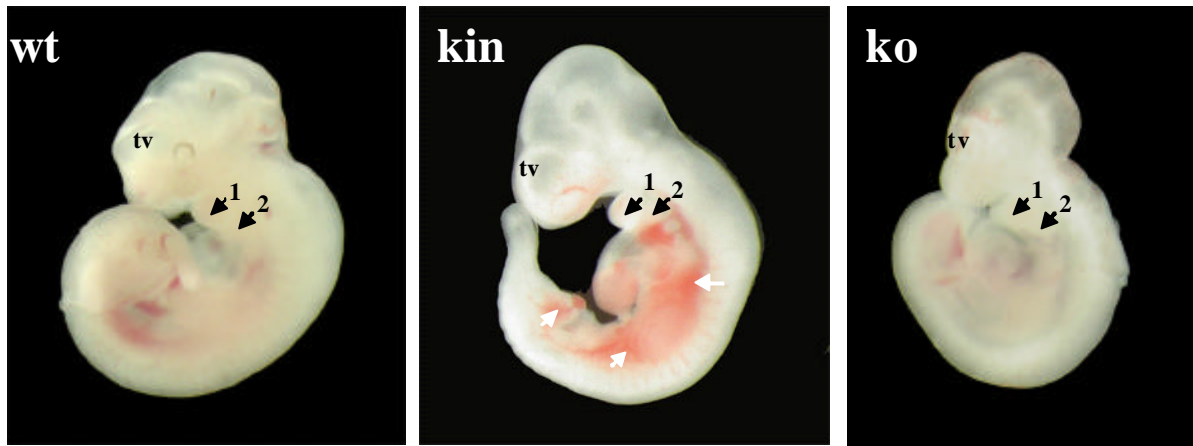


Fig. 2-6 B. Example of observed phenotypes of WT, KIN and KO embryos at E10.5d on 129 Sv/Bl6 background. White arrows indicate bleedings in body cavity. Note the gradually increased abnormalities in WT-KIN-KO (size reduction, head development). Black arrows 1, 2 correspond to first and second branchial arches respectively. **tv** - telencephalic vesicles (future cerebral vesicles).

bleeding (Fig. 2-6 B, KIN) and its littermates were lysed and subjected to Western blot analysis using α -PARP antibodies. In apoptosis the nuclear chromatin associated PARP (Poly (ADP-ribose) polymerase) is cleaved by caspases from its 116 kD intact form into 85 kD and 25 kD fragments. The apoptotic process was defined only in this KIN embryo (Fig 2-6 C). In other experiments with normal KIN embryos no apoptosis was detected (data not shown). When phosphorylated, ERK shuttle kinase is known to be survival and proliferation promoting factor [169]. The reduced ERK phosphorylation was also detected in the same KIN embryo using phospho-specific α -pERK1/2 (pThr202/204) antibodies (Fig. 2-6 C), demonstrating in this case insufficient kinase activity of chimeric A-Raf to rescue endothelial apoptosis.

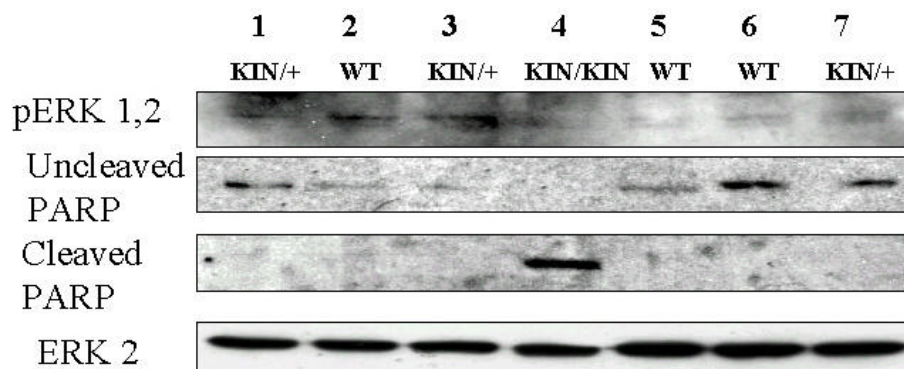


Fig. 2-6 C. Western blot demonstrates the enhanced apoptosis in whole KIN embryo Nr4 displaying hemorrhages. The PARP cleavage was measured using α -PARP antibodies. The reduced phosphorylation of total ERK in the same embryo coincides with increased apoptosis. Phospho-specific α -pERK1/2 (pThr202/204) antibodies were used. The total amount of ERK detected by α -ERK2 antibodies was not changed.

E12.5d, 129Sv/BL6 KO and KIN embryos.

At the E12.5d on 129Sv/Bl6 background, one of three not reorbed KO embryos was still alive, but displayed very weak heart beating, overall growth retardation and bleedings. In cephalic region the palate shelves were widely separated and nasal area was delayed in development corresponding to the stage E10.5-11.5d. Also the twisting midbrain region was observed. Two of three analyzed KIN embryos were alive, where one showed a similar phenotype to KO embryo, and the other was smaller by size without any visible defects in development but demonstrated multiple hemorrhages and enlarged blood vessels (Fig. 2-6 D).

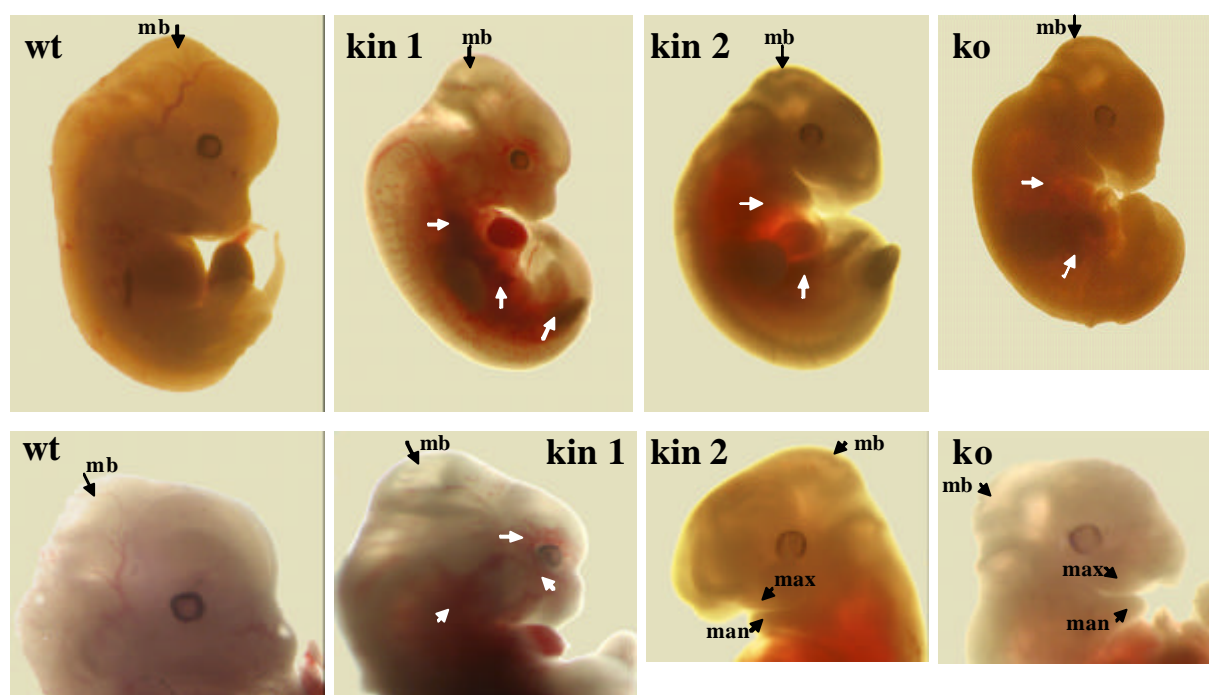


Fig. 2-6 D. Different phenotypes of WT, KIN and KO embryos, E12.5d on 129 Sv/Bl6 background. White arrows indicate bleedings in body cavity and enlarged blood vessels. Compare the similar abnormalities in KIN 2 and KO embryos - the twisting midbrain, not closed palate, retardation in nasal area development. **mb** - midbrain, **max**, **man** – maxillary and mandibular parts of pharyngeal arch.

E15.5d, 129Sv/BL6, only KIN embryos are alive.

At the later stages of development no living KO embryos were found. The introduction of CD-1 outbred instead of inbred C57Bl6 genetic background (129 Sv/CD-1 instead of 129 Sv/Bl6) which was made in order to rescue the early lethality (as was shown for c-Raf-1 deficient embryos [1, 72]) did not increase the KO embryonic life span (Fig. 2-6 A).

At the further developmental stages one smaller KIN embryo, without any obvious developmental defects was found at E15.5d on 129Sv/Bl6 background (Fig. 2-6 A, 2-6 E).

E12.5d-13.5d (129Sv/B16/CD-1=37.5/37.5/25) and E16.5d (129Sv/B16/CD-1=1/1/2) living KIN embryos.

When diluted with CD-1 outbred background (129Sv/B16/CD-1=37.5/37.5/25), the KIN founders were alive at E12.5d and E13.5d. They were normally developed, but were all reduced in size (Fig. 2-6 A, F, G). At E16.5d another living fetus (129Sv/B16/CD-1=1/1/2) was isolated. It was also smaller than littermates, and showed normal development (Fig. 2-6 A, 2-10 A, B). All these findings demonstrate that genetic background related modifier genes could be involved in cooperation with B-Raf protein in different developmental processes.

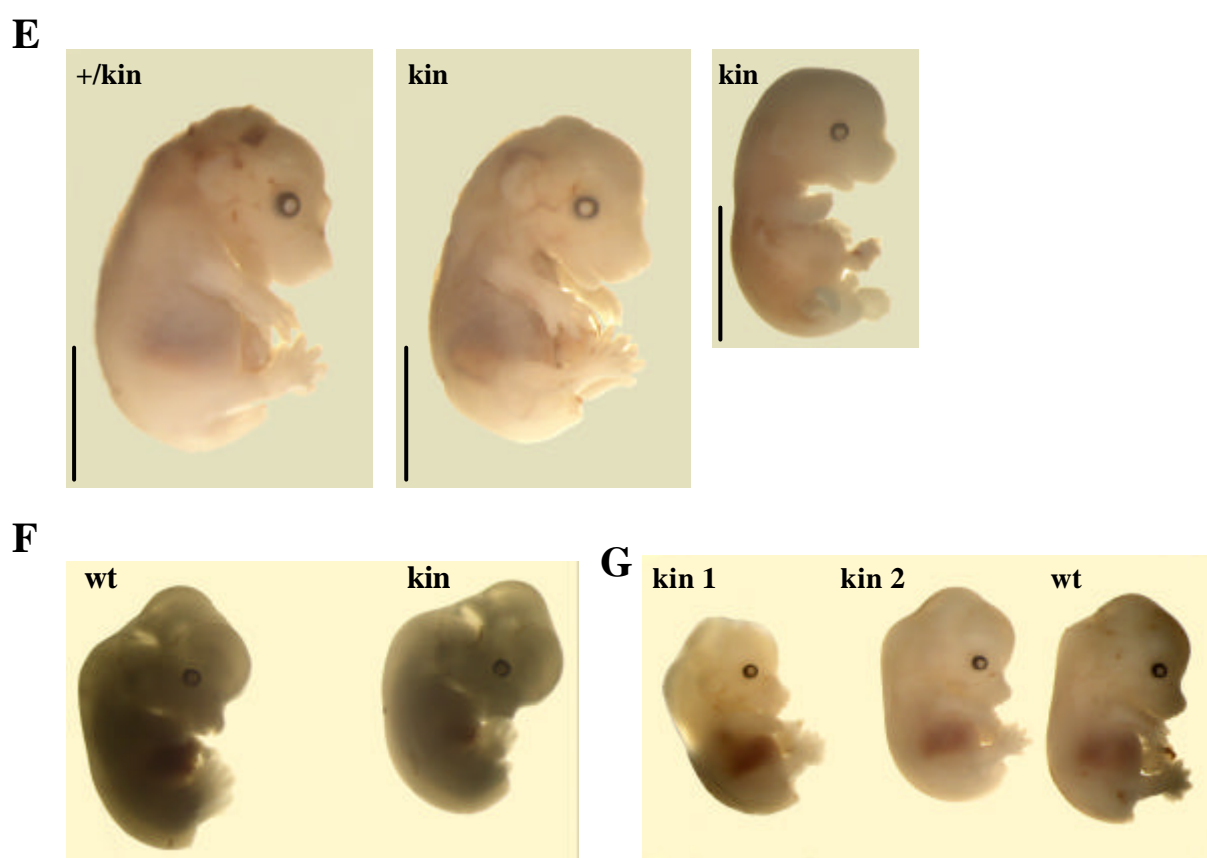


Fig. 2-6 E. Phenotypes of WT and KIN embryos, E15.5d, 129 Sv/B16 background. One KIN embryo (right) is dead, but is not yet resorbed. Alive embryo (in the middle) is normal and around 20% smaller than heterozygous littermate. Scale bars correspond to 0.5cm. **F.** E12.5d embryos on (129Sv/B16/CD-1=37.5/37.5/25) background. **G.** E13.5d embryos on (129Sv/B16/CD-1=37.5/37.5/25) background. In E, F, G all survived KIN embryos manifest the reduced size and normal development. At E12.5d and later no normal KO embryos were detected on different genetic backgrounds.

2-7. Obtaining adult KIN mouse, and its biochemical characterization.

One adult three weeks old (p20) KIN female on 129Sv/B16 was obtained. This mouse was two fold reduced in body weight, but did not display any visible behavioral abnormalities and developmental defects. All organs appeared normal and proportional to body size, excluding

thymus and spleen which were very small and 10 fold reduced by weight compared to heterozygous littermate organs (Fig. 2-7 A).

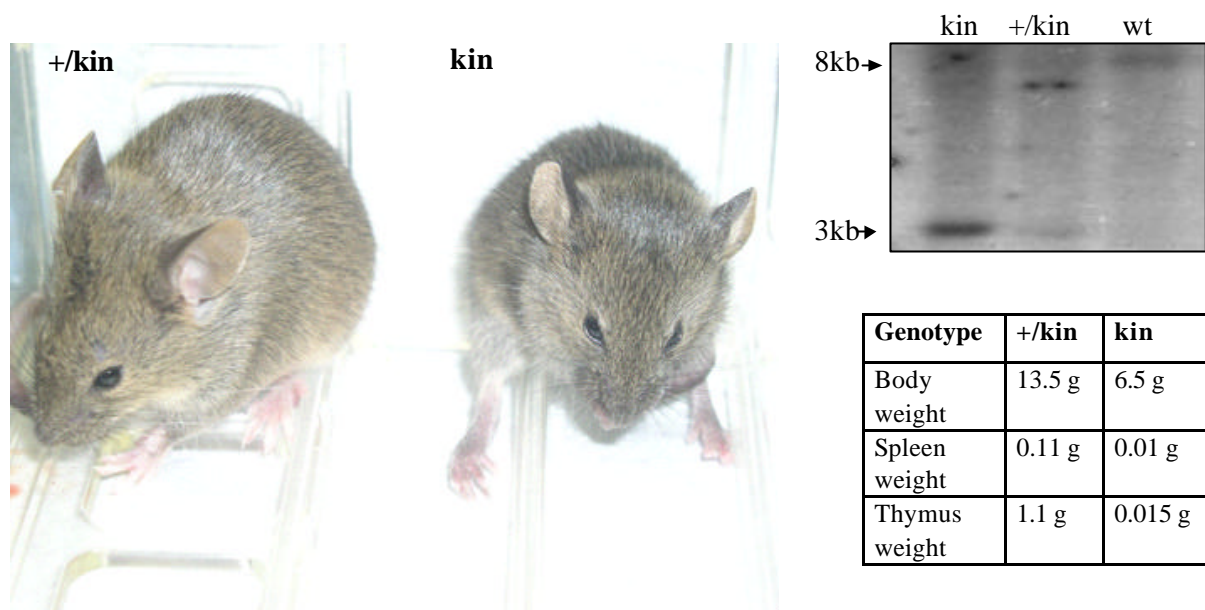


Fig. 2-7 A. Adult p20 +/KIN and KIN females on 129 Sv/B16 background. Note the size reduction of KIN mouse. Southern hybridization probing with 3'end 1.3 kb EcoRI/BamHI fragment confirms the genotypes. After BamHI restriction and probing the bands at 8 kb and 3 kb appear corresponding to WT and KIN alleles respectively. Table indicates the difference in weights of body and organs.

Western blot analysis of different tissues and brain compartments showed no expression of B-Raf protein in KIN mouse. In KIN mouse the fraction of phosphorylated ERK1/2 in the same samples was significantly reduced with exception of hindbrain compared to heterozygous littermate (Fig. 2-7 B).

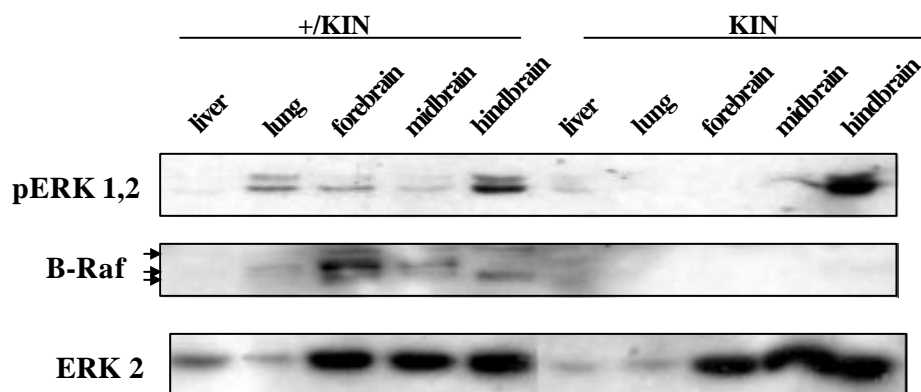


Fig. 2-7 B. Western blot using a-B-Raf antibodies confirms the absence of B-Raf expression in any tested tissue of p20 KIN mouse. Significant reduction in ERK1,2 phosphorylation in near all tested tissues excluding hindbrain in KIN mouse, a-pERK1/2 (pThr202/204) antibodies were used.

2-8. Histochemical and immunochemical analysis of E12.5d embryos.

The surviving embryos of three genotypes: +/KIN, KIN and KO at E12.5d on 129Sv/B16 background (Fig. 2-6 D) were embedded in paraffin, cut in microsections and stained by hematoxylin-eosin to compare their histological structure. The comparison of KIN +/- and KIN main organ structure and development did not reveal a significant difference. In KIN embryo they were proportional to the body size (Fig. 2-8 A, B, D, E, G). No blood vessel ruptures were detected. In contrast, KO embryo demonstrated the irregular brain structure

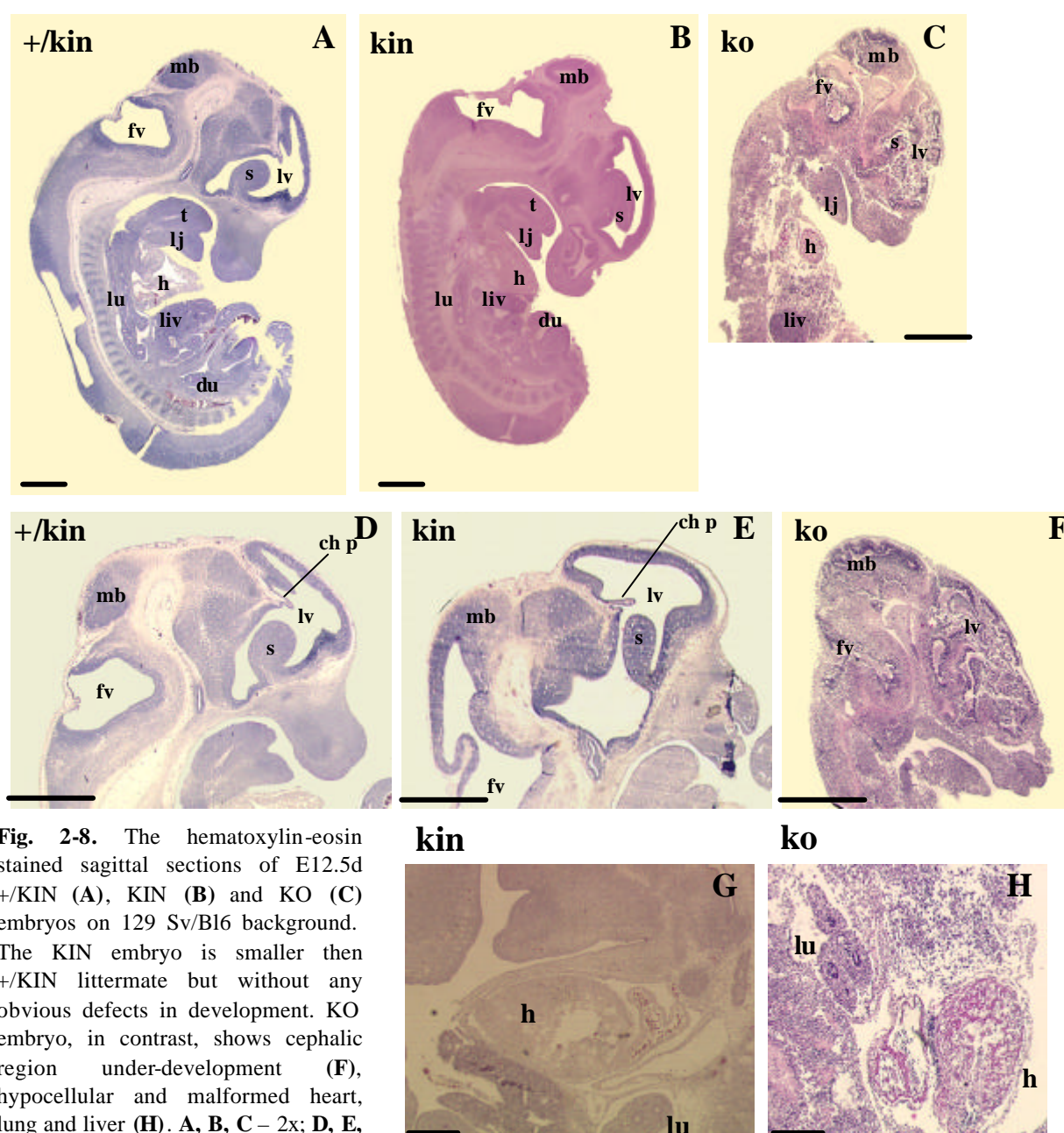


Fig. 2-8. The hematoxylin-eosin stained sagittal sections of E12.5d +/KIN (A), KIN (B) and KO (C) embryos on 129 Sv/B16 background. The KIN embryo is smaller than +/KIN littermate but without any obvious defects in development. KO embryo, in contrast, shows cephalic region under-development (F), hypocellular and malformed heart, lung and liver (H). A, B, C – 2x; D, E, F – 4x; G, H – 10x magnification

In A-F scale bar corresponds to 1mm, in G,F to 250 μ m. **ch p**-choroid plexus, **du**-duodenum, **fv**-fourth ventricle, **h**-heart, **lv**-lateral ventricle, **lj**-lower jaw, **liv**-liver, **lu**-lung, **mb**-midbrain, **s**-striatum, **t**-tongue

(no obvious fourth and lateral ventricle areas and striatum, twisted midbrain), non-developed lower jaw, smaller heart and liver and overall hypocellularity (Fig. 2-8 C, F, H).

Since B-Raf is highly expressed in adult brain and implicated in PC12 cells proliferation and differentiation [27, 28, 169] it would be interesting to compare the proliferative ability of the neural stem cells (NSC) or neuronal progenitor cells (NPC) in embryos of different genotypes. KO embryo does not display any clearly recognizable structure in brain to be compared with, and rather manifests the overall massive apoptosis than proliferative processes. A good marker for proliferating cells is a 36 kD PCNA (Proliferating Cell Nuclear Antigen) protein, also known as cyclin or the polymerase-associated protein. It is synthesized in early G1 and S phases of the cell cycle. The immunohistochemical staining using α -PCNA antibodies revealed a much higher proliferation in +/KIN than in KIN subventricular zone (SVZ) of fourth and lateral ventricles, and in striatum (Fig. 2-8 I).

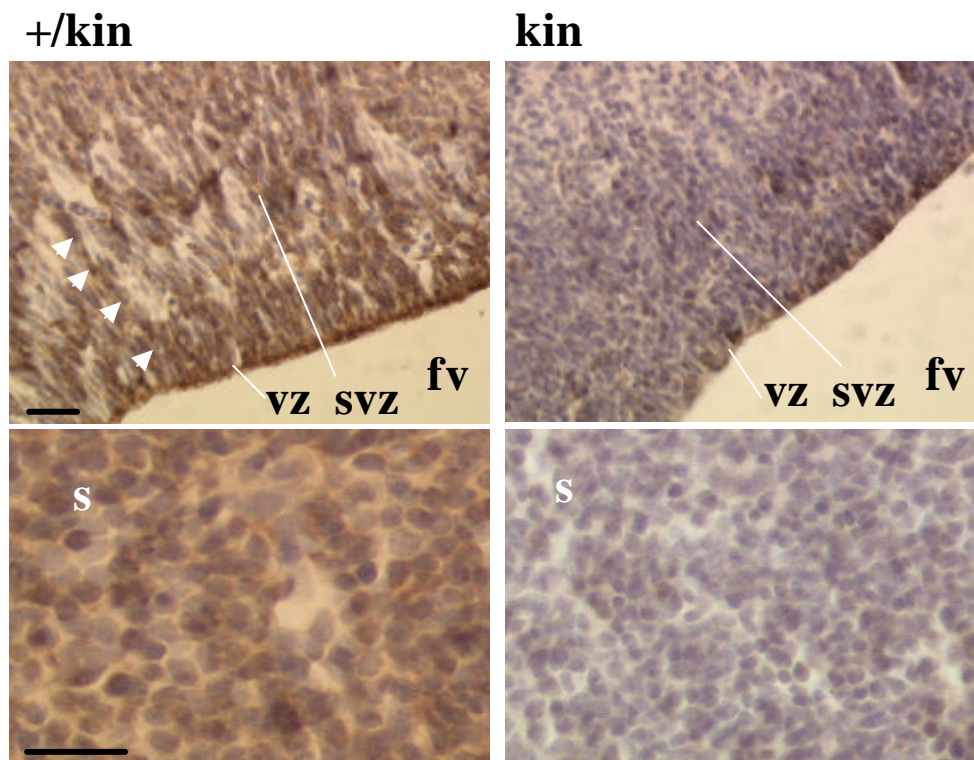


Fig. 2-8 I. Immunohistochemistry using α -PCNA antibodies shows less proliferation in ventricular (VZ) and subventricular (SVZ) zones of fourth ventricle (fv) and in striatum (s) in KIN E12.5d embryo. The cells in S-phase are brown stained. Possibly the migration of neurons from VZ towards SVZ is also affected in KIN embryo since no polarity is seen in this direction in contrast to +/KIN. White arrows indicate the migration process. fv-20x; s-40x magnification. Scale bars correspond to 100 μ m.

These areas are known to be NSC or NPC compartments. At mid-gestation after proliferation in the germinal ventricular zone (VZ) young neurons migrate perpendicular to the ventricle wall guided by radial glia, and form a second germinal zone – subventricular zone (SVZ) [177]. In addition to decrease in proliferation the migration process seems to be impeded in KIN embryo (Fig. 2-8 I).

2-9. Histochemical and immunochemical characterization of E13.5d embryos.

The comparison of KIN and +/KIN hematoxylin-eosin stained whole embryo slices at E13.5d on (129Sv/B16/CD-1=37.5/37.5/25) background (Fig. 2-6 G) did not reveal a basis for the considerable difference in organ formation and development. Excluding the reduced size, no evident abnormalities were detected in KIN embryo. (Fig. 2-9 A).

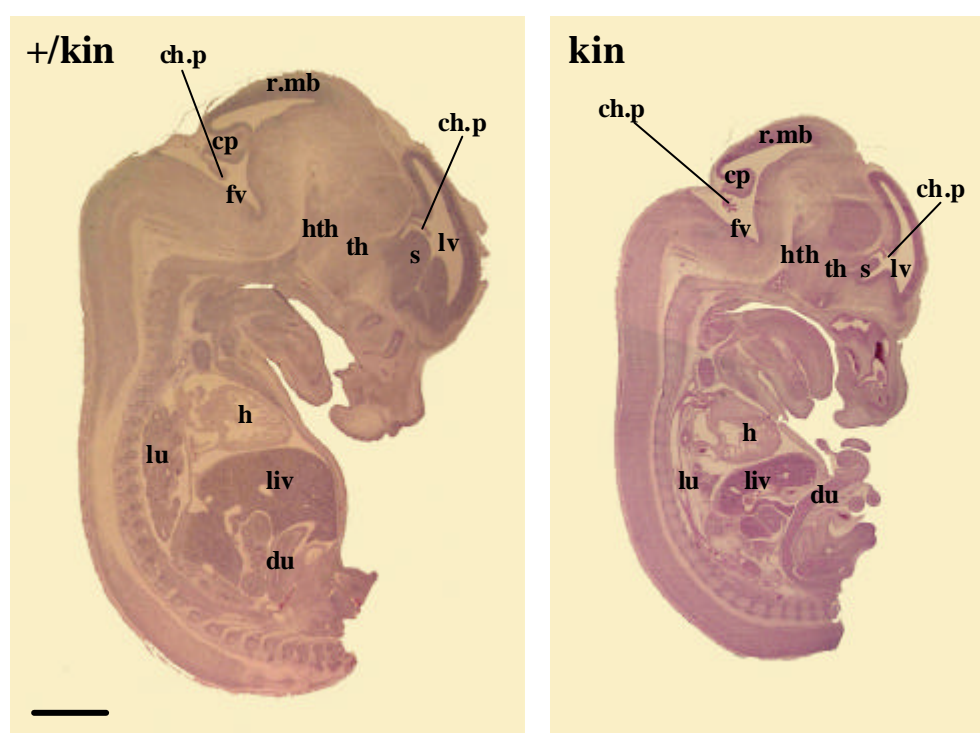


Fig. 2-9 A. The hematoxylin-eosin stained sagittal sections of E13.5d +/KIN and KIN embryos on (129Sv/B16/CD-1=37.5/37.5/25) background. The KIN embryo is smaller but does not display any visible defects in development. 2x magnification. Scale bar corresponds to 1 mm.

ch.p-choroid plexus, **cp**-cerebellar primordium, **du**-duodenum, **fv**-fourth ventricle, **h**-heart, **hth**-hypothalamus, **lv**-lateral ventricle, **liv**-liver, **lu**-lung, **mb**-midbrain, **r.mb**-roof of midbrain, **s**-striatum, **th**-thalamus.

The TUNEL (TdT – mediated dUTP nick end labeling) method was used to detect the level of apoptosis in different embryonic compartments. This method is based on the enzymatic

labeling of apoptosis induced DNA strand breakages by terminal deoxynucleotidyl transferase (TdT). The level of apoptosis was found to be higher in liver, lung, veins, striatum and SVZ of KIN embryo compared to heterozygous littermate. In many of these organs the clusters of apoptotic cells could be recognized, whilst in +/KIN tissues only single dispersed apoptotic cells are observed (Fig. 2-9 B). The structure of most tissues was more irregular and hypocellular in KIN fetus than in its heterozygous littermate. This can be caused by an elevated apoptotic process. In E13.5d KIN embryo the migration process from VZ to SVZ is also partially disturbed since much fewer cells in SVZ are polarized toward the migration direction compared to +/KIN (Fig. 2-9 B). These data indicate that at this embryonic stage of development high B-Raf kinase activity is required for its survival function.

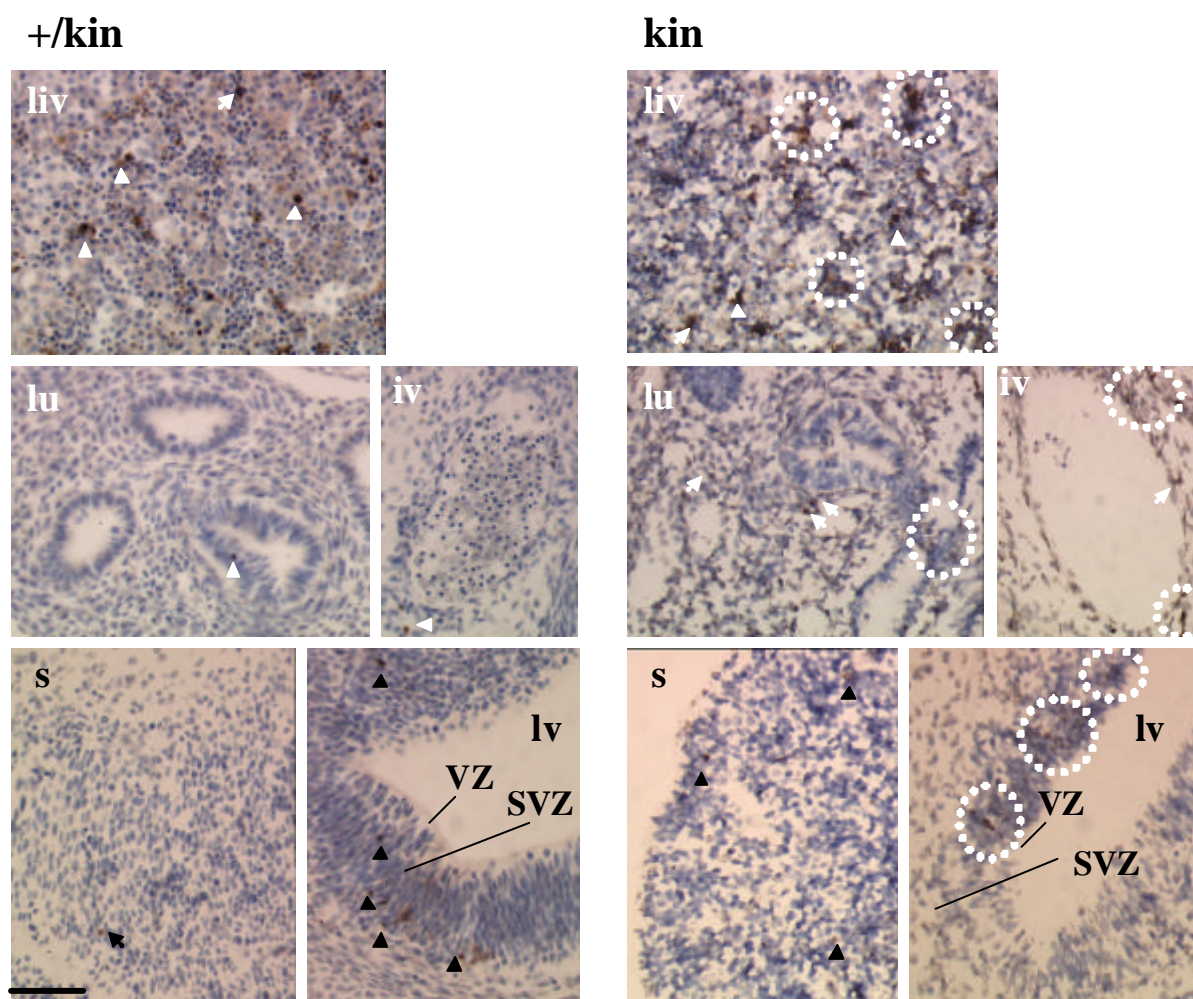
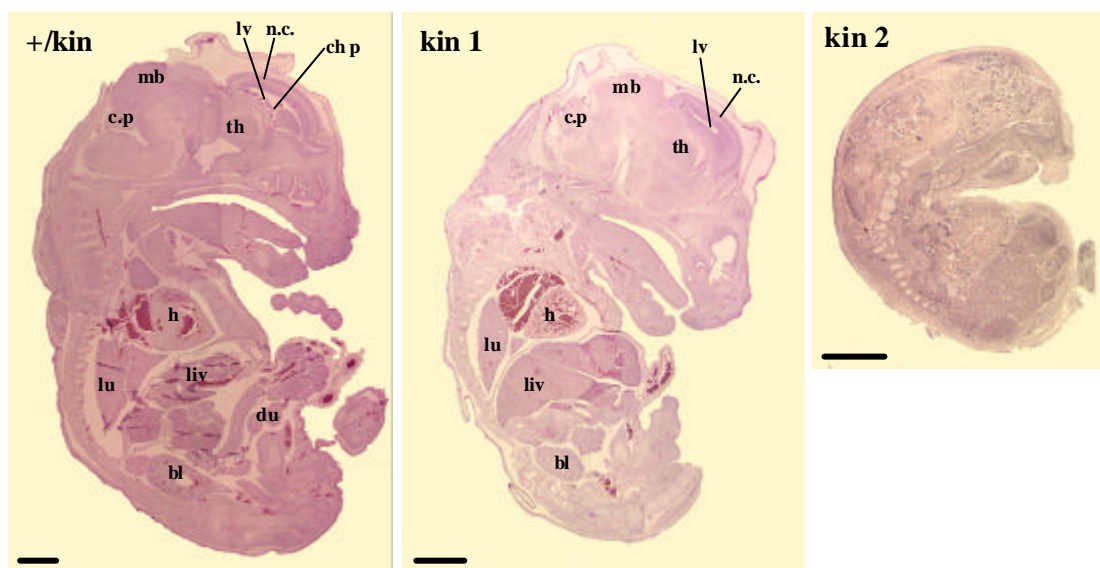


Fig. 2-9 B. The TUNNEL assay demonstrates more apoptotic cells in different tissues of E13.5d KIN embryo compared to +/KIN littermate, apoptotic cells are brown stained and indicated by arrows. Clusters of apoptotic cells are encircled. The structure of KIN tissues is more irregular and hypocellular. The SVZ in KIN fetus is thinner and migration process is affected. 40x magnification. Scale bar corresponds to 100 μ m. **liv**-liver, **lu**-lung, **iv**-iliac vein, **s**-striatum, **lv**-lateral ventricle, **VZ**-ventricular zone, **SVZ**-subventricular zone..

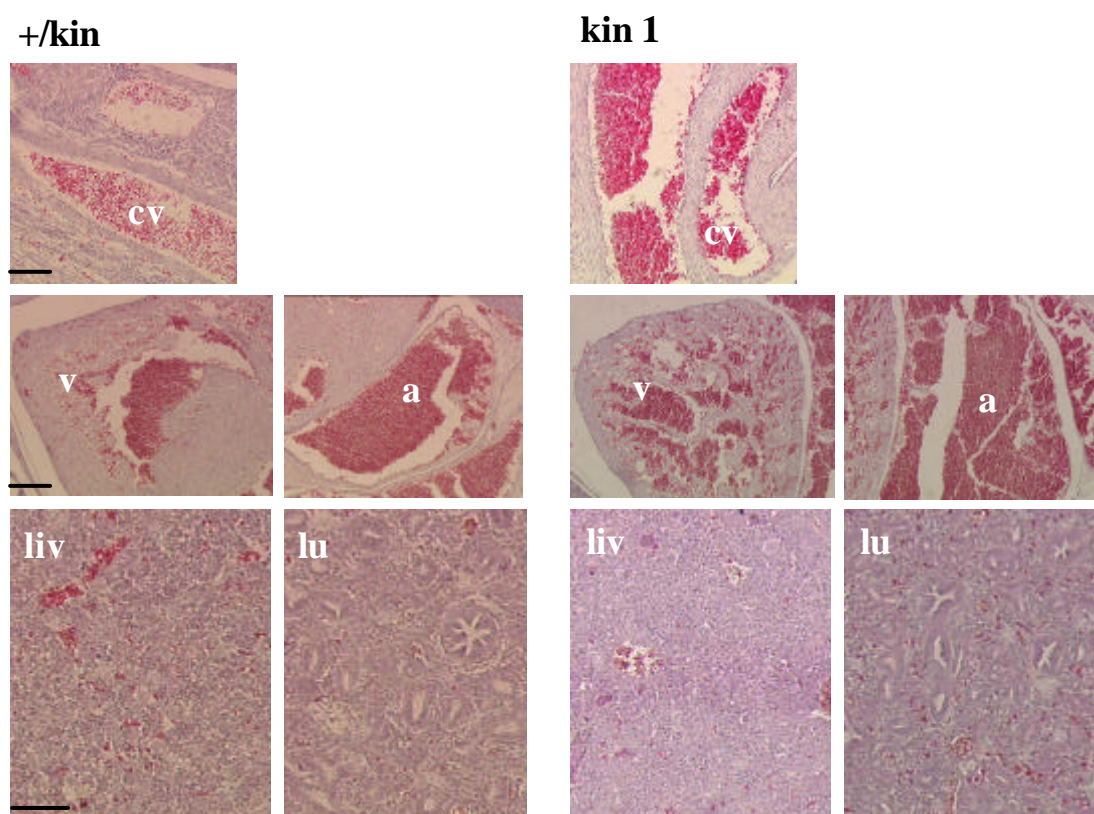
2-10. Histochemical and immunochemical comparison of E16.5d embryos.

At a later stage of development, one living KIN1 embryo was isolated on (129Sv/Bl6/CD-1=1/1/2) genetic background. It was also subjected to histochemical investigation by hematoxylin-eosin staining, in order to find the dissimilarity with its heterozygous littermate (Fig. 2-10 A, B, C).

A



B



C

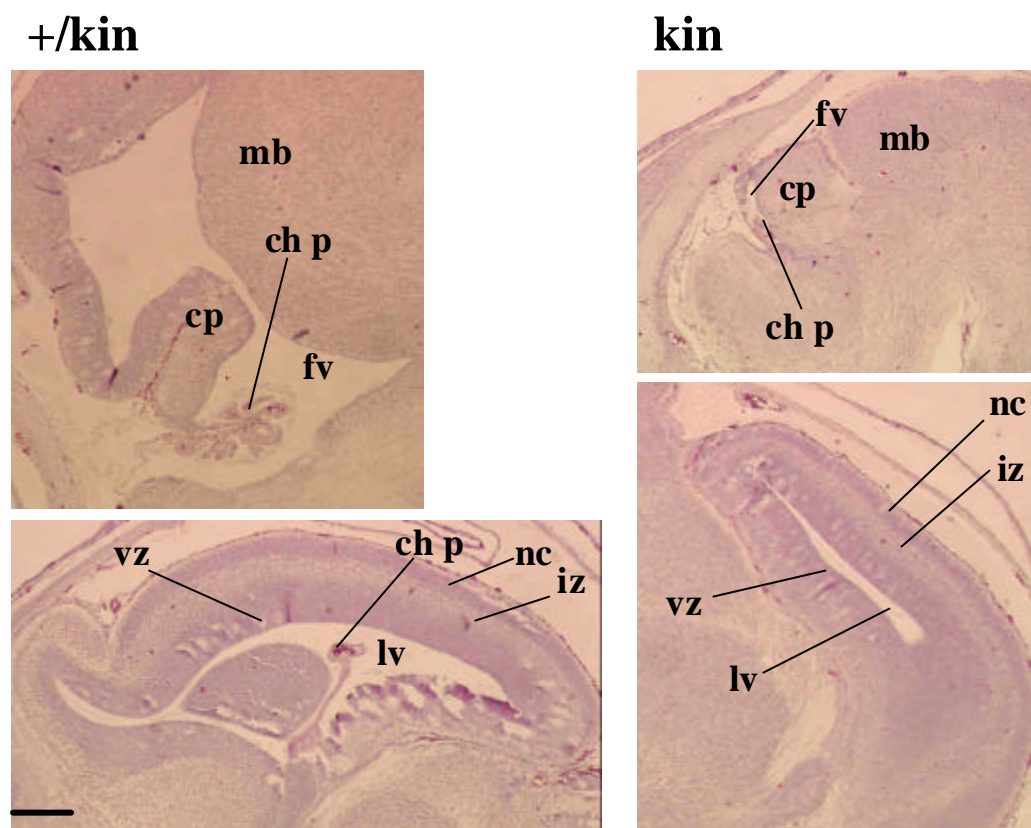


Fig. 2-10 A. The hematoxylin-eosin stained sagittal sections of E16.5d +/KIN, alive KIN1 and dead KIN2 embryos on (129Sv/B16/CD-1=1/1/2) background. The alive KIN embryo is smaller by size without any obvious developmental abnormalities, 2x magnification. Scale bars correspond to 1mm. **B.** Tissues of heterozygous and KIN1 embryos. Note the enlarged atrium and loose ventricle structure in KIN1 heart. **cv** - 20x, scale bar corresponds to 50 μ m; **v, a, liv, lu** - 10x magnification. In **v, a** scale bar corresponds to 200 μ m, in **liv, lu** to 50 μ m. **C.** Different regions of hind- and forebrain. All corresponding structures are present in KIN1 embryonic brain, 4x magnification. Scale bar corresponds to 250 μ m.

a-atrium of heart, **b**bladder, **ch p**choroid plexus, **cp**-cerebellar primordium, **cv**-caudal vein, **du**-duodenum, **fv**-fourth ventricle, **h**-heart, **iz**-intermediate zone, **lv**-lateral ventricle, **liv**-liver, **lu**-lung, **mb**-midbrain, **nc**-neopallial cortex, **th**-thalamus, **v**-ventricle of heart, **vz**-ventricular zone.

Again, like in previous findings in all alive embryos after E12.5d, no visible diversity between +/KIN and KIN embryos was found at this stage. In KIN fetus all organs were properly formed and all corresponding structures in brain were found (Fig. 2-10 A, B, C).

The only difference that was observed, was found in loose structure of the heart ventricle and enlarged atrium in KIN embryo. The other KIN tissues at this stage showed the normal cellularity in contrast to E13.5d (Fig. 2-9 B). In the hindbrain region, the cerebellar primordium and choroid plexus were present in KIN1 embryo. In the forebrain, the neopallial cortex (future cerebral cortex), intermediate zone and ventricular zone layers were well formed and had the same thickness in KIN1 and +/KIN embryos (Fig. 2-10 C).

The dead KIN2 embryo demonstrated no visible structures and was used as a positive control for TUNEL assay (Fig. 2-10 A, D).

The level of apoptosis detected by TUNEL was comparable in KIN and +/KIN embryos in most of tested tissues (Fig. 2-10 D). In contrast to E13.5d, at E16.5d in KIN1 embryo, no visible elevation of programmed cell death (PCD) was observed in various brain compartments (data not shown).

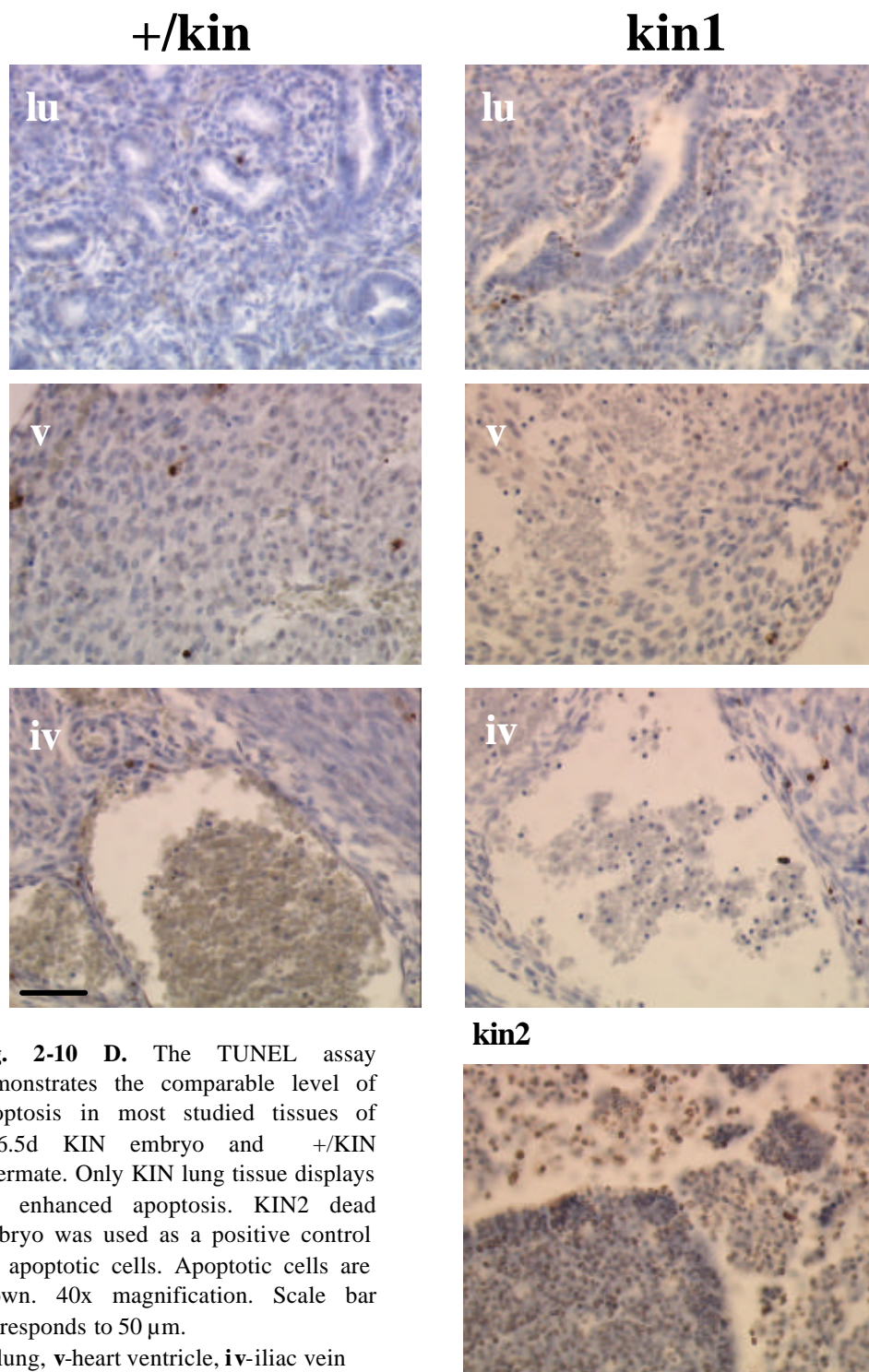


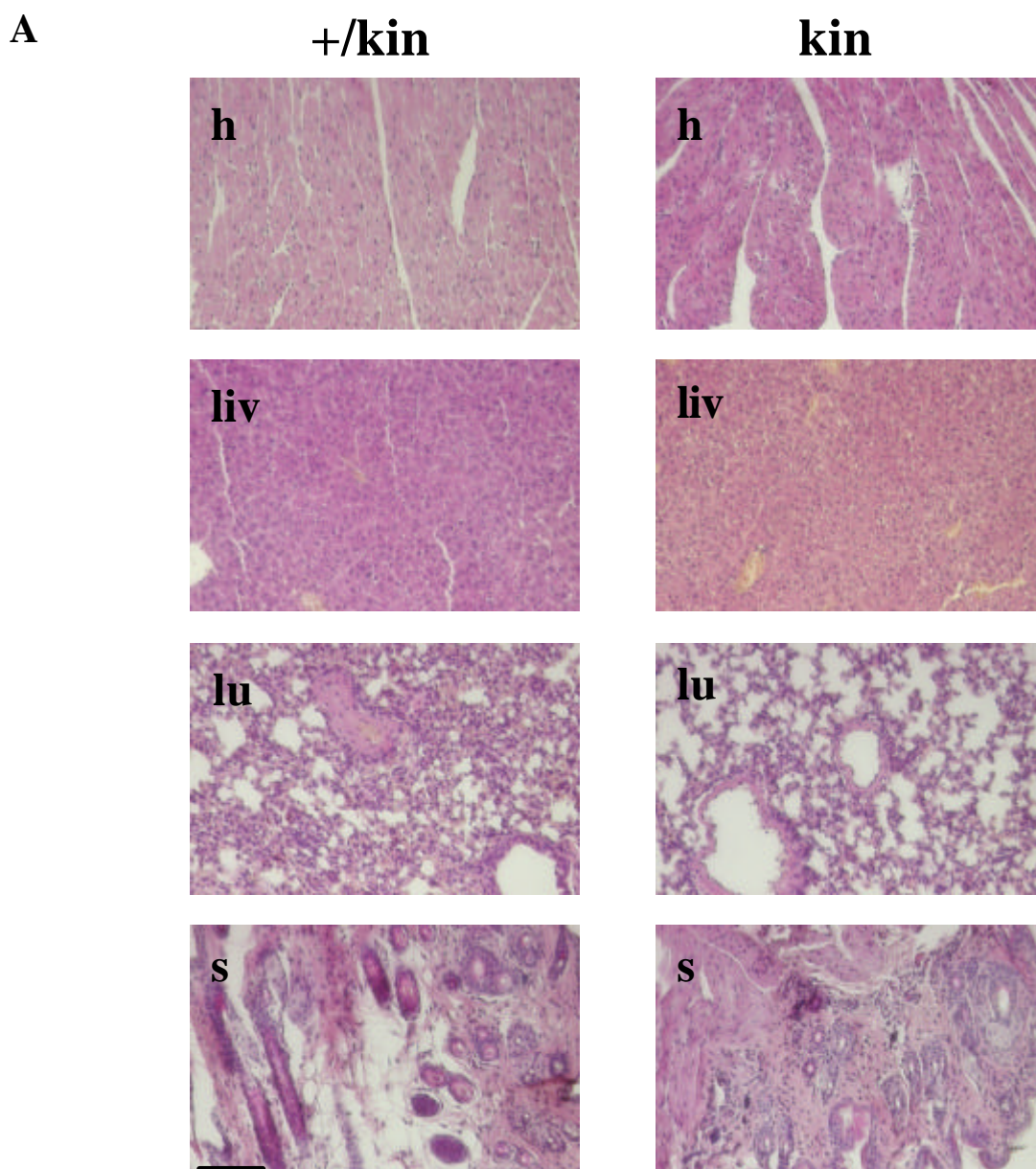
Fig. 2-10 D. The TUNEL assay demonstrates the comparable level of apoptosis in most studied tissues of E16.5d KIN embryo and +/KIN littermate. Only KIN lung tissue displays the enhanced apoptosis. KIN2 dead embryo was used as a positive control for apoptotic cells. Apoptotic cells are brown. 40x magnification. Scale bar corresponds to 50 μ m.

lu-lung, **v**-heart ventricle, **iv**-iliac vein

Increased apoptotic activity was found only in the KIN1 lung. When quantified, the number of apoptotic cells was $16/\text{mm}^2$ and $34/\text{mm}^2$ for heterozygous and KIN1 lung respectively. Despite the loose heart ventricle structure in KIN1, no increase of apoptosis level was detected in this tissue. The iliac vein in KIN1 fetus was enlarged but the level of PCD was the same as in heterozygous littermate (Fig. 2-10 D). All these data suggest that at E16.5d the strong kinase activity of B-Raf is not as necessary for cell survival as it is at the earlier stages of development.

2-11. Comparison of adult p20 mouse tissues.

The hematoxylin-eosin staining of the major organs and tissues from +/KIN and KIN p20 mice did not reveal any significant distinction in morphology between the two genotypes.



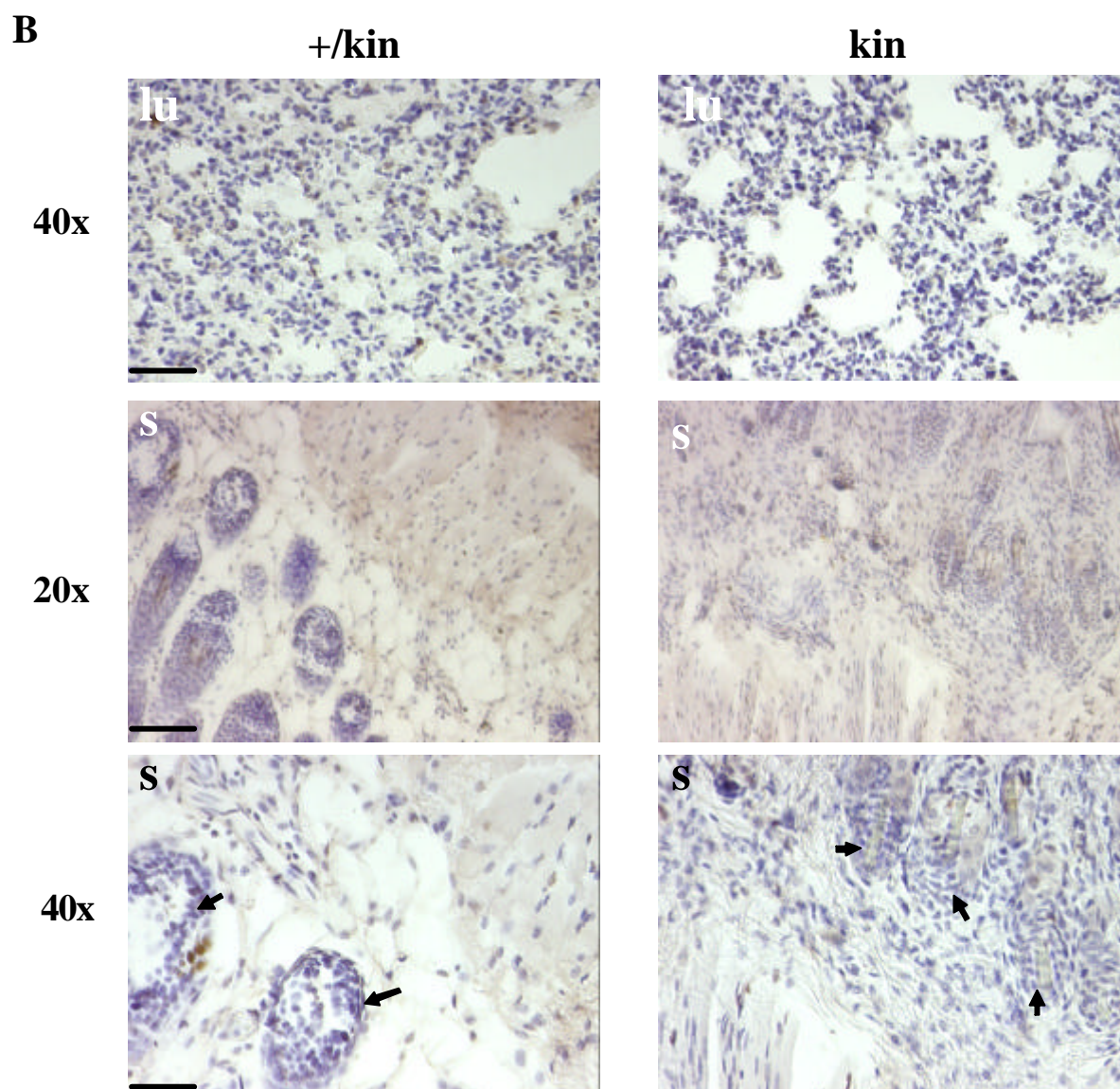


Fig. 2-11 A. The hematoxylin-eosin staining of different tissues, p20 adult +/KIN and KIN mice on 129Sv/B16 background. In KIN lung hypocellularity and larger alveoli are observed. In KIN skin the hair follicles are reduced in size. 20x magnification. Scale bar corresponds to 100 μ m. **B.** TUNEL assay demonstrates no visible increase of apoptosis in KIN tissues. Arrows indicate hair follicles. 20x and 40x magnifications are indicated. Scale bars correspond to 100 μ m at 20x and to 50 μ m at 40x magnification.

h-heart ventricle, **liv**-liver, **lu**-lung, **s**-skin

The KIN lung structure displayed larger and less numerous alveoli and reduced pneumocyte number than in +/KIN littermate. This phenomenon is possibly related with increased lung apoptosis found at the late embryonic days in KIN fetus. Also, skin hair follicles were reduced in size in KIN (Fig. 2-11 A). To study the apoptotic process in adult tissues the TUNEL assay was performed. The level of apoptosis in all tested heterozygous and KIN tissues was comparable and was not elevated in lung and skin of KIN animal (Fig. 2-11 B)

2-12. Characterization of neurogenesis in p20 adult +/-KIN and KIN mouse brains using cell lineage specific markers.

Previous results (chapters 2-8, 2-9) demonstrate the role of B-Raf kinase in proliferation and survival of NSCs or neural progenitor cells (NPCs) at the mid-gestational time window. At the E16.5d no difference in survival was observed in different brain compartments of KIN and heterozygous embryos. To study the adult neurogenesis in the viable KIN p20 adult mouse (Fig. 2-7 A) the immunohistochemistry using different neuronal markers (Table 2-12) was used. In all experiments the heterozygous littermate was used as a positive control.

Markers	Lineage cell label
TuJ-1 (anti- β -tubulin isotype III)	Neuronal precursor, neurites
GFAP (anti-glial fibrillary acidic protein)	Astrocytes
Neu N	Mature neurons

Table 2-12. Different markers of neurogenesis used in experiment.

Neurogenesis occurs in discrete regions of the adult mouse brain including the rostral subventricular zone (SVZ) of the lateral ventricles [211] and the subgranular zone (SGZ) of the dentate gyrus (DG) in hippocampus [185]. Delayed neurogenesis is also known to occur in a transient cell layer (external granular layer (EGL)) of the assembling cerebellar cortex, where postmitotic cells generate the granule cells for the internal granular layer [212].

The present study of neurogenesis is mostly concentrated on hippocampal SGZ and surrounding regions: CA1-3, fimbria fornix and SVZ. The hematoxylin-eosin staining did not reveal a significant difference in structure, thickness of granular (GCL), subgranular (SGZ) and molecular (ML) cell layers and in overall cell number in +/-KIN and KIN hippocampus (Fig. 2-12 A).

The immunohistochemistry using α -TuJ-1 antibodies (Table 2-12) detected more neuronal precursor cells in SGZ and neurofilaments of pyramidal neurons in the Hilus region (H) and in CA1-3 regions of the hippocampus in the +/-KIN mouse (Fig. 2-12 B). In other brain compartments: olfactory bulb (OB), cerebellum and SVZ no dissimilarity between KIN and +/-KIN was observed (data not shown). To find the possible link between the more abundant NPC fraction in +/-KIN SGZ and increased cell proliferation, the immunohistochemical analysis using α -PCNA antibodies was applied. No elevation in S-phase cell number was found in

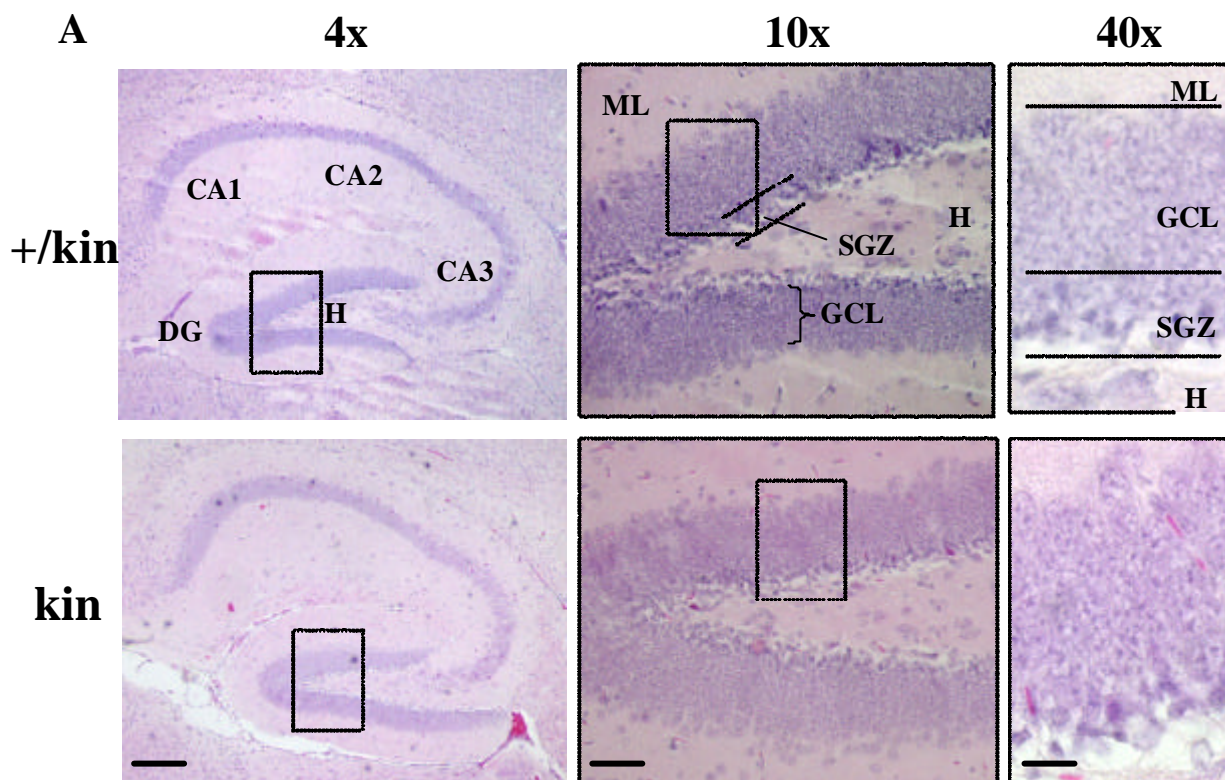


Fig. 2-12 A. Hematoxylin-eosin staining of hippocampus region in KIN and +/KIN p20 adult mice on 129Sv/B16 background. All corresponding structures are present in KIN hippocampus. No difference in thickness of SGZ, GCL and ML in KIN and heterozygous littermate is detected. The different magnifications 4x, 10x and 40x are indicated. Scale bars correspond to 100 μ m at 4x, to 40 μ m at 10x, to 10 μ m at 40x. **DG**-dentate gyrus, **H**-Hilus region, **CA1-3**-cornu ammonis regions 1-3, **ML**-molecular layer, **SGZ**-subgranular zone, **GCL**-granular cell layer.

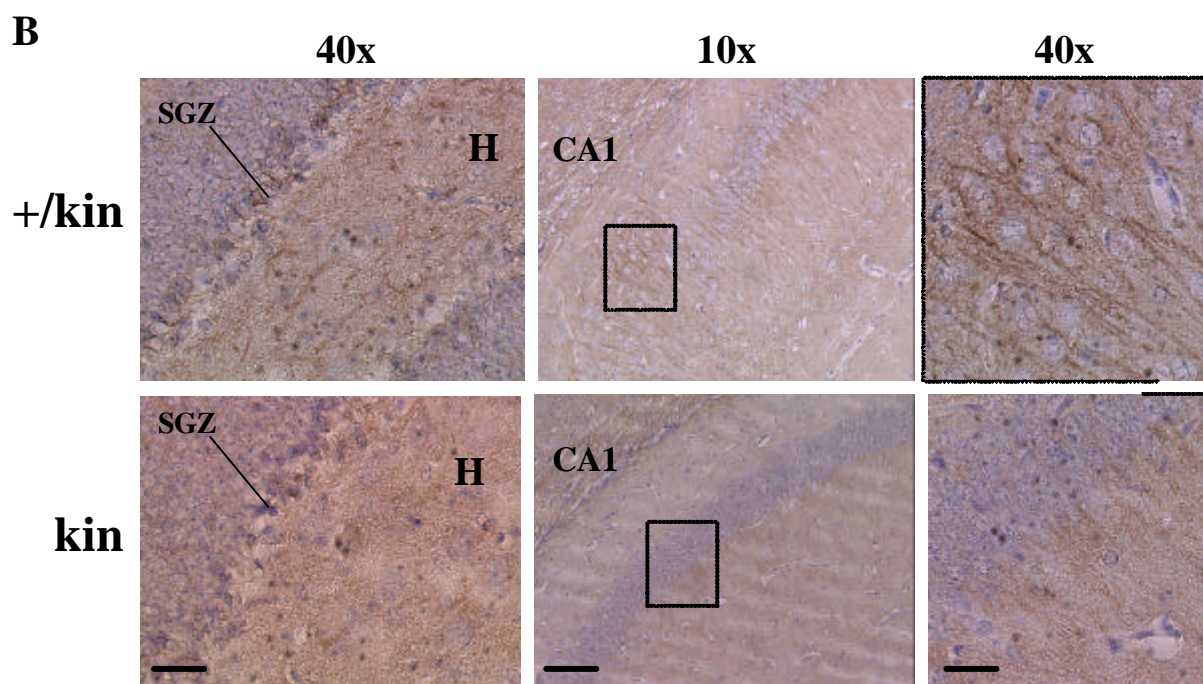


Fig. 2-12 B. Immunohistchemistry of hippocampus regions in KIN and +/KIN p20 adult mice using a-TuJ-1 antibodies. More TuJ-1 positive cells are observed in SGZ, and more neurofilaments of pyramidal neurons are detected in Hilus region of DG, and in CA1-3 hippocampal regions of +/KIN. 10x and 40x magnification indicated. Scale bars correspond to 40 μ m at 10x, to 10 μ m at 40x. **H**-Hilus region, **CA1**-cornu ammonis region 1, **SGZ**-subgranular zone.

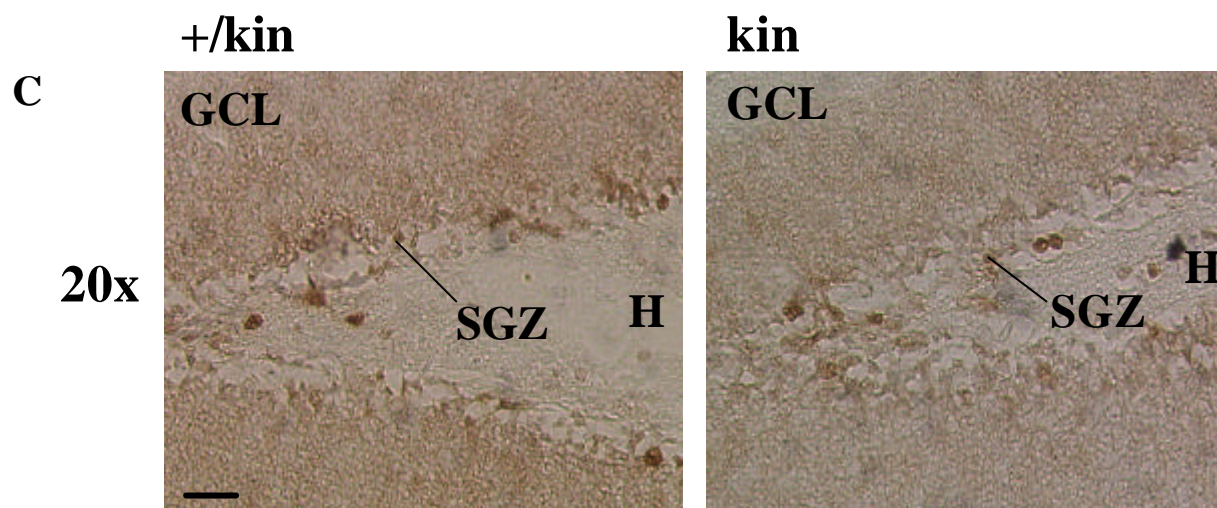


Fig 2-12 C. Dentate gyrus of hippocampus, α -PCNA immunohistochemistry reveals no difference in SGZ proliferating cells between KIN and +/KIN genotypes. PCNA positive cells are brown. 20x magnification. Scale bar corresponds to 20 μ m. **GCL**-granular cell layer, **H**-Hilus region, **SGZ**-subgranular zone.

SGZ and Hilus region in heterozygous mouse (Fig. 2-12 C). These findings suggest the requirement of B-Raf to sustain at least some NSC/NPC populations in hippocampus and this maintenance is not associated with its role in proliferation.

To study the process of neuronal differentiation, the α -NeuN antibodies were applied (Table 2-12). The intensity of staining which marks mature postmitotic neurons did not significantly differ between +/KIN and KIN animals in hippocampus, however at higher magnification the density of neurons in KIN GCL seems to be lower (Fig. 2-12 D). To

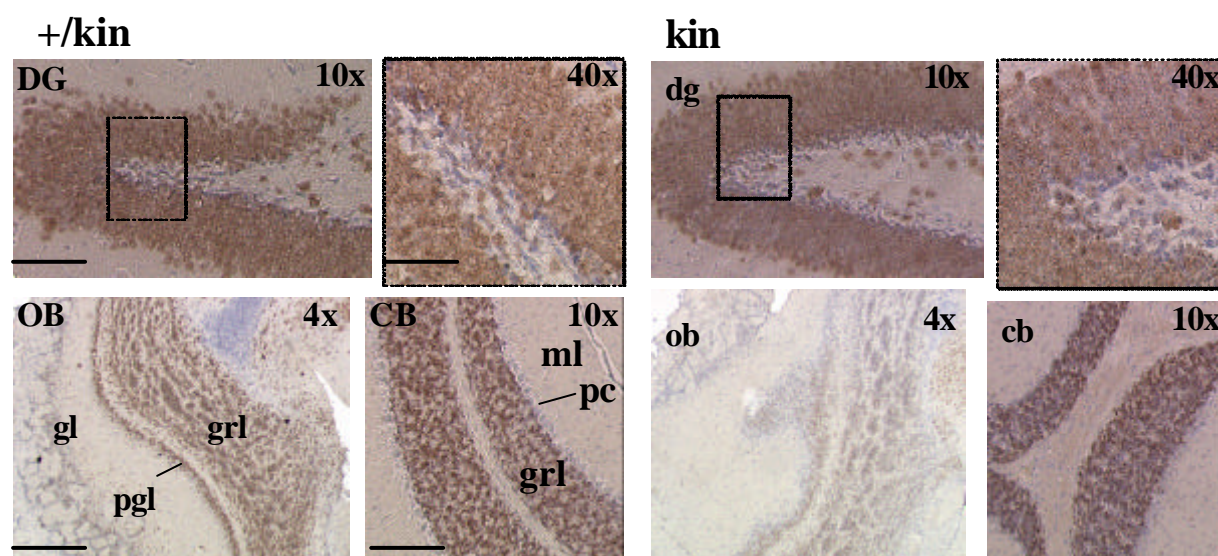


Fig. 2-12 D. Immunohistochemistry of DG, cerebellum and OB in KIN and +/KIN p20 adult mice using α -NeuN antibodies. At higher 40x magnification it is possible to distinguish the higher density of NeuN-positive cells in SGZ of +/KIN animal. In granular (**grl**) and periglomerular (**pgl**) cell layers of OB in KIN animal there is a significant reduction in neurons. No distinction is seen in cerebellum. Magnifications 10x, 20x and 40x are indicated. In **DG** scale bars correspond to 100 μ m at 10x, to 50 μ m at 40x; in **OB** to 200 μ m; in **CB** to 75 μ m. **DG**-dentate gyrus, **OB**-olfactory bulb, **CB**-cerebellum, **gl**, **pgl**, **grl**, **ml**-glomerular, periglomerular, granular, molecular cell layers, **pc**-purkinje cells

examine this further quantification analysis is required. The most obvious difference was found in granular cell layer (GRL) of olfactory bulbs (OB). In heterozygous OB a much greater number of NeuN positive cells in GRL was found compared to KIN. In cerebellum no significant diversity was found (Fig. 2-12 D).

The NPCs of SVZ migrate to the OB via rostromigratory stream (RMS), where they differentiate into the interneurons of the OB: granule cells and periglomerular cells [213]. The above results raise the question whether the migration process via RMS in hypomorphic/isomorphic B-Raf mutant is disturbed, or differentiation into interneurons is ablated, or maybe both processes are affected. Since migration of neuronal cells is guided by glia [177], the gliosis process in +/KIN and KIN brains was examined using GFAP marker (Table 2-12). The immunohistochemical analysis did not reveal a reduced number of GFAP-positive cell number in RMS of KIN brain (data not shown) suggesting rather a role for B-Raf in differentiation. An increased number of GFAP expressing cells was also found in +/KIN SGZ of dentate gyrus compared to KIN (Fig. 2-12 E).

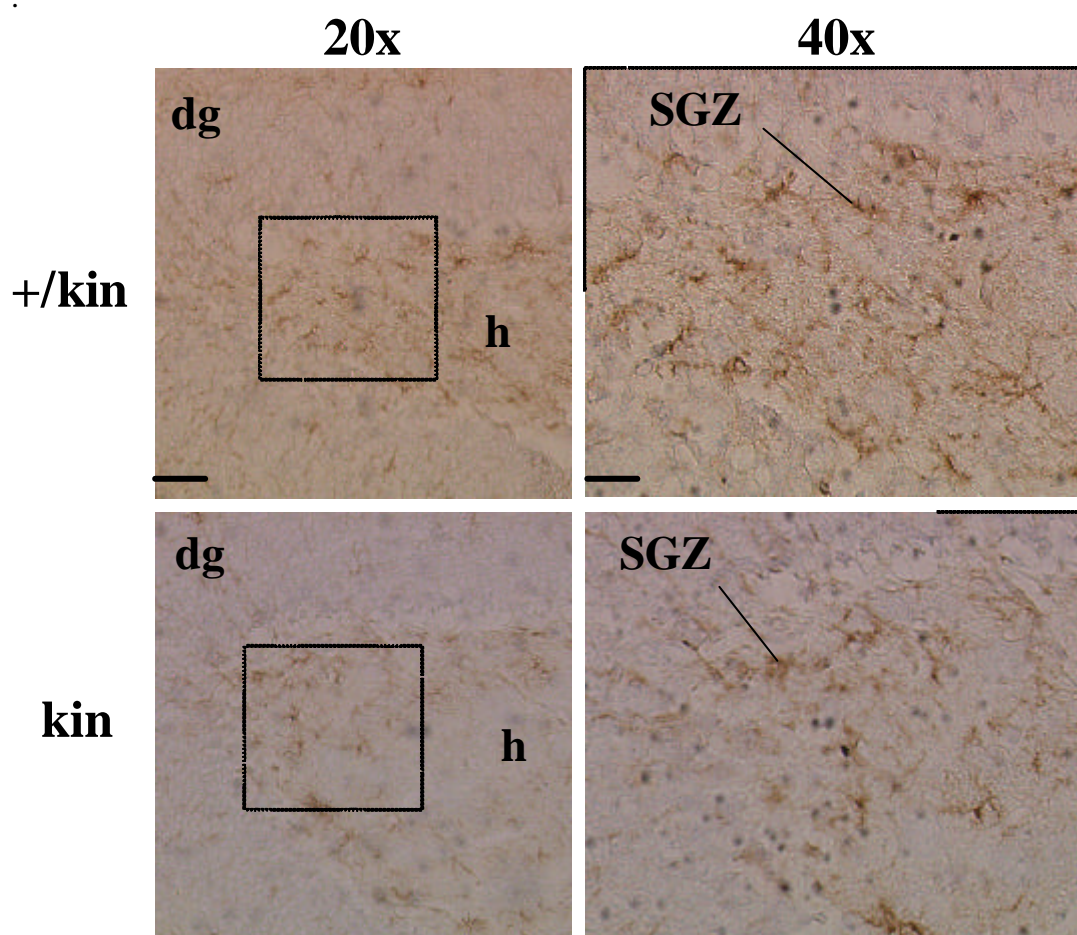


Fig. 2-12 E a-GFAP immunohistochemistry shows the higher number of GFAP-positive cells in **SGZ** and Hilus of **DG** in heterozygous mouse compared to KIN. Magnifications 20x and 40x are indicated. Scale bars correspond to 30 μ m at 10x, 15 μ m at 40x.

DG-dentate gyrus, **H**-Hilus region, **SGZ**-subgranular zone.

2-13. Establishment of primary mouse embryonic fibroblasts (MEF) culture and characterization of proliferative capacity.

To understand the mechanisms and the role of B-Raf in cell proliferation and survival a culture of primary mouse embryonic fibroblasts (MEFs) were established from embryos of different genotypes at E10.5d-11.5d. After embryo body trypsinization and dissociation, the single cells were plated in culture, and after 2-3 passages they were used for experiments. B-Raf null MEFs on 129sV/C57Bl6 and 129sV/CD-1 genetic backgrounds did not proliferate in culture and only a few cells attached to the plate displaying a senescent phenotype: flat and spread shape. Hence, no experiments with primary KO MEFs could be performed. In contrast, KIN MEFs when established, were proliferating well and reached confluence 2-3 days after plating. To compare the proliferative ability in culture of KIN, +/KIN and WT MEFs, the MTT assay was performed. The yellow tetrazolium MTT (3-(4,5-dimethylthiazolyl-2)-2, 5-diphenyltetrazolium bromide) is oxidized by metabolically active cells, in part by action of dehydrogenase enzymes, to generate reducing equivalents such as NADH and NADPH. The resulting intracellular purple formazan can be solubilized and quantified by spectrophotometric means. After four days in culture KIN cells proliferated very slowly whereas +/KIN and WT MEFs displayed exponential growth until day 5 and 6 respectively. After six days in culture cell number in all three genotypes dramatically reduced corresponding to the limited number of cell divisions and G1 arrest commonly known for primary, non immortalized cell cultures (Fig. 2-13 A).

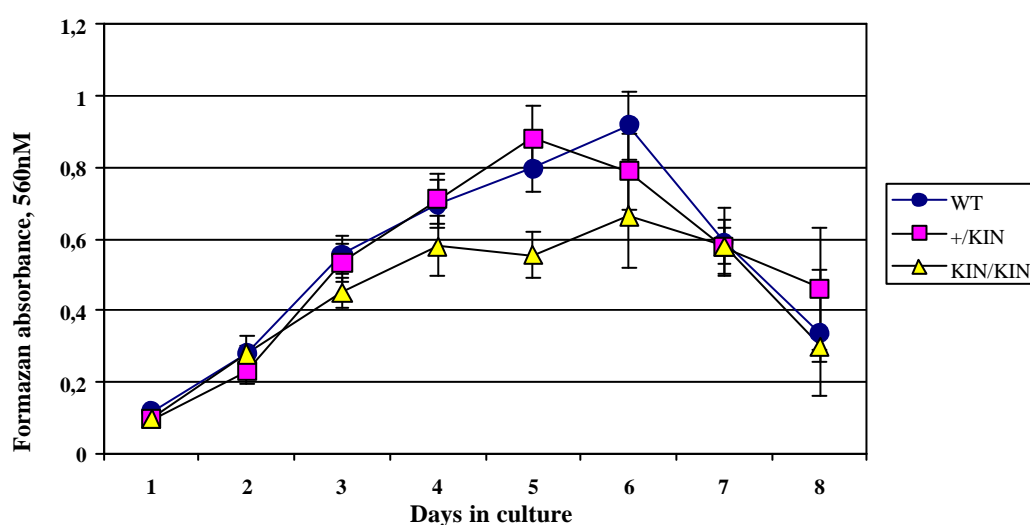
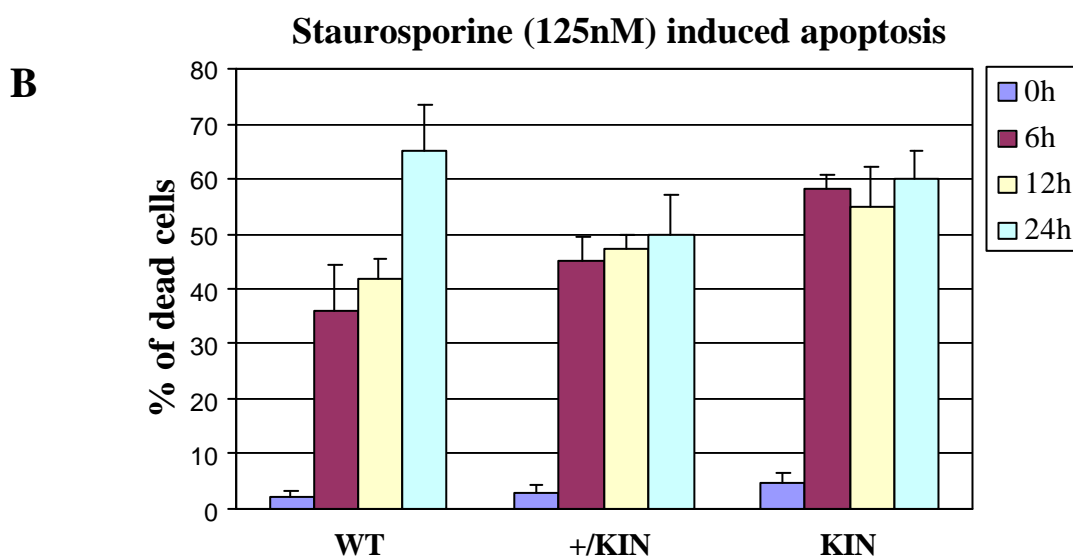
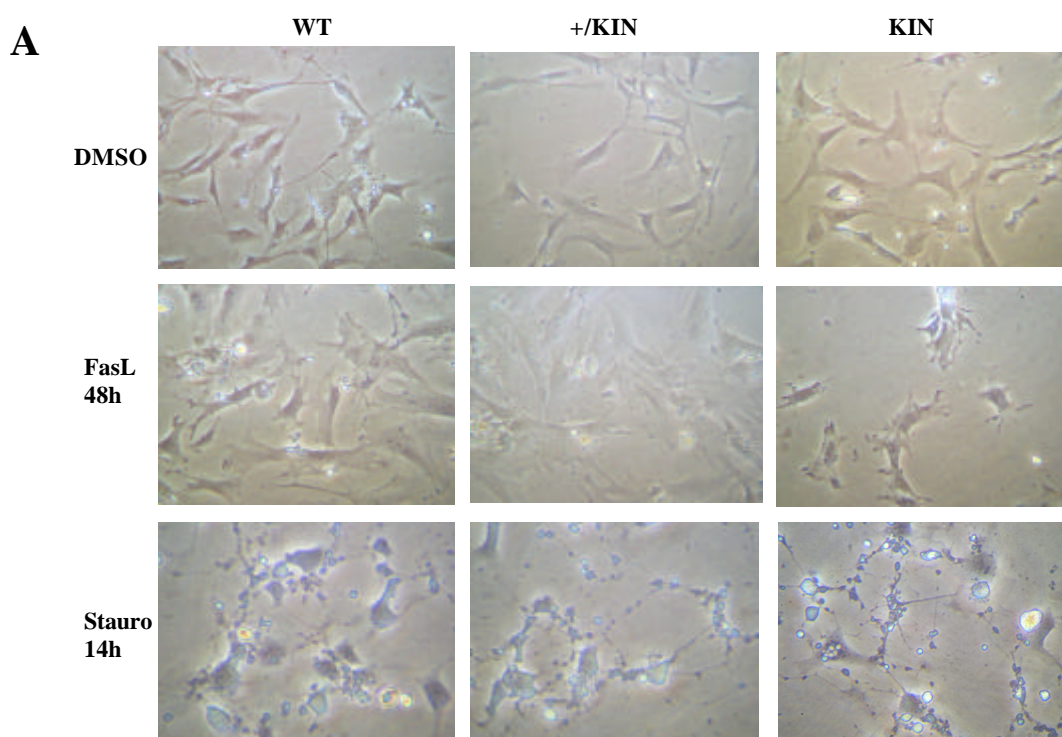


Fig. 2-13 A. MTT proliferation assay demonstrates the reduced proliferation of KIN MEFs. Fibroblasts were derived from E11.5d embryos and cultured for three passages. Initially 5000 cells/well of 96 well plate were plated in triplicates for each genotype and number of viable cells was measured every day during eight days by formazan spectrophotometric quantification at 560nm. Bars indicate standard deviation.

2-14. Different survival of MEFs after induction of apoptosis.

To study the protective antiapoptotic role of B-Raf, apoptosis induction experiments were performed with primary KIN, +/KIN and WT MEFs. Apoptosis was induced either by the broad specific kinase inhibitor staurosporine leading to mitochondrial type of apoptosis, or Fas ligand (FasL) acting through Fas receptor, adaptor protein FADD and caspases 8,10 [214]. Staurosporine evoked the apoptotic process very fast, already during the first hours after application. After 6 hours 35% of WT, 45% of +/KIN and 58% of KIN cells were dead. After 24 hours no significant difference in cell death between three genotypes was observed accounting 50-60% (Fig 2-14 A, B).



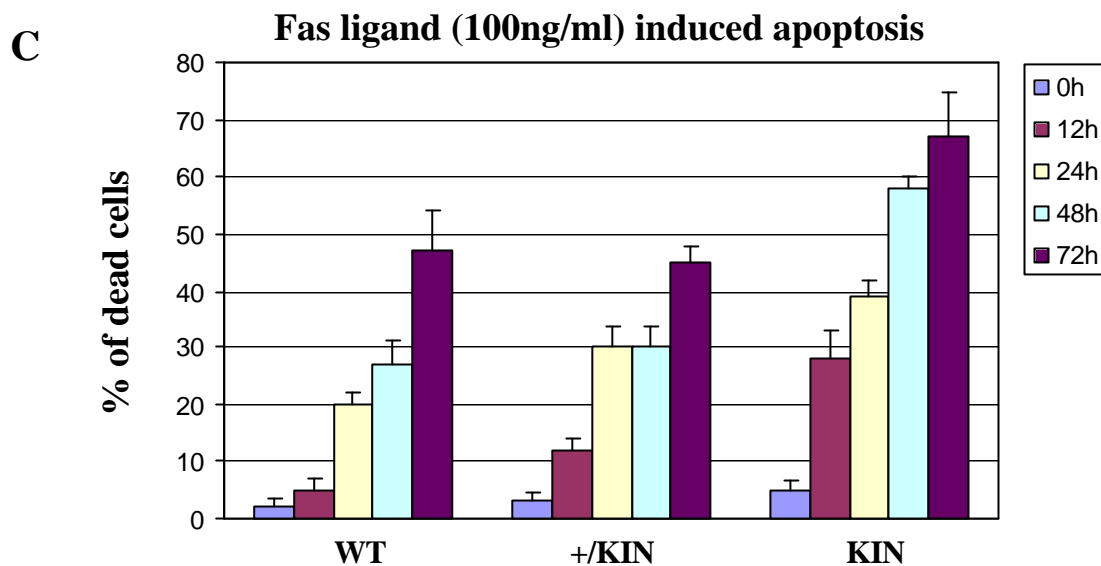


Fig. 2-14 A. MEF phenotypes observed after FasL (100ng/ml) and staurosporine (125nM) induced apoptosis. No difference was found before induction (see DMSO). After 48h of FasL administration the reduced number and less adherent phenotype in KIN MEFs was detected. Typical apoptotic cells are shown after 14h of staurosporine application, no significant difference in WT, +/KIN and KIN MEF phenotypes. **B.** Quantification of staurosporine (125nM) induced apoptosis in MEFs of different genotypes. **C.** Quantification of FasL (100ng/ml) induced apoptosis in MEFs of different genotypes. After induction the cells were collected at different time points and stained with trypan blue. 200 cells/point in duplicates were counted and % of blue cells was referred as % of apoptotic cells. Bars indicate standard deviation.

A significant difference in resistance to FasL induced apoptosis was demonstrated amongst the various MEFs. 12 hours after FasL administration two fold more dead cells in KIN than in +/KIN and seven fold more than in WT were detected. After 48 hours this difference consisted two fold more apoptotic cells in KIN than in +/KIN and WT. Even after three days the difference was 20% (Fig. 2-14 C). The reduced number and apoptotic phenotype of KIN cells after 48h of FasL application compared to WT and +/KIN is clearly seen on Fig. 2-14 A.

2-15. The kinetic of ERK activation is delayed in KIN fibroblasts.

To understand the mechanisms involved in poor proliferation and less resistance to apoptosis of KIN MEFs the integrity of Raf-MEK-ERK survival and proliferative pathway in KIN fibroblasts was examined. As a positive control WT cells were used. The cells were starved in low 0.5% serum medium for 18 hours and then stimulated with 10% serum. The ERK activation at different time periods was detected by phospho-specific α -pERK1/2 (pThr202/204) antibodies (Fig 2-15 A). The quantification of pERK1/2 level demonstrates the reduced ERK phosphorylation in non starved proliferating cells (nt). ERK activation by serum is delayed in KIN fibroblasts and at 30 min is already significantly reduced compared to WT. The activation of B-Raf and chimeric A-Raf as upstream effectors of ERK was measured by Western blot using antibodies against pSer621 of c-Raf-1 cross-reacting with homologous

epitopes of B-Raf (pSer 728) and A-Raf (pSer 582). In contrast to B-Raf, no up-regulation of chimeric A-Raf upon serum stimulation was observed (Fig 2-15 A). These findings confirm the important role of B-Raf in ERK activation. The weak kinase activity of chimeric A-Raf is insufficient to support normal level of phosphorylated ERK in cells and the proper response to the growth factors.

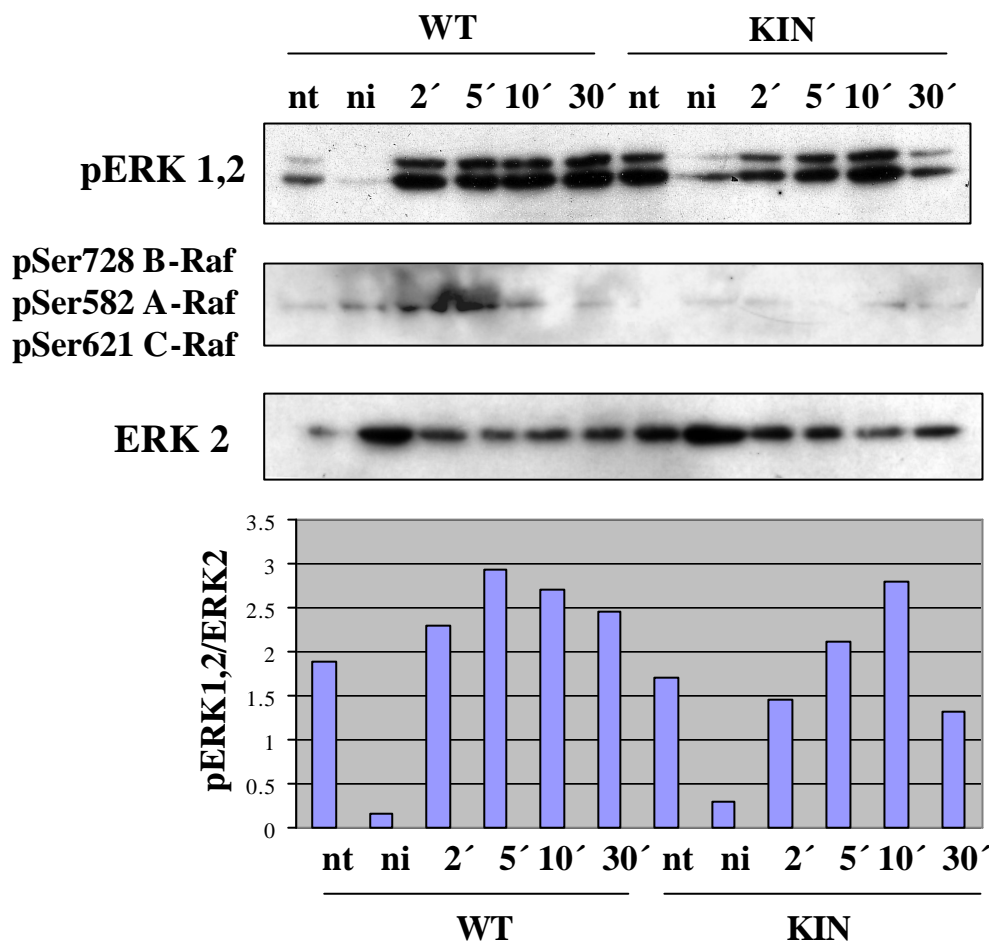


Fig. 2-15 A. Western blot using a-pERK1/2 (pThr202/204) antibodies demonstrates the reduced phospho-ERK in non treated (nt) proliferating KIN cells and delayed kinetic of ERK activation by serum after starvation in KIN fibroblasts. Passage 3 MEFs were grown in 10% FCS medium until 80% of confluence. After 18h starvation in 0.5% serum (ni) they were stimulated by 10% serum and collected at different time points: 2, 5, 10 and 30 min. The pERK level was calculated as a ratio between pERK1,2 and total ERK2 (detected by a-ERK2 antibodies) measured by densitometry. C4B monoclonal house antibodies were used to detect both pB-Raf (pSer728) and pA-Raf (pSer582). Chimeric A-Raf has the same size at 84kD as B-Raf in MEFs. The total B-Raf in MEFs is not detected by a-B-Raf antibodies, probably because of their lower sensitivity compared to C4B. a-HA tag antibodies detect chimeric A-Raf in KIN MEFs at the same position as C4B (data not shown).

2-16. Akt pathway is disturbed in KIN MEFs.

Akt (PKB) plays a critical role in controlling the balance between survival and apoptosis [202]. It is activated by insulin and many other growth and survival factors. For activation Akt is recruited to the plasma membrane through interaction with PIP3 (phosphatidylinositol

(3,4,5) trisphosphate) and phosphorylated at Thr308 and Ser473 by PDK1 [203]. When activated, Akt promotes cell survival by inhibitory phosphorylation of Bad, Forkhead transcription factor, GSK3 and caspase-9. In proliferating KIN MEFs the level of pAkt was reduced, assessed by Western blot using phospho-specific a-pAkt (pSer473) antibodies. In serum induction experiments the phosphorylation of Akt was significantly delayed and moderate in KIN cells compared to WT (Fig. 2-16 A). The level of inactive pBAD (pSer136), a target of active Akt, as well as B-Raf [207], was dramatically reduced in non treated proliferating KIN cells. After serum stimulation, BAD phosphorylation in KIN fibroblasts was not persistent – it was highly reduced at 10 min and was not detected at 30 min in contrast to WT (Fig. 2-16 A).

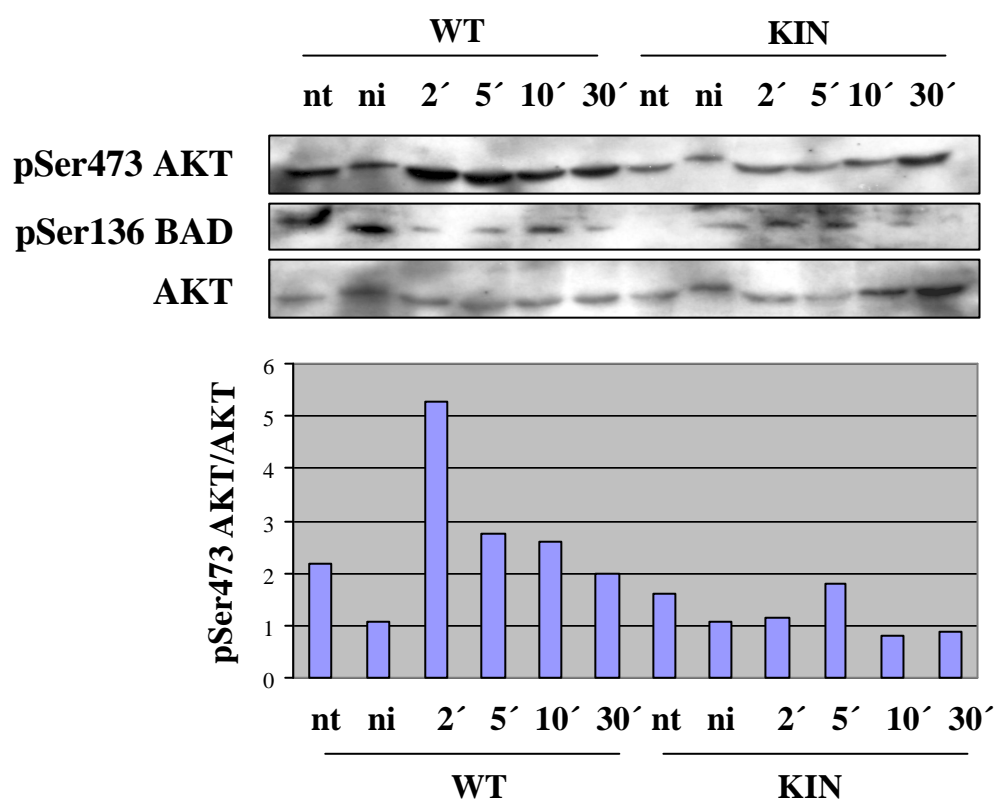


Fig. 2-16 A. Western blot using a-pAkt (pSer473) antibodies demonstrates the reduced phospho-Akt fraction in not treated (**nt**) proliferating KIN MEFs. The moderate activation of Akt by serum after starvation in KIN fibroblasts compared to WT is shown. Phospho-BAD was detected by a-pBAD (pSer136) antibodies. In KIN pBAD is not detected in **nt** cells and persists for shorter time after stimulation. The total Akt was detected by a-Akt antibodies. The cells were grown and activated as described in Fig. 2-15 A.

2-17. Chimeric A-Raf possesses moderate kinase activity compared to B-Raf.

In order to compare kinase activity of endogenous B-Raf and chimeric A-Raf, the *in vitro* coupled kinase assay was performed. Both proteins were immunoprecipitated from 10 min

serum stimulated heterozygous MEFs using α -B-Raf and α -HA tag antibodies respectively. The *in vitro* kinase reaction was done using ATP, immunoprecipitated proteins, recombinant MEK1 and ERK2. The level of ERK phosphorylation was measured by Western blot using α -pERK1/2 (pThr202/204) antibodies. As a positive control the recombinant constitutively active c-Raf-1 mutant was used. With comparable levels of precipitated endogenous chimeric A-Raf and B-Raf, chimeric A-Raf was barely able to phosphorylate ERK, in contrast to B-Raf (Fig. 2-17 A). These data confirm all previous observations that moderate biochemical activity of B-Raf isomorph/hypomorph allele (KIN) could rescue embryos from severe defects in mid-gestation, but is not sufficient to prevent poor cell proliferation and apoptosis in different cell lineages at different stages of development.

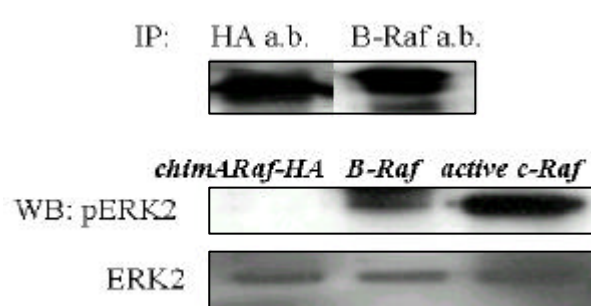


Fig. 2-17 A. IP: Immunoprecipitation of endogenous B-Raf and chimeric A-Raf from 10 min serum activated heterozygous fibroblasts using α -B-Raf and α -HA tag antibodies respectively. 10^6 cells were used for each IP since B-Raf expression in fibroblasts is very low. The coupled *in vitro* kinase assay was performed with precipitated proteins. *active c-Raf* – positive control used in kinase reaction. **WB:** pERK2 was detected by Western blot using α -pERK1/2 (pThr202/204) antibodies. The total ERK2 was detected by α -ERK2 antibodies.

3. DISCUSSION

3-1. A-Raf rescues B-Raf KO embryonic lethality with a low incidence.

Targeted disruption of *raf* genes in mouse demonstrated that their functions are not fully redundant since null mutations for each gene resulted in distinct phenotypes and confirmed that B-Raf is the major MEK activator in vivo [72, 93, 95-97], but requires C-Raf activity for its normal functioning [96]. No or moderate defect in cell proliferation and normal ERK activation has been observed in mouse embryonic fibroblasts derived from knock-outs of the C-Raf and A-Raf genes in contrast to those of B-Raf [72, 93, 96, 98]. The studies on the chicken B lymphocyte DT40 cell line demonstrated that null mutation of C-Raf has no effect on B-cell antigen receptor-mediated ERK activation, whereas loss of B-Raf leads to a significant reduction in ERK activation [158]. Since in fibroblasts, lymphocytes, neuronal tissue, melanoma cell lines B-Raf has a far stronger ability to activate MEK/ERK than the other two Raf proteins [72, 90-92], it could reflect the main role of B-Raf as a MEK activator in these cell types. However, NSCs derived from C-Raf null embryos demonstrated significantly reduced proliferation. No neurospheres could be obtained from B-Raf deficient animals [159]. The cooperative effect of C- and B-Rafs promoting fully ERK activation for survival could be essential in this cell type [96], [157]. Moreover, until determination of specified cell lineages in mid-gestation, C-Raf alone can fully compensate B-Raf function in cell proliferation and survival [1] and vice versa [72, 93, 98]. Double knock-out experiments demonstrate that A-Raf alone can not compensate B- and C-Raf functions but raise the possibility of cooperation between A-Raf and either B- or C-Raf in rescue before mid-gestation [96].

Recent studies using C-Raf and A-Raf deficient MEFs containing the immortalising large T antigen from SV40 showed that oncogenic Ha-ras transformation was not prevented in the absence of C-Raf or A-Raf [4, 97] suggesting that cooperative action of different Rafs mediates oncogenic effect of Ha-ras. Indeed, both B-Raf and C-Raf kinase activity towards MEK was significantly increased in the A-Raf deficient MEFs [97].

B-Raf has a higher affinity for its substrate [7, 94] and more than 50-fold greater ability to activate MEK by phosphorylation than C-Raf [13, 89]. Therefore B-Raf, which is more closely related to D-Raf than A-Raf and C-Raf [160], is likely to be functional homologue of ancestral Raf proteins in invertebrates, whereas A-Raf and C-Raf have deviated in their regulation and function.

B-Raf deficient mice die at E12.5d to vascular hemorrhaging caused by increased apoptosis of endothelial cells [1]. These animals also suffer from a range of other defects that arise as a consequence of a significant disruption to ERK activation in these cells [96]. However, no specific role of B-Raf in mouse development after mid-gestation was demonstrated so far. In this work, the attempt to overcome the lethality caused by endothelial apoptosis in B-Raf KO embryos by creation of hypomorphic/isomorphic B-Raf knock-in mice was done. The targeting construct was designed to express A-Raf, known to have much less kinase activity than C-Raf and B-Raf [89] under control of endogenous B-Raf promoter. Since B-Raf has multiple splice isoforms and exon 3 is present in all of them [6], cDNA of human WT A-Raf was introduced in frame with the third exon of B-Raf at the beginning of its own RBD. The resulting chimeric A-Raf includes the first unique N-terminal part of B-Raf combined with the remainder of A-Raf (Fig. 2-1 A, B, C). These properties of the chimeric protein could help to clarify the unknown function of the B-Raf specific N-terminal glycine rich region that may be implicated in the regulation of proteosomal activity and thereby survival [120, 124-126].

The homologous recombination in ES cells was obtained (Fig. 2-2 A-C) and the expression of expected 84 kD chimeric A-Raf in selected ESC clones was confirmed by RT PCR and Western blot (Fig. 2-3 A, B). Such early activity of the *B-raf* promoter corresponding to E3.5d suggests the role of B-Raf in early mouse development before implantation. However its function is mostly redundant before mid-gestation [96] since no obvious developmental abnormalities excluding growth retardation before this time are observed in B-Raf null embryos [1].

The F1 +/KIN mice were obtained displaying no visible phenotype suggesting no possible dominant negative function of chimeric protein (chapter 2-4). The absence of B-Raf (Fig. 2-5 C) and the expression of 84 kD chimeric A-Raf (data not shown) in F2 homozygous KIN embryos was confirmed by Western blot. The specific expression of chimeric A-Raf was also confirmed for heterozygous and homozygous KIN but not for WT MEFs. No up-regulation in C- and A-Raf expression was detected in KIN embryos (data not shown). The phenotype and survival of homozygous KIN embryos strongly depends on genetic background, like in C-Raf and A-Raf null mice [72, 93, 95, 98]. The life span of KIN mice is ranging from E12.5d to three weeks old adult animal depending on combination and proportion of inbred and outbred genetic backgrounds (Fig. 2-6 A). A correlation between reduced embryonic viability and higher proportion of inbred C57BL6 background usually was observed. In overall KIN embryos displayed less abnormalities than KO suggesting a partially

compensatory role of the isomorphic allele. No living KO embryos were obtained after E12.5d despite the introduction of outbred CD-1 background. In contrast, normal but smaller KIN embryos were found at E13.5-16.5d. It is likely that with some incidence (Fig. 2-6 A), chimeric A-Raf in cooperation with unknown genetic background related modifiers rescued the lethal phenotype at the crucial time window in mid-gestation from endothelial apoptosis and further development was not seriously affected. Indeed, all survived KIN embryos after E12.5d did not display developmental anomalies with exception of size reduction (Fig. 2-6 D-G; 2-8 B, E, G; 2-9 A; 2-10 A, B, C).

3-2. KIN embryo phenotype.

Fraction of KIN embryos displays phenotype similar to B-Raf KO.

At E10.5d-12.5d KIN embryos could be divided into two fractions: one with severe developmental abnormalities similar to those of B-Raf KO, and a second, in which developmental defects were compensated (Fig. 2-6 B, D). The apoptotic process was observed in some KIN embryos at E10.5d displaying hemorrhages (Fig 2-6 B, C). In other experiments with normal KIN embryos no apoptosis was detected (data not shown). The apoptotic process in KIN embryo was accompanied by the reduced ERK phosphorylation (Fig 2-6 C).

In the first fraction of KIN embryos, besides the bleedings in body cavity some neurological abnormalities and cephalic under-developments were observed. In facial region the palate closure, pharyngeal arches and nasal area were delayed in development corresponding to the stage E10.5-11.5d. Also the twisting midbrain region was observed (Fig. 2-6 D). Histochemical analysis of these defects revealed the irregular brain structure (not obvious fourth and lateral ventricle areas and striatum, undulated midbrain), under-developed lower jaw and nasal part, smaller heart and liver and overall hypocellularity (Fig. 2-8 C, F, H).

During mouse development the neural crest cells are migrating from different brain regions to the facial part contributing near all skeletal and connective tissues (Fig 3-1). The developmental delay and under-development of this region in KO and some KIN embryos could be related to either disturbed neural crest cell migration or differentiation of migrated cells.

The first suggestion comes from the observation that MEK-1 deficient fibroblasts fail to migrate on fibronectin [161]. Moreover ERK influences the expression of integrins

involved in cell-cell interaction and migration [162]. Active ERKs are also able to directly phosphorylate myosin light chain kinase leading to enhanced myosin light chain phosphorylation and stress fiber assembly [163]. Recent studies have shown that B-Raf^{-/-} fibroblasts have reduced ERK activation, disrupted actin stress fibers and altered motility [4].

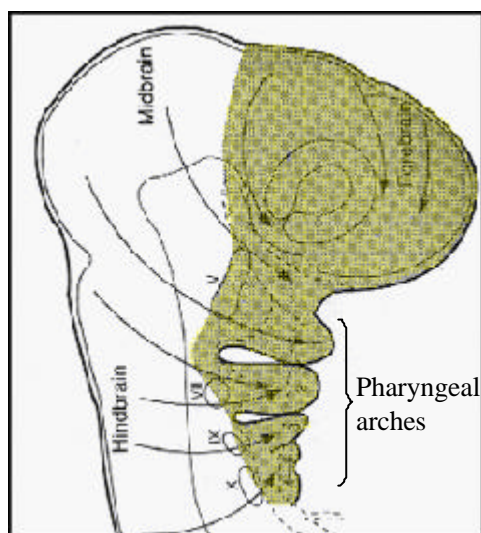


Fig. 3-1 Facial region development, E10.5d. Arrows indicate the origin and destinations of neural crest cell populations. In the facial region neural crest cells produce the craniofacial mesenchyme that differentiate into cartilage and bone, cranial neurons and glia and connective tissues of the face. Other cells enter pathways traversing pharyngeal structures where they give rise to the connective tissue of the thymus, odontoblasts of the tooth primordia and the bones of the middle ear and jaw.

The second possibility, is related with high B-Raf expression in neural cells [164] as well as in cells originating from neural crest, such as PC12 cells [165, 166] and melanocytes [167]. In all these cell types B-Raf activity is stimulated by cAMP [168]. At the same time cAMP is known to inhibit C-Raf kinase activity via phosphorylation by cAMP-dependent PKA [29]. This sustained B-Raf activity correlates with differentiation of PC12 cells while proliferative activity is mediated by a spike of C-Raf activation [28], [169].

The vascular phenotype of B-Raf KO embryos and observed in part of the KIN embryos is caused by increased apoptosis of differentiated endothelial cells and is associated with high proliferation of not differentiated endothelial cells [1]. This is reminiscent of the situation with PC12 cell differentiation [28], where B-Raf mediated ERK sustained activity is required for cell differentiation. On the other hand the role of B-Raf in survival of differentiated endothelial lineage cells could be related with its signaling through Tie-1, Flk-1 (VEGFR2) and Flt-1 (VEGFR1) RTKs, since their knock-out phenotypes are similar to B-Raf null phenotype [170-172]. Mice lacking C-Raf also displayed vascular defects in yolk sack and placenta [72, 98] and two recent works demonstrated the central role of C-Raf in protection from vascular apoptosis. In the first issue J. Hood and colleagues created mutant form of C-Raf that fails to bind ATP and blocks endothelial cell C-Raf activity in culture.

This mutant also blocks angiogenesis on the chick chorioallantoic membrane in response to bFGF or VEGF. Systemic injection of nanoparticle associated mutant that specifically targets angiogenic blood vessels in tumor-bearing mice resulted in apoptosis of tumor associated endothelium [173]. The second study was done by *A. Alavi et al.* on endothelial cell (EC) culture. They demonstrated that VEGF protected cells from FasL or TNF- α induced apoptosis (extrinsic) via C-Raf activation by Src and ERK dependent pathway. bFGF signaling protected ECs from intrinsic apoptosis through ERK independent pathway and resulted in C-Raf activation by PAK-1 and subsequent mitochondrial translocation. In contrast, B-Raf was not activated by VEGF and was only weakly induced by bEGF [70]. Active ERK may also induce the expression of angiogenic factors such as vascular endothelial growth factor (VEGF) [174] and this autocrine signaling mediated by B-Raf/ERK can protect endothelial cells via C-Raf activation from apoptosis .

Ets-1 and 2 transcription factors are expressed in early vascular sites and could propagate signals through Flk-1 or Tie-2 RTKs and Raf kinases thus converting endothelial cells to the angiogenic phenotype by inducing the expression of matrix metalloproteinase and integrin beta-3 [162, 171, 172, 175]. It appears that integrins not only provide structural links to extracellular matrix for attachment and motility, they also bind metalloproteinases or inactive fragments to regulate endothelial invasiveness [176]. The ruptures in blood vessels of B-Raf KO and some KIN embryos could be caused not only by apoptosis, but also by loose cell-cell integrin-mediated interactions.

How chimeric A-Raf with moderate kinase activity overcomes all these developmental disorders in some of the embryos (Fig. 2-6 A) remains to be elucidated. An intriguing possibility is the heterodimerization of chimeric A-Raf via its B-Raf N-terminus with C-Raf and its full activation leading to ERK signaling. Such interaction of B-Raf and C-Raf was demonstrated by *Weber et al.*, however B-Raf interacting domain was not mapped [157]. Another possible explanation may be the survival function of an unknown B-Raf effector (possibly some modifier gene) not related with B-Raf kinase activity and activated through B-Raf N-terminus interaction. The possible candidate for this role is a PA28 α subunit of the 11S regulator of proteasomes, known to specifically interact with B-Raf N-terminus [120]. Finally, it may be the antiapoptotic function of chimeric A-Raf itself since A-Raf was shown to specifically localize in mitochondria [150].

Some 12.5d KIN embryos are normal but reduced in size, neurological defects are observed.

In viable E12.5d KIN embryo, displaying no visible developmental defects the reduced proliferation was detected in the subventricular zone (SVZ) of fourth and lateral ventricles and in striatum (Fig. 2-8 B). These areas contain actively dividing neural stem cells (NSCs) and neural precursor cells (NPCs). During mid-gestation, after proliferation in the germinal ventricular zone (VZ) young neurons are migrating away guided by radial glia and form a second germinal zone – subventricular zone (SVZ) [177]. In addition to an observed reduction in proliferation, the migration process may be impeded in KIN embryo since migrating cells are not orientated along the migration axis toward SVZ (Fig. 2-8 B).

It is known that nuclei of VZ precursors migrate during the cell cycle. During G1 nuclei rise from the inner (apical) surface of the VZ. During S phase the nuclei reside in the outer (basal) third of VZ. During G2 they migrate apically, and mitosis occurs when the nuclei reach the ventricular surface. The vertical cleavage (perpendicular to the ventricular surface) of progenitor cells generates two similar daughters that retain their apical connections and reenter the cell cycle. The horizontal cleavage (parallel to ventricular surface) produces an asymmetric division in which the apical daughter retains contact with the apical surface and the basal daughter loses this contact. It migrates away from the VZ and later becomes the progenitor of postmitotic neuron [178].

Perhaps, this nuclei fluctuation process during the cell cycle is disturbed in KIN SVZ and related to either interference with G1-S transition or interference with cytoskeletal dynamics. In addition, NSCs culturing from forebrain (telencephalon) of E10.5-12.5d KO and KIN embryos could not be established. Several days after dissociation of KO and KIN forebrains and seeding in culture, only few neurospheres appeared in contrast to thousands in heterozygous or WT forebrains. When similar experiment was done with forebrains of C-Raf deficient embryos, the reduction of neurosphere number was less pronounced [159]. All these data are consistent with a requirement of B-Raf signaling for NSC/NPC proliferation during mid-gestation.

Growth factor requirements define at least two major classes of stem cells in the CNS. One group of cells requires high level of EGF [179] and can be expanded as floating cell aggregates, called neurospheres (heterogeneous clonal group of cells), for many passages without apparent phenotypic change, although they eventually become FGF-responsive [180], [181]. A second group of precursor cells are FGF-dependent. These cells can be grown like EGF-dependent cells, but can also be propagated as adherent cultures [182]. FGF-dependent stem cells do not respond to EGF and do not express the EGFR. It

has been suggested that EGF-dependent cells may arise from FGF-dependent precursors [183]. Both types of neuronal precursors co-exist in multiple brain regions, can self-renew and differentiate *in vitro* into three neural cell types upon growth factor withdrawal. The involvement of B-Raf in NSCs proliferation could be related to the complex interplay between EGF/FGF mediated pathways and requires C-Raf action.

Increased apoptosis in tissues of E13.5d KIN embryo.

At the late stage of mid-gestation, E13.5d, histological examination of a viable KIN embryo and its heterozygous littermate did not reveal significant difference in organ formation and positioning (Fig. 2-9 A). In KIN embryo all structures were found normal but were proportionally reduced in size. TUNEL assay detected more apoptosis in KIN liver, lung, veins, striatum and SVZ. In contrast to dispersed apoptotic cells in +/-KIN, clusters of apoptotic cells could be recognized in KIN littermate tissues. However no massive cell death was detected in any organs (Fig. 2-9 B). Increased apoptosis was accompanied by reduced cellularity in organs, presumably as a result of this process at the earlier stages of development. The neuronal apoptosis could be explained by the observation that sensory and motoneurons from B-Raf deficient embryos do not respond to neurotrophic factors for their survival in contrast to those from C-Raf KO [151].

During neurogenesis neurons extend axons to the vicinity of target cells which secrete limited amounts of survival inducing neurotrophic factors. Neurons that do not receive adequate amounts of these factors die by apoptosis [178]. A similar survival mechanism may be operating in other tissues during development and B-Raf signaling might provide the survival. The above findings may also be explained by a partially compensatory role of hypomorphic chimeric protein in cell survival through possible activation of ERK pathway via C-Raf interacting.

Normal phenotype of E16.5d embryo.

Surprisingly, at E16.5d, as in E13.5d viable KIN embryos, all organs and tissues were well formed and developed (Fig. 2-10 A, B, C), but no increase in apoptosis was observed, excluding lung tissue where apoptotic cell numbers showed a two fold increase over heterozygous lung (Fig. 2-10 D). Also no hypocellularity was observed in any tissue. In hindbrain all structures (cerebellar primordium, choroid plexus, fourth ventricle lumen) could be recognized. In forebrain the neopalial cortex (future cerebral cortex), intermediate zone, ventricular zone and lumen of lateral ventricle are present displaying no significant

structural defect compared with heterozygous littermate (Fig. 2-10 C). The heart ventricle had loose structure, atrium and iliac vein in KIN embryo were enlarged, but all these tissues did not display an increase in apoptosis (Fig. 2-10 C). This observation may suggest a dispensable role of B-Raf in cell survival and proliferation at the late embryonic stages and by existence of compensatory mechanisms leading to reconstitution of lost cell number during mid-gestation. These mechanisms could include up-regulation of G-Raf and ERK activation, mobilization of prosurvival factors like Bcl-2 [128], CREB or NFkB [143, 184] activation of PI3K/Akt pathway and down-regulation of proapoptotic pathways [154, 184]. Further immunochemical experiments to confirm either of these hypotheses need to be performed. The most obvious experiment is to check whether increase of proliferation takes place in KIN tissues and determine by which mechanisms.

3-3. Phenotype of adult KIN mouse.

Hematopoietic defects.

Recently one viable three weeks old (p20) adult KIN female was obtained (Fig. 2-7 A). It did not display any behavior abnormalities, fed normal and was healthy during 20 days observation period. It has reduced size and body weight compared to +/KIN littermate, but all organs were normal and proportionally reduced in size with exception of thymus and spleen. These two organs were 10 fold smaller as measured by weight than those of heterozygous littermate (Fig. 2-7 A).

The preliminary results of FACS analysis of KIN thymus demonstrated the dramatically reduced fraction of naive CD4⁺/CD8⁺ double positive T-cells (16% in KIN versus 81% in +/KIN) and increased fraction of mature CD4⁺ (45% in KIN versus 12% in +/KIN) and CD8⁺ (27% in KIN and 4% in +/KIN) single positive cells. Also the fractions of immature B-cells and erythroblasts in KIN spleen were significantly reduced compared to +/KIN (data not presented). At that time the fraction of mature cells in the spleen was not affected or even increased compared to heterozygous littermate. These data suggest an important role of B-Raf in maintenance of immature cell lineages during hematopoiesis but not in establishment and differentiation of these lineages since all mature blood and lymphatic cells were present in normal proportion in KIN animal. It may be that during late embryogenesis when these immature cell lineages are generated, the role of B-Raf is to

prevent them from apoptosis and induce their proliferation through ERK activation. The study on chicken B-lymphocyte DT40 cell line is consistent with this hypothesis [158].

The apoptosis is not increased in adult KIN tissues.

In the p20 adult KIN mouse only lung tissue displayed enlarged alveoli and hypocellularity, probably as a consequence of increased apoptosis detected at E16.5d in KIN lung (Fig. 2-11 A). Other tissues were normal and only in skin hair follicles were smaller, possibly reflecting the overall decrease in size of KIN mouse. C-Raf deficient adult mice, survived with very low incidence, displayed the similar phenotype (overall size reduction, enlarged alveoli, significant spleen and thymus reduction) (our unpublished data). These overlapping phenotypes prove *in vivo* the overlapping functions of both Rafs and confirm their cooperative function in adult organism.

The apoptosis level was normal in all examined tissues of adult KIN arguing again the more important role of B-Raf in cell survival at the earlier stages of development (Fig. 2-11 B). Western blot analysis of different KIN tissues showed the significantly reduced ERK phosphorylation in all of them with exception of hindbrain. No B-Raf expression was found in any of these tissues. This suggests either the role of B-Raf as a main ERK activator in the affected tissues [72] [90], [92], [91] or the cooperative manner of ERK activation [96, 157]. In hindbrain the compensatory mechanism including for instance C-Raf activation could be mobilized and high ERK activity is restored.

Analysis of neurogenesis in adult KIN brain.

The role of B-Raf in proliferation and survival of NSCs/NPCs during mid-gestation was demonstrated however no obvious involvement of this protein in neurogenic process at the later embryonic stage E16.5d was detected. In KIN E16.5d embryo all structures in brain were present displaying no visible difference or increased apoptosis compared to heterozygous littermate. In order to study the role of B-Raf in adult neurogenesis the presentation of neuronal cell lineages and neural precursors, p20 KIN brain was examined using different cell lineage markers (Table 2-12).

This investigation was mainly focused on hippocampal region where the subgranular zone (SGZ) of dentate gyrus (DG) is known to be germinal zone generating hippocampal interneurons during the adulthood [185]. Such germinal areas were also detected in forebrain subventricular zone (SVZ) of the lateral ventricle [186] and in external granular layer of the assembling cerebral cortex [187]. SVZ generated interneurons are migrating

through rostral migratory stream (RMS) into the olfactory bulb where neuron incorporation continues into adulthood [188] (Fig. 3-3).

The histochemical examination of adult brain did not reveal any differences in structure and morphology compared to +/KIN. All hippocampal (Fig. 2-12 A), cerebellar and other structures were present displaying no under-development. The staining for neural precursor marker Tuj-1 (also marks axons) demonstrated the higher number of Tuj-1 positive cells in SGZ of DG in +/KIN compared to KIN hippocampus. In heterozygous

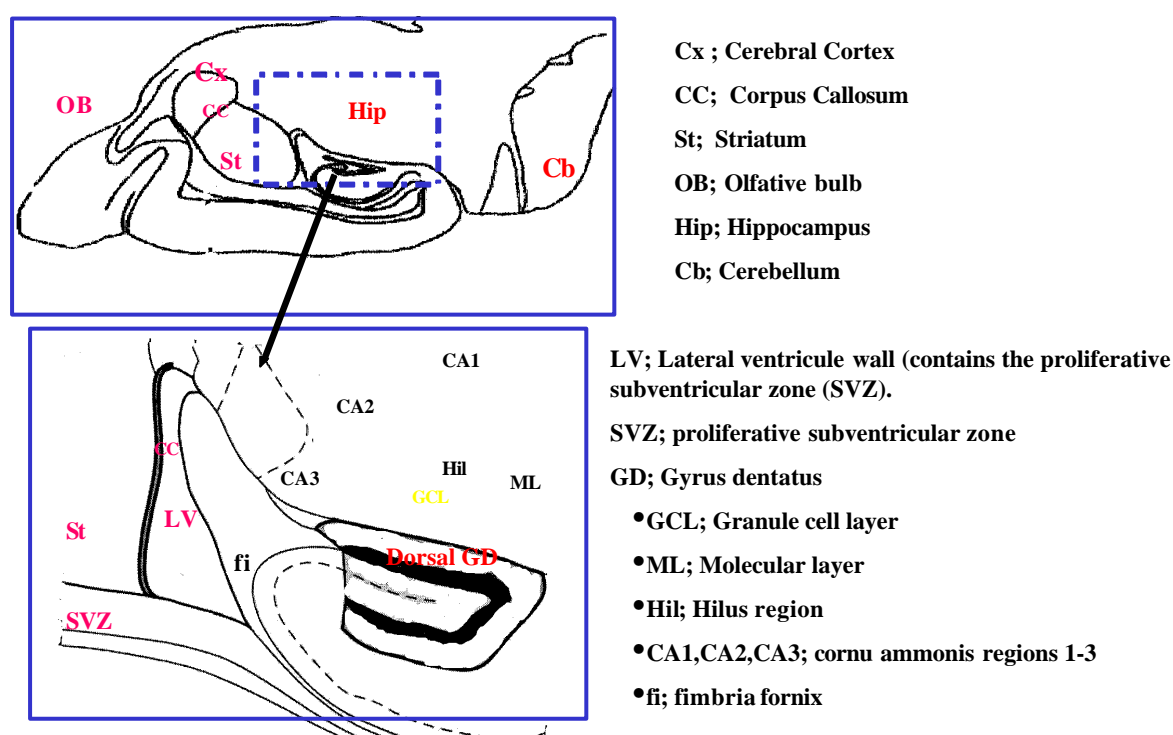


Fig. 3-3 Schematic representation of the main neurogenic regions in adult mouse brain.

animal more neurofilaments were found in Hilus region of DG and in CA1-3 regions of hippocampus (Fig. 2-12 B). In olfactory bulb (OB), cerebellum and SVZ no dissimilarity between KIN and +/KIN Tuj-1 positive cell number was observed (data not shown). The decrease in NPCs number in KIN hippocampus is not associated with proliferation since the number of S-phase cells was similar for both genotypes (Fig. 2-12 C). pERK level, also, was not higher in heterozygous SGZ cells compared to KIN (data not shown). However no significant difference in postmitotic neuron (NeuN positive cells) number in the same regions was detected. The observed lower density of NeuN positive cells at higher magnification in GCL of KIN hippocampus needs to be quantified (Fig. 2-12 D).

The above data point to a specific role of B-Raf in support of NPCs (which is reminiscent to the situation with immature lymphocytes and erythroblasts) but not in their proliferation and differentiation. Also, it is possible, that hypomorphic chimeric A-Raf and C-Raf cooperative activity, or C-Raf up-regulation compensate the latter two functions of B-Raf but not the first one. It is unclear whether this maintenance of NPCs is associated with B-Raf kinase activity toward ERK or other targets, e.g. inactivation of proapoptotic BAD (Heckmann unpub). As no difference in proliferation of SGZ cells and ERK activity was detected in KIN hippocampus it argues for a compensatory mechanism of ERK activation in KIN NPCs population, since ERK activity is required for G1-S transition [189], [190]. The specific B-Raf function in maintenance of this population remains to be elucidated. Further experiments comparing the level of apoptosis and C-Raf activity in SGZ cells are required.

The interpretation of the observation that in KIN hippocampus the axon number was reduced but the number of mature neurons was not affected (Fig. 2-12 B, D) is consistent with data about the different subcellular localization of Raf proteins [191]. In neurons C-Raf is localized in the cytoplasm of soma, whereas B-Raf is present mainly in the neuritic extensions or axons. This different subcellular localization can be associated with their different function and interaction with specific partners e.g. GTPases in the same cell. Recent data clearly showed that Ras GTPases can act differentially [192] and may be implicated in specific neuronal modulations, e.g. synaptic plasticity [193]. B-Raf specific signaling could be involved in establishment of synaptic connections and neurite outgrowth acting via Ras-GRF/CDC25mM, neuronal-specific guanine-nucleotide-exchange factor which induces Ras in response to Ca^{2+} influx [193]. G protein coupled receptor (GPCR) activation can also stimulate neurite outgrowth. PACAP signals through the GPCR type 1 PACAP-preferring receptor (PAC 1) in PC12 cells [194, 195] and like NGF causes robust neurite outgrowth, which requires activation of ERK [196]. Finally CREB transcription factor activation by RSK which in turn is activated by ERK leads to expression of different pro-survival and differentiation promoting factors [197]. Impaired B-Raf activity in KIN can result in reduction of axons and synapses. However, to check this hypotheses the additional staining for specific synaptic and axon markers e.g. synaptophysin and NF70, and quantification analysis are required.

A large difference was found in KIN OB granular and periglomerular cell layers where NeuN positive cell numbers were dramatically reduced (Fig 2-12 D). Since SVZ generated NPCs are migrating through RMS into the olfactory bulb where they differentiate into interneurons [188], two processes could be disturbed in KIN brain: differentiation into

mature olfactory interneurons and their survival and/or migration process. The KIN NPC number in SVZ was not reduced in contrast to those in hippocampus and it is possible that SVZ NPCs are not able to differentiate or die after differentiation. Recent data demonstrated the involvement of endocannabinoid anandamide (AEA) in suppression of neuronal differentiation by interfering with Rap1/B-Raf/ERK pathway [198]. The reduced B-Raf activity may lead to impaired differentiation in this case. In order to distinguish between these possibilities TUNEL assays to detect apoptotic processes in differentiated cells and PSA-NCAM staining to investigate the integrity of migration pathway are required.

The process of gliosis in KIN and heterozygous brains was examined using GFAP marker. A distinction was found in reduced GFAP-positive cell number in KIN SGZ of hippocampus that correlates with a decrease in Tuj-1 positive cells. These findings could support the theory that SGZ precursors are similar to NPCs in SVZ which are supposed to be astrocyte-like cells expressing GFAP and nestin [199, 200]. Likewise, in developing cortex the radial glial cells generate neurons and glial cells [201]. It is obvious that B-Raf is involved in maintenance of this cell population in SGZ of hippocampus.

3-4. Cell culture experiments on KIN MEFs.

KIN fibroblasts display reduced proliferation and are more susceptible to apoptotic stimuli.

The cell culture experiments on fibroblasts derived from KO, KIN and WT E10.5d embryos clearly demonstrated the important role of B-Raf in cell proliferation. The number of KO MEFs attached to the dish after embryo dissociation was very low and these cells failed to proliferate and displayed senescent phenotype. KIN MEFs displayed reduced proliferative ability compared to +/KIN and WT (Fig. 2-13 A).

The resistance to apoptotic stimulation was also reduced in KIN MEFs both in staurosporine and FasL induced apoptosis (Fig. 2-14 A, B). Since staurosporine evoked apoptosis very fast, in a few hours after application, and the number of dead cells was measured first after six hours after induction, the more detailed measurements at the earlier time points are required. However even after 6 hours after induction there were twice more dead KIN cells than WT (Fig. 2-14 A). In FasL induced apoptosis, 12 hours post induction, the apoptotic cell death was 7 and 2 times higher in KIN than in WT and +/KIN MEFs respectively. This difference was decreasing during the time after FasL administration (Fig. 2-14 B). Interestingly, heterozygous MEFs were more susceptible to FasL induced apoptosis than WT, suggesting B-Raf dosage effect in apoptosis resistance. In proliferation assay this

effect was not observed since WT and heterozygous MEFs proliferated similarly (Fig. 2-13 A).

ERK and Akt signaling pathways are disturbed in KIN MEFs

To dissect the mechanisms involved in lowering proliferative ability and apoptosis resistance of KIN MEFs the ability of ERK activation upon growth factor stimulation was examined. Fig. 2-14 A demonstrates the delayed and reduced kinetic of ERK activation in KIN fibroblasts. In proliferating KIN cells (not treated) ERK phosphorylation was slightly reduced compared to WT. In WT fibroblasts ERK serum activation was associated with increased B-Raf phosphorylation at Ser728, homologous to Ser621 in C-Raf. In C-Raf this pSer621 interacts with 14-3-3 proteins and is required for C-Raf activation [61], [77]. So far no data about involvement of pSer728 in B-Raf activation are available. In contrast, no increased phosphorylation upon stimulation at A-Raf homologous Ser528 was detected in KIN cells. No or poor defect in cell proliferation and ERK activation has been observed in mouse embryo fibroblasts derived from C-Raf and A-Raf KO embryos [72],[93, 97]. These data confirm the role of B-Raf in ERK signaling in fibroblasts and connect this pathway with cell survival. Even barely detectable kinase activity of the hypomorphic chimeric A-Raf, demonstrated *in vitro* by coupled kinase assay (Fig. 2-16 A) is sufficient to rescue B-Raf deficient MEFs from death and allows them to proliferate. One can speculate that chimeric A-Raf bearing some properties of B-Raf, e.g. N-terminal part, can heterodimerizes with and activate C-Raf, since B-Raf/C-Raf interaction *in vitro* was shown [157].

The PI3K/Akt survival pathway integrity in KIN MEFs was examined in order to understand the mechanism lying in their increased susceptibility to apoptotic stimuli. Akt (PKB) plays an important role in controlling the balance between survival and apoptosis [202]. It is activated by insulin and many various growth and survival factors. Ligation of the growth factor receptors results in recruitment of phosphoinositide3-kinase (PI3K) into receptor-associated signaling complex. For activation Akt is recruited to the plasma membrane through interaction with PIP3 (phosphatidylinositol (3,4,5) trisphosphate) generated by PI3K and phosphorylated at Thr308 and Ser473 by PDK1 [203]. When activated, Akt promotes cell survival by inhibitory phosphorylation of pro-apoptotic kinases (e.g. GSK3 α and β , ASK1), caspase-9, BAD, Forkhead transcription factor [204]. In not treated proliferating KIN MEFs the basal level of pAkt was reduced and, inactivated pBAD was not detected compared to WT cells. The kinetics of Akt and BAD phosphorylation upon stimulation were delayed resulting in very poor Akt activation and transient BAD inactivation

in KIN MEFs. In contrast, WT fibroblasts demonstrated much faster and pronounced Akt activation and more persistent BAD inactivation. These findings demonstrate a role of Akt pathway and BAD inactivation for MEFs survival, and synergistic connection between Akt and ERK signaling pathways in cell survival. Both these pathways are required for 32D cell survival upon growth factor withdrawal [205].

BAD is known to be phosphorylated and inactivated by C-Raf [128] and this phosphorylation could occur in cooperative manner with BAG-1 and Akt. The experiments on Bcl-2 deficient fibroblasts demonstrated the Bcl-2 independent role of mitochondrial C-Raf in apoptosis suppression [130]. Suppression of mitochondrial C-Raf activity rendered Akt-expressing cells susceptible to apoptosis induced by growth factor deprivation and was accompanied by inhibition of BAD phosphorylation [206]. In hypomorphic B-Raf cells BAD Ser136 phosphorylation was dramatically reduced. The above findings for C-Raf can be applied for B-Raf since B-Raf was shown to directly phosphorylate BAD on Ser112 and 136 [207].

The results also suggest that Akt activation depends on B-Raf activity either directly or through ERK signaling and autocrine loop. Akt is reported to negatively regulate B-Raf protein by direct phosphorylation at Ser364 [208] and C-Raf by phosphorylation at Ser259 [52]. On the other hand Akt can indirectly activate C-Raf in PKC-dependent manner [206]. There is no evidence that Akt can be directly activated by Raf proteins. However this activation could occur through autocrine loop since Raf/ERK signaling can enhance the expression of growth factors activating PI3K/Akt pathway [205, 209]. The analysis of ERK induced transcripts in epithelial cells demonstrated up-regulation of heparin-binding EGF (79 Rapp), a transcriptional target downstream of ERK (73). The experiments with PI3K and Akt inhibitors support this model demonstrating the requirement of PI3K activity for MEK1 responsive growth and survival [205], [210].

All presented experiments demonstrate that in overall the reduced ERK activity is not essential for survival and function in adulthood but is crucial at earlier embryonic stages of development, especially during mid-gestation. The survival role of B-Raf for many cell lineages during this time period is associated with its kinase activity and ERK/Akt pathway cooperation. Once mid-gestational crisis is overcome with the help of isomorphic/hypomorphic chimeric A-Raf (at very low incidence and depending on genetic background modifier genes) the further development is normal and increased ERK activity in WT or heterozygous animals compared to KIN is only required to maintain the minor processes in organism. This is in some contrast with the recent bulk of data suggesting the

central role of B-Raf in ERK signaling and indicates on redundancy of Raf isozymes in adult organism functioning.

4. MATERIALS AND METHODS

The methods described in this section are all based upon today's standard molecular and cellular biology techniques.

4-1. Materials

4-1.1. Instruments

Hardware

Bacterial incubator
 Bacterial shaker
 Cell culture incubator
 Cell culture microscope
 Cell culture Hood
 Cell Tram vario
 Cover glasses
 Developing machine
 Deparaffinization machine
 DNA Sequencer
 Electrophoresis power supply
 Electrophoresis unit, small
 Fine scale
 Heat block
 Homogenizer
 Horizontal electrophoresis gel
 Injection microscope
 Mega centrifuge

 Mikrotome
 Microscope Slides, Super Frost[®] Plus
 Mini centrifuge

 Paraffin embedding machine
 pH meter
 Phosphoimager

Manufacturer

Heraeus B 6200
 New Brunswick Scientific innova 4330
 Heraeus Instrument
 Leica
 Heraeus Instrument
 Eppendorf
 Marienfeld
 Agfa
 Shandon Elliott LTD
 ABI PRISM 373, ABI
 Bio-Rad
 Bio-Rad Mini-Protean II
 Scaltec SBC 21
 Liebisch, Type 2099-DA
 Ultra-Turrax[®]
 MWG Biotech
 Leica
 J-6B, Beckman; Megafuge 1.0 R, Heraeus;
 RC 5B plus, Sorval
 Leitz Wetzlar
 Menzel-Gläzer
 5417R, Eppendorf
 Biofuge 15, Heraeus
 AutoTechnicon
 Microprocessor, WTW
 Fujix BAS-2000 III, Fuji,

Shakers	with plates BAS-MP 2040P, Fuji Heidolph, Unimax 2010, Edmund Bühler WS5
Scale	BP2100S, BP310S, Sartorius
Spectrophotometer	Ultraspec 3000, Pharmacia Biotech
Thermocycler	PE9600, Perkin Elmer; T3, Biometra®
Ultraviolet Crosslinker	UVC500 Hoefer Scientific Instruments
Vortex	Scientific Industries Genie-2
Water bath	GFL 1083, Amersham-Buchler

4-1.2. Chemical reagents and general materials

<i>Reagent</i>	<i>Purchased from</i>
[α - ³² P]dCTP	Amersham
1 kb DNA ladder	Gibco, MBI
Acrylamide (30%)/Bisacrylamide (0,8%)	Roth
Adenosin-5'Triphosphate (ATP)	Sigma
Agarose, ultra pure	Life Technologies, Inc.
Ammonium Acetate	Sigma
Ammonium peroxydisulfate (APS)	Sigma
Ampicillin	Sigma
AntifoamA	Sigma
Aprotinin	Roth
Bacto-Agar	Roth
Bovine serum albumin (BSA)	Sigma
Bradford-reagent	Biorad
Bromphenolblue	Sigma
β -Mercaptoethanol	Roth
Calciumchloride (CaCl ₂)	Sigma
Chloroform	Roth
Cloralhydrate	Roth
CircleGrow (GC)	Dianova
Deoxycholate (DOC)	Sigma
Diethyl pyrocarbonate (DEP)	Merck
Dimethylsulfoxide (DMSO)	Sigma
Dithiothreitol (DTT)	Sigma
dNTP	MBI
Ethylenediaminetetraacetic acid-disodium salt (EDTA)	Sigma
EGTA	Sigma
Ethanol	Roth
Ethidiumbromide	Life Technologies, Inc.
Formaldehyde	Roth
Formamide	Roth
Glutathion-sepharose	Pharmacia
Glycerol	Sigma
Guanidine thiocyanate	Roth

Hydrochloride (HCl)	Roth
Hybond-N, Hybond TM -P membrane	Amersham
IGEPAL (NP-40)	Sigma
Isopropyl-1-thio-β-D-thiogalactopyranoside (IPTG)	Roth
Isopropanol	Merck
Leupeptin	Sigma
L-Arginine	Sigma
L-Lysine	Sigma
L-Methionine	Sigma
L-Phenylalanine	Sigma
L-Threonine	Sigma
L-Tryptophan	Sigma
Magnesiumchloride	Sigma
3-(N-morpholino)propanesulfonic acid (MOPS)	Sigma
Paraffin wax (Histosec Pastillen)	Merk
Pefablock	Roth
Phenol	Roth
Phenol:Chloroform:Isoamylalcohol	Roth
Phenol/Chloroform (TE saturated)	Roth
Ponceau S	Sigma
Potassium acetate (KAc)	Sigma
Potassiumchloride (KCl)	Sigma
Potassiumdihydrophosphate (KH ₂ PO ₄)	Merck
Protein A-agarose	Roche
Protein G-agarose	Roche
Protein ladder, BenchMark TM	Invitrogen
SDS ultra pure	Roth
Sodium citrate	Merck
Sodiumdihydrophosphate (NaH ₂ PO ₄)	Merck
Sodiumhydrophosphate (NaHPO ₄)	Merck
Sodiumhydroxide (NaOH)	Sigma
sodium morpholineethanesulfonate (Na-MES)	Sigma
Sodium orthovanadate	Sigma
Sonicated salmon sperm	Invitrogen
TEMED	Roth
Tris-(hydroxymethyl)-aminomethane (Tris)	Roth
Triton-X100	Sigma
Tyrosine	Sigma
Uracil	Sigma
Whatman 3MM Paper	Schleicher & Schüll
X-gal	Sigma
X-ray film	Amersham
Xylencyanol	Roth
Yeast extract	Life Technologies, Inc.

4-1.3. Cell culture and embryo manipulation materials

<i>Reagent</i>	<i>Source</i>
β-mercaptoethanol	Sigma
DMEM	Life Technologies, Inc.
ES cell injection medium: 10 ml DMEM, 0.026 g	MSZ

Hepes, 100 BSA, 5U/ml DNaseI	
FAS ligand	Alexis
Foetal calf serum (FCS)	PAN
FCS tested for ES cell	Gibco #10119-162
	Lot3703359A or
	Biospa Lot701GD1
G418 sulfate	Calbiochem
Gancyclovir (Cymeven i.v.)	Roche
L-Glutamine	Gibco
LIF	Gibco or supernatant from
	CHO cells transfected with
	LIF (1:250) (from
	L.Nitschke)
M2 embryo flashing medium	Sigma
M16 embryo incubation medium	Sigma
Mineral oil (embryo tested)	Sigma
Mitomycin C	Sigma
MTT solution: 5 mg MTT/1ml PBS	Roth
Non-essential amino acids	Gibco
Phosphate buffered saline (PBS)	Gibco
Penicillin /Streptomycin	Life Technologies, Inc.
Staurosporine	Sigma
Trypsin-EDTA	Gibco
Trypanblue	Sigma
Cell Freezing Medium: 70% Complete	MSZ
DMEM/RPMI 1640 (10% FCS, P/S), 20% Fetal	
Bovine Serum, 10% DMSO	

4-1.4. Antibodies used for Western blot

<i>Antibodies</i>	<i>Antigens</i>	<i>Source</i>
a-12CA5 (mouse monoclonal)	Hemagglutinin (HA)	MSZ Würzburg
anti-AKT(rabbit polyclonal)	AKT	Cell signaling
anti-pSer473 AKT (rabbit polyclonal)	pAKT	Cell signaling
anti-pSer136 BAD (rabbit polyclonal)	PBAD	Cell signaling
anti-B-Raf	B-Raf	Santa Cruz
anti-ERK2 (rabbit polyclonal)	ERK2	Santa Cruz
anti-p(Thr202/Tyr204) ERK1/2 (rabbit polyclonal)	PERK1/2	Cell signaling
anti-Rabbit IgG conjugated peroxide (POD)		Amersham-Life Sciences
anti-Mouse IgG conjugated		Amersham-

peroxidase (POD)		LifeSciences
PARP (rabbit polyclonal)	Cleav. (89kD) and uncleav. (116kD) PARP	Cell signaling
Protein-A conjugated Agarose-beads		Roche
Protein-G conjugated Agarose-beads		Roche

4-1.5. Enzymes

<i>Items</i>	<i>Source</i>
Calf Intestinal Phosphatase (CIP)	New England Biolabs (NEB)
Bio Therm DNA polymerase	Gene Craft
DNaseI, PCR grade	Gibco
M-MuLV-RT (reverse transcriptase)	MBI
Proteinase K	Roth
Pfu polymerase	Stratagene
RNaseA	Roche
T4 Ligase	NEB
Restriction Endonucleases	MBI, Boehringer Mannheim, NEB, Amersham

4-1.6. Kits

<i>Items</i>	<i>Source</i>
ECL Western blotting detection reagents	Amersham
In Situ Cell Death Detection Kit, POD	Roche
QIAEX II Gel Extraction Kit	Qiagen
QIAGEN Plasmid Kit (Midi, Maxi)	Qiagen
QIAquick PCR purification Kit	Qiagen
rediprime TM II random prime labelling system	Amersham Pharmacia
	Biotech
Vectastain [®] ABC-peroxidase kit	Vector

4-1.7. Plasmid DNA

<i>Plasmids</i>	<i>Source</i>
Vectors	
pBluescript II SK+/- (pBSK)	Stratagene
pGEM-T Easy vector	Promega
pCDNA3	Invitrogen
pKS TK/NEO LoxP	I. Girkontaite, K.D. Fischer
B-Raf genomic clones	
pBSK-BamHI(8kb)Ex3-BRaf (p7)	L. Wojnowski
pBSK-BamHI/EcoRI(6.8kb)Ex3-BRaf (p7 6.8)	B. Fröhlen
pBSK-BamHI/XhoI(5kb)In2-BRaf (p7 4.5)	B. Fröhlen
pBSK-XhoI/EcoRI(2.8kb)Ex3-BRaf (p7 2.8)	O.Tyrsin
Human A-Raf cDNAs	
pCMV5-hA-Raf(WT)	K. Weber
pCMV5-hA-Raf(HAtag WT)	K. Weber
pCMV5-hA-Raf(K338M)	K. Weber
pCMV5-hA-Raf(DD)	K. Weber
KIN targeting vectors	
pKS TK/NEO LoxP-Araf(WT)	O.Tyrsin
pKS TK/NEO LoxP-Araf(K338M)	O.Tyrsin
pKS TK/NEO LoxP-Araf(DD)	O.Tyrsin

4-1.8. Oligonucleotides

<i>Primer name</i>	<i>Sequence</i>
Targeting vector cloning primers	
HA-tag forw (EcoRI)	5'-gcgcggaattcatgactggttac -3'
hGHPolyA rev (Sall)	5'-gcgcgctcgactactgagtggacccaacgc-3'
hGHPolyA rev (KpnI)	5'-gcgcggttacactactgagtggacccaacgc-3'

A-Raf forw (PstI)	5'-cgcgcgctgcagtgggcaccgtcaaag-3'
A-Raf rev (SacI)	5'-ctcgacaatgagctcctcgcc-3'
C-Raf forw (PstI)	5'-cgcgcgctgcagatgatggcaaactcac-3'
C-Raf rev (HindIII)	5'-gaaggcaagcttcaggaac-3'
C-Raf forw (BglII)	5'-ctccccagatcttagtaag-3'
C-Raf rev (EcoRI)	5'-cgcgcggaattcgaagacaggcagcctcgg-3'
Contr B-Raf 3' arm	5'-tgtgtatcgatctgtcccgtacaccatg-3'
Sequencing primers	
T3 promoter	5'-aattaaccctcactaaagg-3'
T7 promoter	5'-aatacgactcactatagg-3'
SP6 promoter	5'-atntagtgacactatag-3'
A-Raf seq1 forw	5'-tcaccagcagcagcgc-3'
A-Raf seq2 (EheI) forw	5'-gccatgcgggcctgctg-3'
68 (5' neo)	5'-gttggcgctaccggtggatgtgg-3'
65 (3' neo)	5'-gggccagctcattcctcccactcat-3'
mB-Raf intr2-5' seq	5'-ctcaagctagcaagatgg-3'
mB-Raf 3' arm seq	5'-aattaaccctcactaaagg-3'
RT PCR primers	
mβ-actin sen	5'-gtcgtaccacaggcattgtgatgg-3'
mβ-actin asen	5'-gcaatgcctgggtacatggtgg-3'
mB-Raf Ex1 sen	5'-gccgcggcctcttcggctg-3'
mB-Raf Ex2 sen	5'-gtggagagcataaaccaccatc-3'
5' template primers (for Southern probe)	
5' kin B-Raf sen	5'-atgtggaagtaataaac-3'
5' kin B-Raf asen	5'-aacgtctcaccgtcata-3'
Genotyping primers	
MB3-1	5'-gcctatgaagagtacaccagcaagctagatgcc-3'
Mbdel	5'-taggtttctgtggtgacttggggttgtccgtga-3'
NeoL	5'-agtgccagcggggctgctaaa-3'
A-Raf (SacI) long	5'-ggacctcgacaatgagctcctcgcc-3'

4-1.9. Cell lines, mouse lines and bacterial strains

<i>Cell lines:</i>	<i>Source:</i>
CJ7	Mouse embryonic stem cells, passage 11, 129Sv background (L. Fedorov, originally from T.Gridley, Jackson Lab.)
MEF	Primary mouse embryonic fibroblasts (established from embryos)
<i>Mouse lines:</i>	<i>Source:</i>
C57Bl6	All mouse strains were obtained from Harlan Winkelmann GmbH
CD-1	
129Sv	
B6D2F1	
<i>Bacterial strains:</i>	<i>Source:</i>
DH5 α	Bethesda Research Laboratories. Optimised for DNA transformation and replication

4-2. Solutions and buffers**4-2.1. Bacterial medium and DNA isolation buffers*****LB (Luria-Bertani) medium***

10g/L Bacto-tryptone

10g/L NaCl, 5g yeast extract

Adjust pH to 7.5 with NaOH

For plates, add 15 g Bacto-aga

Sob medium

20g/L Bacto-tryptone

0.5g/L NaCl, 5g yeast extract

10ml/L 250mM KCl

Adjust pH to 7.5 with NaOH

(before use add 5ml/L 2M MgCl₂)

X-Gal stock solution

20mg/ml X-gal (5-Bromo-4-Chloro-3-Indolyl- β -D-Galactopyranosid) dissolved in DMF and aliquoted at -20°C in darkness.

Buffer P1 (resuspension buffer)

50nM Tris-HCL

10mMEDTA

10 μ g/ml RNaseA

pH 8.

Buffer P2 (Lysis buffer)

10% SDS

200 mM NaOH

Buffer P3 (Neutralization buffer)

3 M potassium acetate, pH5.5

Buffer QBT (Equilibration buffer)

15% ethanol

0.15% Triton X-100

Buffer QC (Wash buffer)

2.0 M NaCl

50 mM MOPS, pH7.0

15% ethanol

Buffer QF (Elution buffer)

1.25 mM NaCl

50 mM Tris-HCl, pH 8.5

15% ethanol

4-2.2. RNA buffers

TRIzol[®] LS reagent (Gibco)

(Total RNA isolation Reagent for Liquid samples)

DEPC-H₂O

20 μ l DEPC to 100ml H₂O, leave 1hr before autoclaving.

10x RNA Gel Loading Buffer

See 10x DNA loading buffer

4-2.3. DNA buffers

STE

0.1M NaCl

20 mM Tris (pH 7.4)

10mM EDTA (pH8.0)

Phosphate buffer

89g NaH₂PO₄·2H₂O

4ml 85% Phosphoric acid

made up to 1L, pH 7.2

Hybridisation/prehybridisation buffer

7% SDS

0.5M Phosphate buffer

1mM EDTA

Washing buffer 1

40mM Phosphate buffer

1mM EDTA

5% SDS

Washing buffer 2

40nM Phosphate buffer

1mM EDTA

1% SDS

1x CIP Buffer

50 mM NaCl

10 mM Tris-HCl

10 mM MgCl₂

1 mM dithiothreitol, pH7.9

10x DNA Gel Loading Buffer

40% (w/v) saccharose

0.25% bromphenolblue

0.25% xylencyanol, use as 1x solution

1x Tris-Acetate-EDTA (TAE)

40 mM Tris-HCl,

40 mM acetic acid,

2 mM EDTA; pH7.8

10x Tris-Buffered Saline (TBS)

1 mM Tris-HCl,

150 mM NaCl

Tail Lysis Buffer

50 mM EDTA; pH8.0

50 mM Tris-HCl; pH8.0

0.5% SDS

4-2.4. Protein analysis buffers

TBST

1x TBS + 0.05% Tween

Blotting Buffer

39 mM Glycine

48 mM Tris

0.037% SDS

10% Methanol

Blocking Buffer

5% (w/v) of non-fat dry milk in TBST

Kinase Buffer

10 mM MgCl₂

25 mM HEPES, pH 7.5

25 mM β-glycerophosphate

1 mM Sodium vanadate

0.5 mM DTT

NP40 lysis buffer

10 mM Hepes pH 7.4

145 mM KCl

5 mM MgCl₂

1 mM EGTA

0.2% IGEPAL

1 mM pefablock

1 mM sodium vanadate

5 mM benzamidine

5 μg/ml aprotinin

5 μg/ml leupeptin

Running Buffer (for SDS-PAGE)

25 mM Tris

250 mM Glycine

0.1 % SDS

5x SDS-loading Buffer (for SDS-PAGE)

31 mM Tris HCl, pH6.8

1% SDS

5 % Glycerin

2.5 % Mercaptoethanol

0.05 % Bromphenoblu, 1x solution

Sodium Tris-EDTA Buffer (STE)

100 mM NaCl

10 mM Tris-HCl, pH 8.0

1 mM EDTA

10´TE

0,1 M Tris-HCL

10 mM EDTA (pH 7.5)

4-2.5. Immunochemical buffers

Eosin solution

1% Eosin in H₂O

Hematoxylin solution (per 100 ml)

1 g Hematoxylin

0.2 g NaIO₃

50 g KAl(SO₄)₂·12H₂O

1 g Citrate

25 g Chloralhydrat

4-3. Methods

4-3.1. Bacterial manipulation

Plasmid transformed bacteria are selected on LB plates with the appropriate antibiotic for 24 hr. For overnight mini cultures, single colonies are picked and inoculated in LB medium with antibiotic and shaken overnight at 37°C. This preculture is then used for preparing frozen glycerine cultures, plasmid DNA or protein purification. For storage of bacteria, a glycerol stock culture is prepared by growing bacteria to an OD of 0.8 at a wavelength of 600nm in culture medium. 500µl bacterial culture is taken and added to 500 µl 80% glycerine and then mix thoroughly in a small 1.5ml tube. This stock solution is subsequently frozen at –80°C. To inoculate an overnight culture again, take out bacteria and hold at room temperature (RT) until surface is thawed. Pick a small amount of cells and mix into 2-5 ml culture medium and leave to grow for several hours at 37°C in a bacterial culture shaker. The frozen stock is immediately returned to the -80°C.

4-3.1.1. Preparation of competent cells (CaCl₂ method)

On the first day, inoculate an overnight preculture from a single colony on a prestreaked plate (from glycerol stock) in 2ml LB or 2x TY media by incubation at 37°C and shaking to aerate.

The second day, inoculate 1 ml of the preculture in 100ml fresh media and grow the culture at 37°C until OD at wavelength 600nm of the culture reaches between 0.2 and 0.3. Cool down the culture on ice for at least 15 min. (The following procedures should be carried out at 4°C in pre-cooled sterile tubes). Harvest the cells in a centrifuge at 5000 g for 5 min, and discard the supernatant. Resuspend the bacterial pellets thoroughly in a small volume of ice-cold 100mM CaCl₂. Dilute the suspension with the CaCl₂ solution to a final volume of 30-40 ml, and leave on ice for 25 min with occasional shaking. Spin down the cells as before, discard the supernatant carefully and resuspend the pellets in 5 ml glycerol/CaCl₂. The suspension can be aliquoted in 100 to 400 µl aliquots and stored at -70°C. The transformation efficiency of the bacteria prepared by this method should reach at least 10⁶.

4-3.1.2. Transformation of competent bacteria

Thaw the competent bacteria from a desired origin on ice. Add a maximum of 20ng ligated DNA or purified plasmid-DNA to 100 µl competent cells in a cold 1.5 ml microfuge tube. Mix carefully and keep on ice for 20 min or longer. Heat-shock the bacteria then at 42°C for 90 sec, add 1 ml antibiotic-free LB medium, and aerate at 37°C for 30 min. Selection of transformed bacteria is done by plating 100 µl of the bacterial suspension on antibiotic containing agar plates. Only bacteria that have taken up the desired plasmids, which normally contain ampicillin resistance cassette, can grow on the agar plates. A single colony can then be expanded in LB medium and used for DNA preparation.

4-3.2. DNA methods

4-3.2.1. Electrophoresis of DNA on agarose gel

Double stranded DNA fragments with lengths between 0.5 kb and 10 kb can be separated according to their lengths on agarose gels. Agarose is added to 1x TAE to obtain a final concentration between 0.7-2%. Boil the suspension in the microwave until the agarose is completely solubilised. Allow the agarose to cool down to around 50°C before adding ethidium bromide up to 0.5 µg/ml and pour into the gel apparatus. Add DNA gel loading buffer to the DNA sample and apply on the gel. Electrophorese in 1x TAE buffer at 100 volts. The DNA can be visualised under UV-light.

4-3.2.2. Isolation of plasmid DNA from agarose (QIAEX II agarose gel extraction protocol)

This protocol is designed for the extraction of 40-bp to 50-kbp DNA fragments from 0.3-2% standard agarose gels in TAE or TBE buffer. DNA molecules are adsorbed to QIAEX II silica particles in the presence of high salt. All non-nucleic acid impurities such as agarose, proteins, salts, and ethidium bromide are removed during washing steps.

Excise the desired DNA band from the agarose gel under the UV light. Weigh the gel slice and add 3 volumes of Buffer QG to 1 volume of gel for DNA fragments 100-bp-4 kbp; for DNA fragments more than 4 kbp, add 2 volume of QG plus 2 volumes of H₂O. Resuspend QIAEA II by vortexing for 30 sec; add 10 µl (or 30 µl) of QIAEX II to the sample containing not more than 10 µg of DNA (between 2-10 µg). Incubate at 50°C for 10 min to solubilise the agarose and bind the DNA. Mix by vortexing every 2 min to keep QIAEX II in suspension. Centrifuge the sample for 30 sec and carefully remove supernatant with a pipette. Wash the pellet with 500 ml of Buffer QG and then twice with Buffer PE. Air-dry the pellet and elute the DNA in 10 mM Tris-HCL or H₂O and resuspend the pellet by vortexing. Incubate at RT for 5 min (or at 50°C for 5 min) for DNA fragments not more than 4 kbp (for DNA fragments between 4-10 kbp). Centrifuge for 30 sec and carefully pipette supernatant into a clean tube.

4-3.2.3. Purification of plasmid DNA (QIAquick PCR purification kit)

This protocol is designed to purify single- or double-stranded PCR products or DNA plasmids ranging from 100 bp to 10 kbp. DNA adsorbs to the silica-membrane in the presence of high salt while contaminants pass through the column. The impurities are washed away and pure DNA is eluted with Tris buffer or H₂O.

Add 5 volume of buffer PB to 1 volume of the contaminants and mix. Place a QIAquick spin column in a 2 ml collection tube. Apply the mixed sample to the QIAquick column and centrifuge 30-60 sec. Discard flow-through and place QIAquick column back into the same collection tube. Add 0.75 ml Washing Buffer PE to column and centrifuge 30-60 sec. Discard flow-through and place QIAquick column back into the same collection tube. Centrifuge column for an additional 1 min at maximum speed. Place QIAquick column in a clean 1.5 ml microfuge tube. Add 50 µl Elution Buffer EB or H₂O to the centre of the QIAquick column and centrifuge for 1 min. Store the purified DNA at - 20°C.

4-3.2.4. Ligation of DNA fragments

Calf-intestinal-phosphatase (CIP) reaction (5' phosphorylation)

Alkaline phosphatase catalyses the removal of 5' phosphate groups from DNA, RNA and ribo- and deoxyribonucleoside triphosphates. For blunt end ligation, the 5' phosphate group of the vector must be removed by CIP reaction. This reaction is also used to prevent the re-ligation of the vectors. 2.5 µg of DNA fragments is phosphorylated at 37°C for 30 min in 100 µl of reaction volumes consisting of 1x CIP buffer and 1 µl of phosphatase. 5 mM EDTA is then added to the reaction and incubated with the reaction at 65°C for 15 min to inactivate the enzyme. The DNA fragments are purified by phenol and ethanol precipitation before ligation reaction.

4-3.2.5. Cohesive-end ligation

Prepare the plasmid DNA or DNA fragment by cutting it with suitable restriction enzymes, which is followed by purification. 1:3 molar ratio of vector: insert DNA fragments together with 1 µl of T4 ligase are incubated in 1x Ligation Buffer in a total volume of 20 µl for 4 hr at RT or overnight at 16°C. Heat the mixture at 65°C for 10 min to inactivate the enzyme.

4-3.2.6. Mini-preparation of plasmid DNA

Grow 3 ml overnight culture in LB, 2x TY, or GC media with 100 µg/ml ampicillin at 37°C overnight. Pellet the cells at 14,000 rpm for 1 min. Remove the supernatant and resuspend the pellets in 100 µl Buffer. Add 200 µl Buffer P2 (Lysis Buffer) and incubate at RT for 5 min. Add 150 µl ice-cold 3 M acidic KOAc (Neutralisation Buffer), mix by inverting the tubes for 6-7 times and incubate on ice for 5 min. Centrifuge at 15,000 rpm for 3 min. Transfer the supernatant to a fresh Eppendorf tube and add 900 µl of pre-cooled 100% ethanol, precipitate at -70°C for 10 min. Centrifuge the pellet at 15,000 rpm for 10 min. Wash the pellet with 200 µl 70% ethanol. Air-dry the pellet and resuspend it in 30-50 µl 10 mM Tris-HCl, pH 7.8.

4-3.2.7. Maxi-preparation of plasmid DNA

Grow culture in 50 ml LB media containing plasmids or recombinant plasmids overnight in a 37°C incubator with shaking at 220 rpm. Collect the bacteria and isolate DNA plasmids by using a Quiagen Plasmid Maxi Kit. This extraction method is based on Birnboim's alkali lysis principle. Resuspend the bacterial pellet in 10 ml of Buffer P1. Add 10 ml of Buffer P2, mix gently, and incubate at RT for 5 min. Add 10 ml of chilled Buffer P3, mix immediately,

and incubate on ice for 20 min. Centrifuge at 4,000 rpm for 30 min at 4°C. Filter the supernatant over a prewetted, folded filter. Apply the supernatant to a equilibrated QIAGEN-tip 500 and allow it to enter the resin by gravity flow. Wash the QIAGEN-tip twice with Buffer QC. Elute DNA with 15 ml Buffer QF. These processes result in the isolation of a DNA-salt pellet, which is precipitated by 0.7 volumes (10.5 ml) of isopropanol and centrifuged further at 4000 rpm for 30 min. Washed the resulting pellet twice with 70% ethanol and air-dry at RT. The pellet is then carefully resuspended in TE buffer and used for transfection of cultured mammalian cells.

4-3.2.8. Measurement of DNA concentration

The DNA concentration is determined by using an UV spectrophotometer at wavelength of 260 nm. The absorption of 1 at 260 nm corresponds to a concentration of 50 µg/ml double stranded DNA. Identity, integrity and possible purity of the DNA can be subsequently analysed on an agarose gel.

4-3.2.9. DNA Sequencing (Sanger Dideoxy Method)

DNA can be sequenced by generating fragments through the controlled interruption of enzymatic replication [152]. DNA polymerase I is used to copy a particular sequence of a single-stranded DNA. The synthesis is primed by complementary fragment, which may be obtained from a restriction enzyme digest or synthesised chemically. In addition to the four deoxyribonucleoside triphosphates (ddNTP), the incubation mixture contains a 2', 3'-dideoxy analogue of one of them. The incorporation of this analogue blocks further growth of the new chain because it lacks the 3'-hydroxyl terminus needed to form the next phosphodiester bond. A fluorescent tag is attached to the oligonucleotide primer, a differently coloured one in each of the four chain-terminating reaction mixtures. The reaction mixtures are combined and electrophoresed together. The separated bands of DNA are then detected by their fluorescence as they pass out the bottom of the tube, and the sequence of their colours directly yields the base sequence.

1. Sequencing Reaction:

The "Taq Cycle Sequencing" is performed by using "PRISM™ Ready Reaction DyeDeoxy™ Terminator Cycle Sequencing Kit". Mix the following reagents in a 0.6 ml double-snap-cap microfuge tube:

Terminator premix*	9.5 µl
DNA template	100ng-1.0 µg

Primer				10 pmol
dH ₂ O				Adjust the final reaction volume to 20 μl
*A-Dye	Terminator	labelled	with	
				dichloro[R6G]
C-Dye	Terminator	labelled	with	
				dichloro[TAMRA]
G-Dye	Terminator	labelled	with	
				dichloro[R110]
T-Dye	Terminator	labelled	with	
				dichloro[ROX]

Place the tubes in a thermal cycler preheated to 96°C which is followed by 25 cycles of thermal cycling steps: 96°C for 15 sec; 48°C for 15 sec; 60°C for 4 min; and keep at 4°C after the reaction.

2. Removal of the excess dye terminators by using CENTRI-SEP Columns:

CENTRI-SEP Columns are designed for the fast and efficient purification of large molecules from small molecules.

Prepare the CENTRI-SEP columns according to the standard procedures (PRINCETON SEPARATIONS, INC.) Transfer the DyeDeoxyTM terminator reaction mixture to the top of the gel. Carefully dispense the sample gently onto the centre of the gel bed at the top of the column without disturbing the gel surface. Place the column into the sample collection tube and place both into the rotor. Maintain proper column orientation. Spin the column and collection tube at 750 g for 2 min. The purified sample will be collected in the bottom of the sample collection tube. Dry the sample in a vacuum centrifuge.

3. Preparation and Loading of the samples:

Resuspend the pellet in 4 μl of the following reagent mixture containing 5 μl deionized formamide and 1 μl 25 mM EDTA with blue dextran (50 mg/ml). Centrifuge the solution to collect all the liquid at the bottom of the tube. Denature the samples at 95°C for 2 min and transfer them immediately on ice. The samples are then separated on polyacrylamide gel on the ABI PRISM 373 DNA Sequencer with the appropriate run module, DT {dR Set Any-Primer} mobility file, and matrix file.

DNA sequencing is done by R. Krug (MSZ, Würzburg).

4-3.2.10. Isolation of genomic DNA from cell and tissue

Digest small piece of mouse tail (0.5-1 cm), 50-100 mg of tissue or 5×10^6 cells in 250 μ l of the Tail Lysis Buffer with 0.4 mg/ml Proteinase K ON at 55°C. Vortex and spin to pellet the cellular debris. 1 μ l of the digest can be directly used for genotyping in 50 μ l PCR reaction. For DNA isolation transfer the SN to the new tube and add 80 μ l 6M NaCl. Vortex, incubate 5 min at RT and centrifuge at 10,000 rpm for 15 min. Transfer the SN to the new tube, add 200 μ l Isopropanol, mix carefully (do not Vortex). Fish DNA with a glass capillary. Wash with 75% Ethanol, air dry, dissolve in 150-200 μ l TE. Measure concentration, and store at +4°C.

4-3.2.11. Southern blot

Digest genomic DNA by specific restriction enzymes, separate the fragments on 0.7-1% TAE agarose gel with ethidium bromide at 3V/cm, ON. Photograph the gel, and then capillary transfer DNA onto Hybond-N membrane in 20x SSC Buffer according to manufacturer instruction (Hybond-N, Amersham). Cross-link DNA to membrane using UV-light, 120 mJ/cm². Radioactively label and hybridise a probe. The Southern blots described in this dissertation were probed with 3' and 5' template fragments labelled according to the Rediprime™ kit protocol from Amersham Pharmacia Biotech, which is based upon a standard Klenow based technique. The membrane was first incubated with prehybridising solution for 1 hr at 65°C. The solution was then changed and replaced with hybridisation solution containing the radiolabelled probe and incubated overnight at 65°C. The probe may be frozen, denatured and re-used for up to one week later. Following hybridisation, the membrane is then subjected to washing at 65°C. The membrane is washed once with washing buffer 1, followed by three times with washing buffer 2, each for 15 min. The membrane is then rinsed to remove excess SDS and exposed ON with X-Ray film.

4-3.3. Extracting and handling RNA

4-3.3.1. Isolation of RNA from cell and tissue

RNA is extremely sensitive to degradation by RNases, and should therefore be handled where possible with RNase-free materials. Cells can be directly lysed in TRIzol LS reagent, 5×10^6 cells/1ml. Tissues can be taken fresh or stored at -80°C. Frozen or fresh tissues should be put in TRIzol LS reagent solution, 50-100mg of tissue/1ml (in 15 ml Falcon tube). Homogenise in Ultra-Turrax for 30 sec at speed "5" (speed "6" for bone). Repeat until adequately

homogenised (the mechanical parts may heat up during this procedure, therefore avoid prolonged homogenisation, and keep on ice for 5 min). Add 0.2 ml Chloroform. Mix on a Vortex for 25 sec then place on ice for 15 min. Transfer to an Eppendorf tube and centrifuge at 10,000 rpm for 15 min. Transfer the upper aqueous phase to the new tube, add 0.5 ml Isopropanol, incubate 30 min at RT and centrifuge at 10,000 rpm for 15 min. Wash pellet with 75% Ethanol, air dry and resuspend in 100-150µl DEPC-H₂O. Measure concentration, and store at -20°C under 2.5 volumes ethanol.

4-3.3.2. Running RNA samples on denaturing gels

Centrifuge 10µg RNA at full speed for 15 min, take off SN and air dry (usually requires 1 min, do not dry longer!). Reconstitute with 18 µl probe buffer, pipetting up and down several times. Denature at 56°C for 10 min and add 2µl 10× loading buffer. Dissolve 1 g agarose in 77 ml DEPC water, and boil. Allow cooling to 60°C and then add 5 ml 20× MOPS and 18 ml formaldehyde. Pour gel and allow to set. The gel is run in 1× MOPS buffer. The RNA can be visualized by labelled using ethidium bromide and its integrity can be controlled by the presence of 18S and 28S rRNAs.

4-3.3.3. RT PCR

Total RNA prepared from cells or tissues are treated with amplification grade DNase I. For semiquantitative PCR of RNA, cDNA was prepared by reverse transcription (RT) of 5 µg of each RNA sample using Moloney-murine leukaemia virus reverse transcriptase (M-MuLV-RT) and random hexamer primer according manufacturer instructions. The PCR amplifications were performed in a 50 µl reaction volume containing 1/10 volume of each cDNA. Primers for for β-actin detection were mβ-actin sen/mβ-actin asen; for chimeric A-Raf: mB-Raf Ex1 sen/A-Raf rev (SacI) or mB-Raf Ex2 sen/A-Raf rev (SacI). The conditions for amplification were as follows: 95⁰ C denaturation for 2 min followed by 95⁰ C for 30 sec, 68⁰ C for 30 sec, 72⁰ C for 1 min for 35 cycles with chimeric A-Raf and 25 cycles with β-actin primers followed by 6 min extention at 72⁰ C. PCR control reaction without RT yielded no detectable fragments with either primer pair.

4-3.4. Protein methodologies

4-3.4.1. Immunoprecipitation

For immunoprecipitation of cellular proteins, protein G agarose (PGA) is employed for monoclonal antibodies, whereas protein A agarose (PAA) is used for rabbit polyclonal

antibodies. 20 µl PGA or PAA was incubated with 0.5-4 µg of antibody, 500 µl precleared lysate and the volume made up to 1 ml in an Eppendorf tube using lysis buffer. Lysates are first precleared for 1 hr with the relevant beads. Samples are incubated on a nutator for at least 2 hr at 4 °C and then washed with appropriate wash buffers, depending on the stringency required. The choice of wash buffer should insure low background and maximum preservation of complexed proteins. When analysing novel interactions, a mild wash buffer like NP40 buffer is used in order to insure that interactions between proteins of interest are not destroyed. The immunoprecipitated proteins are boiled in Laemmli buffer and subjected to SDS PAGE and Western blotting, or their activity can be analysed in *in vitro* kinase assays.

4-3.4.2. *In vitro* kinase assay

The kinase activity of an enzyme can be measured *in vitro* by the uptake of [³²P] ATP by its substrate. The immunoprecipitated kinases are washed twice with both lysis buffer and kinase buffer. Add 5 µl 10mM ATP, 2-5 µg of substrates (recombinant MEK and ERK), 0.5 µl 1M MgCl₂, 1 µl 100mM DTT and kinase buffer to 50 µl, incubate the mixture at 30°C for 30 min with shaking 1200 rpm. The reaction is then stopped by adding SDS-loading Buffer and incubated at 95°C for 5 min. The proteins are separated by SDS-PAGE, and then blotted onto nitrocellulose membranes. Western blot is performed using phospho-specific pERK antibodies. Equal loading of the immunoprecipitated kinase is subsequently controlled by immunoblotting with specific antibodies.

4-3.4.3. Measurement of Protein concentration (Bio-Rad protein assay)

The Bio-Rad Protein Assay is based on the observation that when Coomassie Brilliant Blue G-250 binds to the protein, the absorbency maximum shifts from 450 nm to 595 nm. Equal volumes of cell lysate containing 1-20 µg of protein is added to diluted Dye Reagent and mixed well (1:5 dilution of Dye Reagent Concentrate in ddH₂O). After a period of 5-10 min, the absorption at wavelength 595 is measured versus reagent blank (which contains only the lysis buffer).

4-3.4.4. Sodium dodecyl sulfate polyacrylamide gel electrophoresis (SDS PAGE)

Proteins can be easily separated on the basis of mass by electrophoresis in a polyacrylamide gel under denaturing conditions. Cells are harvested, washed, lysed. Cell debris is cleared by centrifugation. Tissues are homogenized in lysis buffer, cleared by centrifugation. Protein content is measured. 5x SDS-loading Buffer is used to denature 30-100 µg of precleared

lysates, whilst for IPs an equal amount of 2x SDS-loading is added, and then heated at 95°C for 5 min. SDS is an anionic detergent that disrupts nearly all noncovalent interactions in native proteins. β -Mercaptoethanol is also included in the sample buffer to reduce disulfide bonds. The SDS complexes with the denatured proteins are then electrophoresed on a polyacrylamide gel in the form of a thin vertical slab. Vertical gels are set in between 2 glass plates with an internal thickness of 1.5 mm between the two plates. In this chamber, the acrylamide mix is poured and left to polymerise for at least 30 min at RT. The gels are composed of two layers: a 6-15% separating gel (pH 8.8) that separates the proteins according to size; and a lower percentage (5%) stacking gel (pH 6.8) that insures the proteins simultaneous entry into the separating gel at the same height.

	Separating gel	Stacking gel
Tris pH 8.8	2.5 ml.	1.25 ml
Acrylamide/bisacrylamide 29:1 (30%)	2.0-5.0 ml	1.7 ml
10% SDS	0.1 ml	0.1 ml
ddH ₂ O	5.4-2.4 ml	6.8 ml
10% APS	0.1 ml	0.1 ml

The separating gel is poured in between two glass plates, leaving a space of about 1cm plus the length of the teeth of the comb. Isopropanol is added to the surface of the gel to exclude air. After the separating gel is polymerised, the isopropanol is removed. The stacking gel poured on top of the separating gel, the comb inserted, and allowed to polymerise. The samples are loaded into the wells of the gel and running buffer is added to the chamber. A cover is then placed over the gel chamber and 45 mA are applied. The negatively charged SDS-proteins complexes migrate in the direction of the anode at the bottom of the gel. Small proteins move rapidly through the gel, whereas large ones migrate slower. Proteins that differ in mass by about 2% can be distinguished with this method. The electrophoretic mobility of many proteins in SDS-polyacrylamide gels is proportional to the logarithm of their mass.

4-3.4.5. Immunoblotting

After the cell extracts are subjected to SDS-PAGE, the proteins are transferred by electroblotting to HybondTM-P membrane. SDS-PAGE gels are electroblotted at 400 mA in blotting buffer for 45 min. Ponceau S fixative dye solution (containing Ponceau S, trichloroacetic acid, and sulfosalicylic acid) is used to check if the transfer has occurred.

Stain for 5 min and wash with de-ionised water. For Western blot analysis, incubate the membranes in blocking buffer for 1 hr at RT or overnight at 4°C on a shaker. Dilute the first antibody in TBST/5% milk (unless otherwise indicated), add to the membrane, and incubate ON at 4°C. Wash the membrane three times with TBST, each time for 10 min. Dilute the appropriate peroxidase-conjugated secondary antibody in TBST (or according to manufacturers instructions), add to the membrane, incubate at RT for 45 min, and wash. This step is followed by the standard enhanced chemiluminescence reaction (ECL-system): incubate the membrane in a 1:1 mix of ECL solutions 1 and 2. This reaction is based on a peroxidase catalysed oxidation of Luminol, which leads to the emission of light photons that can be detected on X-ray film. Thus the peroxidase conjugated secondary antibodies bound to the primary antibody detect the protein of interest.

4-3.4.6. Immunoblot stripping

The removal of primary and secondary antibodies from a membrane is possible, so that it may be reprobbed with alternative antibodies. To make 50 ml stripping buffer, mix 3.125 ml of a 1M Tris solution, 5 ml of a 20% SDS solution, 0.35 ml of 4.3M β -Mercaptoethanol, and make up to 50ml with 42ml distilled H₂O. Incubate the membrane in stripping buffer for 30 min at 50°C. The membrane should be washed at least 5 times with PBST or TBST. The membrane can then be reprobbed as described above.

4-3.5. Cell culture techniques

4-3.5.1. Cell maintenance

The primary mouse embryonic fibroblasts (MEFs) were cultured in Dulbecco's modified Eagle's medium (DMEM) supplemented with 10% (v/v) heat inactivated (30 min., 56°C) foetal calf serum (FCS), 100 U penicillin and streptomycin per ml, and 2 mM L-glutamine, at 37°C in humidified air with 5% CO₂. The CJ7 ES cells were grown on the Mitomycin C treated feeder (MEF) layer in DMEM supplemented with 15% heat inactivated (45 min., 56°C) ES cell tested FCS, 100 U penicillin and streptomycin per ml, 2 mM L-glutamine, 500-1000 U/ml recombinant LIF (or SN from CHO LIF transfected cells, 1:250), 1x non-essential amino acids solution (Gibco), 0.1 mM β -mercaptoethanol at 37°C in humidified air with 5% CO₂. The cells were passaged every two days and the medium was changed every day. The number of cells should never exceed 1.5x10⁷/10 cm plate.

4-3.5.2. Isolation of primary of MEFs

All procedures have to be done in sterile conditions. E10.5d-13.5d pregnant mice were used. To obtain G418 resistant feeder MEFs for ES cell selection use Neo transgenic E13.5d pregnant mice. Sacrifice pregnant mouse by cervical dislocation and isolate the uterus, rinse several times in PBS. Using fine scissors open the uterine walls and release the embryos into Petri dish containing sterile PBS. Remove placenta and membranes (amnion, yolk sac), wash embryos two times with PBS. Using forceps dissect out the liver and attached internal organs, cut off embryo heads. Transfer the bodies into fresh PBS. Take 2ml syringe with 18 gauge needle attached and remove plunger. Drop the embryo bodies inside the syringe and add 1.5 ml Trypsin/EDTA. Squirt contents of syringe into 3-10 cm Petri dish and keep at 37⁰C for 5 min. Add 5-12 ml of MEF medium and pipette up and down a few times to break up the tissue. Incubate the dish at 37⁰C in humidified air with 5% CO₂. This is passage one. Do not disturb MEFs during 1-3 days to allow them to settle and attach. Change the medium after 1-2 days and split after 3-4 days. After a further 2-4 days in culture the cells can be counted and frozen.

4-3.5.3. ES cell transfection and positive clone selection

For electroporation take 30 µg of linearized targeting vector. Use 30x10⁶ ES cells, passage 10-11. Resuspend cells in 600 µl PBS, transfer to electroporation cuvette (BioRad), keep on ice. Apply 240V/500 µF (BioRad Pulser), plate onto 10x10 cm dishes. After one day (24 h) change the medium and start G418 selection, continue until the cells are frozen in 96 well plate. Start Gancyclovir (GANC) selection two days after electroporation. Continue GANC selection for 5-6 days. Prepare every day fresh medium with GANC. Change the medium every day until the colonies are enough big to pick them. It takes 8-12 days. From one 10 cm plate 10-70 colonies, depending on the construct, could be obtained.

4-3.5.4. Independent clone isolation

All procedures have to be done in sterile conditions. At least 300-400 independent colonies should be isolated to screen for homologous recombination. Prepare 96 well flat-bottom plates with Mitomycin C treated feeder MEFs in ESC medium. Prepare 96 well U-bottom plates, add 30 µl Trypsin/EDTA per well. Remove ESC medium and add 10 ml PBS/10 cm dish with ES cell colonies. Pick the colonies under binocular or microscope using P20 white tips. Place the colony in a well of 96 well plate containing Trypsin/EDTA until cell clumps are dispersed. Pipette five times and transfer to the well of 96 well plate with feeder cells.

Grow for 2-3 days, change the medium every day. Trypsinize and split 1:3 (e.g. make 3 master plates) when the cells are almost confluent. Freeze 2 plates, use 1 plate for DNA isolation for PCR or transfer the cells into 48 well plates when prepare DNA for Southern blot.

4-3.5.5. Cell proliferation assay

Grow MEFs in 96 well plate. Add 10 μ l MTT solution (5mg/ml) to each well. Incubate 2-3 h at 37⁰C in humidified air with 5% CO₂. Remove medium, add 100 μ l DMSO, resuspend. Measure the absorbtion at 570 nM in spectrophotometer.

4-3.5.6. Cell survival assay

For the analysis of cell survival and intracellular signalling pathways MEFs from 24 well tissue culture plate were trypsinized, washed in PBS. 2×10^5 cells/well were diluted in 100 μ l PBS. Cell viability was routinely assessed by staining the cells in trypan blue (Sigma).

4-3.5.7. ES cell injection and production of chimeras.

The inbred C57B16 (abbreviated as B6) and (C57B16xDBA2)F1 (abbreviated as B6D2F1) hybrid mice were used for blastocyst production. The B6 and B6D2F2 host embryos are equally well suited for germ line transmission (g.l.t.) of the 129/Sv-derived ES genome (CJ7 ES cells). At day 3.5 post coitum (dpc), blastocysts were flushed from the uteri with prewarmed M2 medium and kept in M16 droplet cultures under mineral oil at 37⁰C, 5% CO₂ until injection. ES cells were prepared for injection as follow: 2 –3 days before injection the cells were plated at the low dense feeder layer and passaged at least one time. At the day of injection they were trypsinized, washed with PBS two times and resuspended in Injection medium containing DNase. Approximately 10–20 ES cells were injected per blastocyst. After reexpansion of the blastocoel (1–2 h), 8–12 blastocysts per female were transferred into 2.5 dpc pseudopregnant NMRI or B6D2F1 fosters. The chimerism of the delivered mice was identified on the basis of agouti pigmentation in the coat eight to nine days after birth. All male and some female chimeras were tested for g.l.t. by breeding with B6 mice. The transmission of transgenes in the germline was analysed by standard PCR and Southern blot methods.

4-3.6. Immunohistochemical methods.

4-3.6.1. Embedding in paraffin

Wash isolated embryos or organs several times in PBS, fix ON in 4% Paraformaldehyde, RT. Incubate as follow: 40 min in 50% Ethanol, 40 min in 70% Ethanol, 40 min in 80% Ethanol, 40 min in 90% Ethanol, 40 min in 95% Ethanol, 3x 40 min in 100% Ethanol, 2x 30 min in 1:1 (Chloroform:Ethanol), 30 min in Chloroform:Ethanol. All procedures perform at RT. Transfer embryos or organs into melted Paraffin, incubate 1h at 65⁰C. Change Paraffin and incubate 2h or ON at 65⁰C. Prepare the Paraffin blocks. Embryos and organs are sectioned into 6-10 µm microsections and can be used for the further TUNEL or immunohistochemistry assays.

4-3.6.1. Hematoxylin/eosin staining

All procedures are performed at RT. After deparaffinization in machine wash the glasses in water, incubate 3 min in Hematoxylin solution. Transfer the glasses into water with ammonium (1 drop of liquid ammonium/100 ml H₂O) for 1 min. Transfer into 1% Eosin solution for 30 sec. Incubate the slides 3x 1min in Ethanol, and then 3x 2min in Ethanol. Transfer in Xylol, incubate 2x 1 min, and 1x 5 min in Xylol. Mount in Depex.

4-3.6.2. TUNEL assay

TUNEL assay was performed on the 6 µm thick paraffin sections according to the manufacturer's protocol using In Situ Cell Death Detection, POD kit (Roche). 3'OH DNA groups in the apoptotic cells were labeled by fluorescein-labeled nucleotids with terminal deoxynucleotidyl transferase (TdT) followed by direct immunoperoxidase labeling of fluorescein-labeled genomic DNA. A TUNEL negative control was obtained by ommiting TdT from labeling mix. The sections were then counterstained with hematoxylin. Positive nuclei were scored both on the basis DAB labeling and morphological features of of apoptosis including nuclear versus cytoplasmic staining, death of single cells, marked condensation of chromatin and cytoplasm, uniformly dense of chromatin, intracellular chromatin fragmentation (micronuclei) and halo effect around the nucleus.

4-3.6.3 Immunohistochemistry

Paraffin-embedded 6 µm thick sections were deparaffinized in machine, rehydrated and microwaved 6 min in 10 mM sodium citrate, pH 5,5 and washed 3x5 min in PBS. Subsequently the slides were incubated 6 min in peroxidase blocking solution (3% H₂O₂ in

PBS) and washed 3x5 min in PBS. After antigen retrieval, slides were rinsed in distilled water, incubated in 20% sucrose/PBS at +4⁰ C 30 min, washed in PBS and placed in blocking buffer (5% goat serum in PBS) for 40 min. Subsequently the slides were incubated in the presence of the first antibodies (see table) in blocking buffer at +4⁰ C, ON. The slides were washed 3x 5 min in PBS, secondary biotinylated antibodies in blocking buffer were applied and the slides were incubated 1h at RT. Antigene-antibody complexes were detected using immunoperoxidase system (Vectastain[®] ABC Kit, Vector) according manufacturer instructions. The sections were then counterstained with hematoxylin to stain the nuclei. All immunohistochemical reactions were carried out in parallel with reactions lacking primary antibodies to ensure the specificity of the observed staining.

First antibody	<u>Dilution</u>	<u>Source</u>	Second antibody	<u>Dilution</u>	<u>Source</u>
PCNA	1:300	Pharmigen	Biotynilated anti-mouse	1:200	Dako
GFAP	1:500	Chemicon	Biotynilated anti-rabbit	1:400	Dako
TuJ-1	1:200	Chemicon	Biotynilated anti-mouse	1:400	Dako
Neu-N	1:100	Chemicon	Biotynilated anti-mouse	1:400	Dako
P-ERK	1:100	Cell Signalling	Biotynilated anti-rabbit	1:200	Dako

5. BIBLIOGRAPHY

1. Wojnowski, L., *et al.*, *Endothelial apoptosis in Braf-deficient mice*. Nat Genet, 1997. **16**(3): p. 293-7.
2. Daum, G., *et al.*, *The ins and outs of Raf kinases*. Trends Biochem Sci, 1994. **19**(11): p. 474-80.
3. Naumann, U., *et al.*, *Raf protein serine/threonine kinases*. In "Protein Phosphorylation", VCH, Weinheim, 1996.
4. Mercer, K.E. and C.A. Pritchard, *Raf proteins and cancer: B-Raf is identified as a mutational target*. Biochim Biophys Acta, 2003. **1653**(1): p. 25-40.
5. Eychene, A., *et al.*, *Chromosomal assignment of two human B-raf(Rmil) proto-oncogene loci: B-raf-1 encoding the p94Braf/Rmil and B-raf-2, a processed pseudogene*. Oncogene, 1992. **7**(8): p. 1657-60.
6. Barnier, J.V., *et al.*, *The mouse B-raf gene encodes multiple protein isoforms with tissue-specific expression*. J Biol Chem, 1995. **270**(40): p. 23381-9.
7. Papin, C., *et al.*, *Modulation of kinase activity and oncogenic properties by alternative splicing reveals a novel regulatory mechanism for B-Raf*. J Biol Chem, 1998. **273**(38): p. 24939-47.
8. Eychene, A., *et al.*, *Quail neuroretina c-Rmil(B-raf) proto-oncogene cDNAs encode two proteins of 93.5 and 95 kDa resulting from alternative splicing*. Oncogene, 1992. **7**(7): p. 1315-23.
9. Storm, S.M., J.L. Cleveland, and U.R. Rapp, *Expression of raf family proto-oncogenes in normal mouse tissues*. Oncogene, 1990. **5**(3): p. 345-51.
10. Luckett, J.C., *et al.*, *Expression of the A-raf proto-oncogene in the normal adult and embryonic mouse*. Cell Growth Differ, 2000. **11**(3): p. 163-71.
11. Mott, H.R., *et al.*, *The solution structure of the Raf-1 cysteine-rich domain: a novel ras and phospholipid binding site*. Proc Natl Acad Sci U S A, 1996. **93**(16): p. 8312-7.
12. Erhardt, P., *et al.*, *Differential regulation of Raf-1 and B-Raf and Ras-dependent activation of mitogen-activated protein kinase by cyclic AMP in PC12 cells*. Mol Cell Biol, 1995. **15**(10): p. 5524-30.
13. Marais, R., *et al.*, *Differential regulation of Raf-1, A-Raf, and B-Raf by oncogenic ras and tyrosine kinases*. J Biol Chem, 1997. **272**(7): p. 4378-83.
14. Kolch, W., *et al.*, *Raf-1 protein kinase is required for growth of induced NIH/3T3 cells*. Nature, 1991. **349**(6308): p. 426-8.
15. Abrams, S.I., *et al.*, *Mutant ras epitopes as targets for cancer vaccines*. Semin Oncol, 1996. **23**(1): p. 118-34.
16. Davies, H., *et al.*, *Mutations of the BRAF gene in human cancer*. Nature, 2002. **417**(6892): p. 949-54.
17. Daub, M., *et al.*, *The RafC1 cysteine-rich domain contains multiple distinct regulatory epitopes which control Ras-dependent Raf activation*. Mol Cell Biol, 1998. **18**(11): p. 6698-710.
18. Cutler, R.E., Jr., *et al.*, *Autoregulation of the Raf-1 serine/threonine kinase*. Proc Natl Acad Sci U S A, 1998. **95**(16): p. 9214-9.
19. Campbell, S.L., *et al.*, *Increasing complexity of Ras signaling*. Oncogene, 1998. **17**(11 Reviews): p. 1395-413.
20. Voice, J.K., *et al.*, *Four human ras homologs differ in their abilities to activate Raf-1, induce transformation, and stimulate cell motility*. J Biol Chem, 1999. **274**(24): p. 17164-70.
21. Prior, I.A. and J.F. Hancock, *Compartmentalization of Ras proteins*. J Cell Sci, 2001. **114**(Pt 9): p. 1603-8.

22. Reuther, G.W. and C.J. Der, *The Ras branch of small GTPases: Ras family members don't fall far from the tree*. *Curr Opin Cell Biol*, 2000. **12**(2): p. 157-65.
23. Weber, C.K., *et al.*, *Mitogenic signaling of Ras is regulated by differential interaction with Raf isozymes*. *Oncogene*, 2000. **19**(2): p. 169-76.
24. Mason, C.S., *et al.*, *Serine and tyrosine phosphorylations cooperate in Raf-1, but not B-Raf activation*. *Embo J*, 1999. **18**(8): p. 2137-48.
25. Graham, S.M., *et al.*, *TC21 and Ras share indistinguishable transforming and differentiating activities*. *Oncogene*, 1999. **18**(12): p. 2107-16.
26. Rosario, M., H.F. Paterson, and C.J. Marshall, *Activation of the Raf/MAP kinase cascade by the Ras-related protein TC21 is required for the TC21-mediated transformation of NIH 3T3 cells*. *Embo J*, 1999. **18**(5): p. 1270-9.
27. Wixler, V., *et al.*, *Differential regulation of Raf isozymes by growth versus differentiation inducing factors in PC12 pheochromocytoma cells*. *FEBS Lett*, 1996. **385**(3): p. 131-7.
28. York, R.D., *et al.*, *Rap1 mediates sustained MAP kinase activation induced by nerve growth factor*. *Nature*, 1998. **392**(6676): p. 622-6.
29. Schramm, K., *et al.*, *Phosphorylation of c-Raf-1 by protein kinase A interferes with activation*. *Biochem Biophys Res Commun*, 1994. **201**(2): p. 740-7.
30. Hu, C.D., *et al.*, *Coassociation of Rap1A and Ha-Ras with Raf-1 N-terminal region interferes with ras-dependent activation of Raf-1*. *J Biol Chem*, 1997. **272**(18): p. 11702-5.
31. Vossler, M.R., *et al.*, *cAMP activates MAP kinase and Elk-1 through a B-Raf- and Rap1-dependent pathway*. *Cell*, 1997. **89**(1): p. 73-82.
32. Grewal, S.S., *et al.*, *Neuronal calcium activates a Rap1 and B-Raf signaling pathway via the cyclic adenosine monophosphate-dependent protein kinase*. *J Biol Chem*, 2000. **275**(5): p. 3722-8.
33. Aitken, A., *14-3-3 proteins on the MAP*. *Trends Biochem Sci*, 1995. **20**(3): p. 95-7.
34. Muslin, A.J. and H. Xing, *14-3-3 proteins: regulation of subcellular localization by molecular interference*. *Cell Signal*, 2000. **12**(11-12): p. 703-9.
35. Fu, H., R.R. Subramanian, and S.C. Masters, *14-3-3 proteins: structure, function, and regulation*. *Annu Rev Pharmacol Toxicol*, 2000. **40**: p. 617-47.
36. Finnie, C., J. Borch, and D.B. Collinge, *14-3-3 proteins: eukaryotic regulatory proteins with many functions*. *Plant Mol Biol*, 1999. **40**(4): p. 545-54.
37. Datta, S.R., *et al.*, *14-3-3 proteins and survival kinases cooperate to inactivate BAD by BH3 domain phosphorylation*. *Mol Cell*, 2000. **6**(1): p. 41-51.
38. Muslin, A.J., *et al.*, *Interaction of 14-3-3 with signaling proteins is mediated by the recognition of phosphoserine*. *Cell*, 1996. **84**(6): p. 889-97.
39. Petosa, C., *et al.*, *14-3-3zeta binds a phosphorylated Raf peptide and an unphosphorylated peptide via its conserved amphipathic groove*. *J Biol Chem*, 1998. **273**(26): p. 16305-10.
40. Yaffe, M.B., *et al.*, *The structural basis for 14-3-3:phosphopeptide binding specificity*. *Cell*, 1997. **91**(7): p. 961-71.
41. Fantl, W.J., *et al.*, *Activation of Raf-1 by 14-3-3 proteins*. *Nature*, 1994. **371**(6498): p. 612-4.
42. Freed, E., F. McCormick, and R. Ruggieri, *Proteins of the 14-3-3 family associate with Raf and contribute to its activation*. *Cold Spring Harb Symp Quant Biol*, 1994. **59**: p. 187-93.
43. Roy, S., *et al.*, *14-3-3 facilitates Ras-dependent Raf-1 activation in vitro and in vivo*. *Mol Cell Biol*, 1998. **18**(7): p. 3947-55.
44. Yip-Schneider, M.T., *et al.*, *Regulation of the Raf-1 kinase domain by phosphorylation and 14-3-3 association*. *Biochem J*, 2000. **351**(Pt 1): p. 151-9.

45. Fu, H., *et al.*, *Interaction of the protein kinase Raf-1 with 14-3-3 proteins*. *Science*, 1994. **266**(5182): p. 126-9.
46. Michaud, N.R., *et al.*, *14-3-3 is not essential for Raf-1 function: identification of Raf-1 proteins that are biologically activated in a 14-3-3- and Ras- independent manner*. *Mol Cell Biol*, 1995. **15**(6): p. 3390-7.
47. Suen, K.L., X.R. Bustelo, and M. Barbacid, *Lack of evidence for the activation of the Ras/Raf mitogenic pathway by 14-3-3 proteins in mammalian cells*. *Oncogene*, 1995. **11**(5): p. 825-31.
48. Rommel, C., *et al.*, *Activated Ras displaces 14-3-3 protein from the amino terminus of c-Raf-1*. *Oncogene*, 1996. **12**(3): p. 609-19.
49. Tzivion, G., Z. Luo, and J. Avruch, *A dimeric 14-3-3 protein is an essential cofactor for Raf kinase activity*. *Nature*, 1998. **394**(6688): p. 88-92.
50. Avruch, J., *et al.*, *Ras activation of the Raf kinase: tyrosine kinase recruitment of the MAP kinase cascade*. *Recent Prog Horm Res*, 2001. **56**: p. 127-55.
51. Rommel, C., *et al.*, *Differentiation stage-specific inhibition of the Raf-MEK-ERK pathway by Akt*. *Science*, 1999. **286**(5445): p. 1738-41.
52. Zimmermann, S. and K. Moelling, *Phosphorylation and regulation of Raf by Akt (protein kinase B)*. *Science*, 1999. **286**(5445): p. 1741-4.
53. Abraham, D., *et al.*, *Raf-1-associated protein phosphatase 2A as a positive regulator of kinase activation*. *J Biol Chem*, 2000. **275**(29): p. 22300-4.
54. Jaumot, M. and J.F. Hancock, *Protein phosphatases 1 and 2A promote Raf-1 activation by regulating 14-3-3 interactions*. *Oncogene*, 2001. **20**(30): p. 3949-58.
55. Wassarman, D.A., *et al.*, *Protein phosphatase 2A positively and negatively regulates Ras1-mediated photoreceptor development in Drosophila*. *Genes Dev*, 1996. **10**(3): p. 272-8.
56. Sieburth, D.S., *et al.*, *A PP2A regulatory subunit positively regulates Ras-mediated signaling during Caenorhabditis elegans vulval induction*. *Genes Dev*, 1999. **13**(19): p. 2562-9.
57. Braselmann, S. and F. McCormick, *Bcr and Raf form a complex in vivo via 14-3-3 proteins*. *Embo J*, 1995. **14**(19): p. 4839-48.
58. Clark, G.J., *et al.*, *14-3-3 zeta negatively regulates raf-1 activity by interactions with the Raf-1 cysteine-rich domain*. *J Biol Chem*, 1997. **272**(34): p. 20990-3.
59. Williams, J.G., *et al.*, *Elucidation of binding determinants and functional consequences of Ras/Raf-cysteine-rich domain interactions*. *J Biol Chem*, 2000. **275**(29): p. 22172-9.
60. McPherson, R.A., *et al.*, *Interactions of c-Raf-1 with phosphatidylserine and 14-3-3*. *Oncogene*, 1999. **18**(26): p. 3862-9.
61. Thorson, J.A., *et al.*, *14-3-3 proteins are required for maintenance of Raf-1 phosphorylation and kinase activity*. *Mol Cell Biol*, 1998. **18**(9): p. 5229-38.
62. Dent, P., *et al.*, *Reversal of Raf-1 activation by purified and membrane-associated protein phosphatases*. *Science*, 1995. **268**(5219): p. 1902-6.
63. Morrison, D.K., *et al.*, *Identification of the major phosphorylation sites of the Raf-1 kinase*. *J Biol Chem*, 1993. **268**(23): p. 17309-16.
64. King, A.J., *et al.*, *The protein kinase Pak3 positively regulates Raf-1 activity through phosphorylation of serine 338*. *Nature*, 1998. **396**(6707): p. 180-3.
65. Fabian, J.R., I.O. Daar, and D.K. Morrison, *Critical tyrosine residues regulate the enzymatic and biological activity of Raf-1 kinase*. *Mol Cell Biol*, 1993. **13**(11): p. 7170-9.
66. Chong, H., J. Lee, and K.L. Guan, *Positive and negative regulation of Raf kinase activity and function by phosphorylation*. *Embo J*, 2001. **20**(14): p. 3716-27.

67. Kolch, W., *Meaningful relationships: the regulation of the Ras/Raf/MEK/ERK pathway by protein interactions*. *Biochem J*, 2000. **351 Pt 2**: p. 289-305.
68. Chaudhary, A., *et al.*, *Phosphatidylinositol 3-kinase regulates Raf1 through Pak phosphorylation of serine 338*. *Curr Biol*, 2000. **10(9)**: p. 551-4.
69. Chiloeches, A., C.S. Mason, and R. Marais, *S338 phosphorylation of Raf-1 is independent of phosphatidylinositol 3-kinase and Pak3*. *Mol Cell Biol*, 2001. **21(7)**: p. 2423-34.
70. Alavi, A., *et al.*, *Role of Raf in vascular protection from distinct apoptotic stimuli*. *Science*, 2003. **301(5629)**: p. 94-6.
71. Tilbrook, P.A., *et al.*, *Erythropoietin-stimulated Raf-1 tyrosine phosphorylation is associated with the tyrosine kinase Lyn in J2E erythroleukemic cells*. *Arch Biochem Biophys*, 2001. **396(1)**: p. 128-32.
72. Huser, M., *et al.*, *MEK kinase activity is not necessary for Raf-1 function*. *Embo J*, 2001. **20(8)**: p. 1940-51.
73. M. Hekmann, U.R.R., *manuscript in preparation*.
74. Kolch, W., *et al.*, *Protein kinase C alpha activates RAF-1 by direct phosphorylation*. *Nature*, 1993. **364(6434)**: p. 249-52.
75. Schonwasser, D.C., *et al.*, *Activation of the mitogen-activated protein kinase/extracellular signal-regulated kinase pathway by conventional, novel, and atypical protein kinase C isoforms*. *Mol Cell Biol*, 1998. **18(2)**: p. 790-8.
76. Dhillon, A.S., *et al.*, *Cyclic AMP-dependent kinase regulates Raf-1 kinase mainly by phosphorylation of serine 259*. *Mol Cell Biol*, 2002. **22(10)**: p. 3237-46.
77. Dhillon, A.S., *et al.*, *Regulation of Raf-1 activation and signalling by dephosphorylation*. *Embo J*, 2002. **21(1-2)**: p. 64-71.
78. Mischak, H., *et al.*, *Negative regulation of Raf-1 by phosphorylation of serine 621*. *Mol Cell Biol*, 1996. **16(10)**: p. 5409-18.
79. Wu, J., *et al.*, *Inhibition of the EGF-activated MAP kinase signaling pathway by adenosine 3',5'-monophosphate*. *Science*, 1993. **262(5136)**: p. 1065-9.
80. Yao, B., *et al.*, *Phosphorylation of Raf by ceramide-activated protein kinase*. *Nature*, 1995. **378(6554)**: p. 307-10.
81. Morrison, D.K., *KSR: a MAPK scaffold of the Ras pathway?* *J Cell Sci*, 2001. **114(Pt 9)**: p. 1609-12.
82. Jelinek, T., *et al.*, *RAS and RAF-1 form a signalling complex with MEK-1 but not MEK-2*. *Mol Cell Biol*, 1994. **14(12)**: p. 8212-8.
83. Wu, X., *et al.*, *Selective activation of MEK1 but not MEK2 by A-Raf from epidermal growth factor-stimulated Hela cells*. *J Biol Chem*, 1996. **271(6)**: p. 3265-71.
84. Xu, S., *et al.*, *Differential regulation of mitogen-activated protein/ERK kinase (MEK)1 and MEK2 and activation by a Ras-independent mechanism*. *Mol Endocrinol*, 1997. **11(11)**: p. 1618-25.
85. Zheng, C.F. and K.L. Guan, *Activation of MEK family kinases requires phosphorylation of two conserved Ser/Thr residues*. *Embo J*, 1994. **13(5)**: p. 1123-31.
86. Yan, M. and D.J. Templeton, *Identification of 2 serine residues of MEK-1 that are differentially phosphorylated during activation by raf and MEK kinase*. *J Biol Chem*, 1994. **269(29)**: p. 19067-73.
87. Alessi, D.R., *et al.*, *Identification of the sites in MAP kinase kinase-1 phosphorylated by p74raf-1*. *Embo J*, 1994. **13(7)**: p. 1610-9.
88. Catling, A.D., *et al.*, *A proline-rich sequence unique to MEK1 and MEK2 is required for raf binding and regulates MEK function*. *Mol Cell Biol*, 1995. **15(10)**: p. 5214-25.
89. Pritchard, C.A., *et al.*, *Conditionally oncogenic forms of the A-Raf and B-Raf protein kinases display different biological and biochemical properties in NIH 3T3 cells*. *Mol Cell Biol*, 1995. **15(11)**: p. 6430-42.

90. Catling, A.D., *et al.*, *Partial purification of a mitogen-activated protein kinase kinase activator from bovine brain. Identification as B-Raf or a B-Raf-associated activity.* J Biol Chem, 1994. **269**(47): p. 30014-21.
91. Jaiswal, R.K., *et al.*, *The mitogen-activated protein kinase cascade is activated by B-Raf in response to nerve growth factor through interaction with p21ras.* Mol Cell Biol, 1994. **14**(10): p. 6944-53.
92. Reuter, C.W., *et al.*, *Biochemical analysis of MEK activation in NIH3T3 fibroblasts. Identification of B-Raf and other activators.* J Biol Chem, 1995. **270**(13): p. 7644-55.
93. Mikula, M., *et al.*, *Embryonic lethality and fetal liver apoptosis in mice lacking the c-raf-1 gene.* Embo J, 2001. **20**(8): p. 1952-62.
94. Papin, C., *et al.*, *Identification of signalling proteins interacting with B-Raf in the yeast two-hybrid system.* Oncogene, 1996. **12**(10): p. 2213-21.
95. Pritchard, C.A., *et al.*, *Post-natal lethality and neurological and gastrointestinal defects in mice with targeted disruption of the A-Raf protein kinase gene.* Curr Biol, 1996. **6**(5): p. 614-7.
96. Wojnowski, L., *et al.*, *Overlapping and specific functions of Braf and Crafl-1 proto-oncogenes during mouse embryogenesis.* Mech Dev, 2000. **91**(1-2): p. 97-104.
97. Mercer, K., *et al.*, *ERK signalling and oncogene transformation are not impaired in cells lacking A-Raf.* Oncogene, 2002. **21**(3): p. 347-55.
98. Wojnowski, L., *et al.*, *Crafl-1 protein kinase is essential for mouse development.* Mech Dev, 1998. **76**(1-2): p. 141-9.
99. Schaeffer, H.J., *et al.*, *MPI: a MEK binding partner that enhances enzymatic activation of the MAP kinase cascade.* Science, 1998. **281**(5383): p. 1668-71.
100. Therrien, M., *et al.*, *KSR, a novel protein kinase required for RAS signal transduction.* Cell, 1995. **83**(6): p. 879-88.
101. Denouel-Galy, A., *et al.*, *Murine Ksr interacts with MEK and inhibits Ras-induced transformation.* Curr Biol, 1998. **8**(1): p. 46-55.
102. Yu, W., *et al.*, *Regulation of the MAP kinase pathway by mammalian Ksr through direct interaction with MEK and ERK.* Curr Biol, 1998. **8**(1): p. 56-64.
103. Cacace, A.M., *et al.*, *Identification of constitutive and ras-inducible phosphorylation sites of KSR: implications for 14-3-3 binding, mitogen-activated protein kinase binding, and KSR overexpression.* Mol Cell Biol, 1999. **19**(1): p. 229-40.
104. Therrien, M., *et al.*, *KSR modulates signal propagation within the MAPK cascade.* Genes Dev, 1996. **10**(21): p. 2684-95.
105. Xing, H., K. Kornfeld, and A.J. Muslin, *The protein kinase KSR interacts with 14-3-3 protein and Raf.* Curr Biol, 1997. **7**(5): p. 294-300.
106. Zhang, Y., *et al.*, *Kinase suppressor of Ras is ceramide-activated protein kinase.* Cell, 1997. **89**(1): p. 63-72.
107. Xing, H.R. and R. Kolesnick, *Kinase suppressor of Ras signals through Thr269 of c-Raf-1.* J Biol Chem, 2001. **276**(13): p. 9733-41.
108. Michaud, N.R., *et al.*, *KSR stimulates Raf-1 activity in a kinase-independent manner.* Proc Natl Acad Sci U S A, 1997. **94**(24): p. 12792-6.
109. Muller, J., *et al.*, *Identification of B-KSR1, a novel brain-specific isoform of KSR1 that functions in neuronal signaling.* Mol Cell Biol, 2000. **20**(15): p. 5529-39.
110. Stewart, S., *et al.*, *Kinase suppressor of Ras forms a multiprotein signaling complex and modulates MEK localization.* Mol Cell Biol, 1999. **19**(8): p. 5523-34.
111. Bell, B., *et al.*, *KSR-1 binds to G-protein betagamma subunits and inhibits beta gamma-induced mitogen-activated protein kinase activation.* J Biol Chem, 1999. **274**(12): p. 7982-6.
112. Peyssonnaud, C., *et al.*, *Induction of postmitotic neuroretina cell proliferation by distinct Ras downstream signaling pathways.* Mol Cell Biol, 2000. **20**(19): p. 7068-79.

113. Levchenko, A., J. Bruck, and P.W. Sternberg, *Scaffold proteins may biphasically affect the levels of mitogen- activated protein kinase signaling and reduce its threshold properties*. Proc Natl Acad Sci U S A, 2000. **97**(11): p. 5818-23.
114. Yeung, K., *et al.*, *Suppression of Raf-1 kinase activity and MAP kinase signalling by RKIP*. Nature, 1999. **401**(6749): p. 173-7.
115. Yeung, K., *et al.*, *Mechanism of suppression of the Raf/MEK/extracellular signal-regulated kinase pathway by the raf kinase inhibitor protein*. Mol Cell Biol, 2000. **20**(9): p. 3079-85.
116. Wakioka, T., *et al.*, *Spred is a Sprouty-related suppressor of Ras signalling*. Nature, 2001. **412**(6847): p. 647-51.
117. Blagosklonny, M.V., *Hsp-90-associated oncoproteins: multiple targets of geldanamycin and its analogs*. Leukemia, 2002. **16**(4): p. 455-62.
118. Wang, H.G., *et al.*, *Bcl-2 interacting protein, BAG-1, binds to and activates the kinase Raf- 1*. Proc Natl Acad Sci U S A, 1996. **93**(14): p. 7063-8.
119. Song, J., M. Takeda, and R.I. Morimoto, *Bag1-Hsp70 mediates a physiological stress signalling pathway that regulates Raf-1/ERK and cell growth*. Nat Cell Biol, 2001. **3**(3): p. 276-82. [taf/DynaPage.taf?file=/ncb/journal/v3/n3/full/ncb0301_276.html](http://www.nature.com/ncb/journal/v3/n3/full/ncb0301_276.html)
[taf/DynaPage.taf?file=/ncb/journal/v3/n3/abs/ncb0301_276.html](http://www.nature.com/ncb/journal/v3/n3/abs/ncb0301_276.html).
120. Kalmes, A., *et al.*, *Interaction between the protein kinase B-Raf and the alpha-subunit of the 11S proteasome regulator*. Cancer Res, 1998. **58**(14): p. 2986-90.
121. Zhang, Z., *et al.*, *Identification of an activation region in the proteasome activator REGalpha*. Proc Natl Acad Sci U S A, 1998. **95**(6): p. 2807-11.
122. Groettrup, M., *et al.*, *A role for the proteasome regulator PA28alpha in antigen presentation*. Nature, 1996. **381**(6578): p. 166-8.
123. Seliger, B., M.J. Maeurer, and S. Ferrone, *TAP off--tumors on*. Immunol Today, 1997. **18**(6): p. 292-9.
124. Drexler, H.C., *Activation of the cell death program by inhibition of proteasome function*. Proc Natl Acad Sci U S A, 1997. **94**(3): p. 855-60.
125. Grimm, L.M., *et al.*, *Proteasomes play an essential role in thymocyte apoptosis*. Embo J, 1996. **15**(15): p. 3835-44.
126. Sadoul, R., *et al.*, *Involvement of the proteasome in the programmed cell death of NGF- deprived sympathetic neurons*. Embo J, 1996. **15**(15): p. 3845-52.
127. Wang, H.G., U.R. Rapp, and J.C. Reed, *Bcl-2 targets the protein kinase Raf-1 to mitochondria*. Cell, 1996. **87**(4): p. 629-38.
128. Wang, H.G. and J.C. Reed, *Bcl-2, Raf-1 and mitochondrial regulation of apoptosis*. Biofactors, 1998. **8**(1-2): p. 13-6.
129. Zha, J., *et al.*, *Serine phosphorylation of death agonist BAD in response to survival factor results in binding to 14-3-3 not BCL-X(L)*. Cell, 1996. **87**(4): p. 619-28.
130. hZhong, J., J. Troppmair, and U.R. Rapp, *Independent control of cell survival by Raf-1 and Bcl-2 at the mitochondria*. Oncogene, 2001. **20**(35): p. 4807-16.
131. Le Mellay, V., *et al.*, *Negative regulation of mitochondrial VDAC channels by C-Raf kinase*. BMC Cell Biol, 2002. **3**(1): p. 14.
132. Benz, R., *Permeation of hydrophilic solutes through mitochondrial outer membranes: review on mitochondrial porins*. Biochim Biophys Acta, 1994. **1197**(2): p. 167-96.
133. Shimizu, S., *et al.*, *Electrophysiological study of a novel large pore formed by Bax and the voltage-dependent anion channel that is permeable to cytochrome c*. J Biol Chem, 2000. **275**(16): p. 12321-5.
134. Shimizu, S., *et al.*, *BH4 domain of antiapoptotic Bcl-2 family members closes voltage-dependent anion channel and inhibits apoptotic mitochondrial changes and cell death*. Proc Natl Acad Sci U S A, 2000. **97**(7): p. 3100-5.

135. Shimizu, S., *et al.*, *Essential role of voltage-dependent anion channel in various forms of apoptosis in mammalian cells*. J Cell Biol, 2001. **152**(2): p. 237-50.
136. Chen, J., *et al.*, *Raf-1 promotes cell survival by antagonizing apoptosis signal-regulating kinase 1 through a MEK-ERK independent mechanism*. Proc Natl Acad Sci U S A, 2001. **98**(14): p. 7783-8.
137. Nantel, A., M. Huber, and D.Y. Thomas, *Localization of endogenous Grb10 to the mitochondria and its interaction with the mitochondrial-associated Raf-1 pool*. J Biol Chem, 1999. **274**(50): p. 35719-24.
138. Peruzzi, F., *et al.*, *Multiple signaling pathways of the insulin-like growth factor 1 receptor in protection from apoptosis*. Mol Cell Biol, 1999. **19**(10): p. 7203-15.
139. Peruzzi, F., *et al.*, *Anti-apoptotic signaling of the insulin-like growth factor-I receptor through mitochondrial translocation of c-Raf and Nedd4*. J Biol Chem, 2001. **276**(28): p. 25990-6.
140. Attar, R.M., *et al.*, *Genetic approaches to study Rel/NF-kappa B/I kappa B function in mice*. Semin Cancer Biol, 1997. **8**(2): p. 93-101.
141. Foo, S.Y. and G.P. Nolan, *NF-kappaB to the rescue: RELs, apoptosis and cellular transformation*. Trends Genet, 1999. **15**(6): p. 229-35.
142. Baldwin, A.S., Jr., *The NF-kappa B and I kappa B proteins: new discoveries and insights*. Annu Rev Immunol, 1996. **14**: p. 649-83.
143. Baumann, B., *et al.*, *Raf induces NF-kappaB by membrane shuttle kinase MEKK1, a signaling pathway critical for transformation*. Proc Natl Acad Sci U S A, 2000. **97**(9): p. 4615-20.
144. Hagemann, C., *et al.*, *The regulatory subunit of protein kinase CK2 is a specific A-Raf activator*. FEBS Lett, 1997. **403**(2): p. 200-2.
145. Stalter, G., *et al.*, *Asymmetric expression of protein kinase CK2 subunits in human kidney tumors*. Biochem Biophys Res Commun, 1994. **202**(1): p. 141-7.
146. Hagemann, C., *et al.*, *A-Raf kinase and pyruvate kinase type M2 link mitogenic signaling with metabolism*. Submitted for publication.
147. Brinck, U., *et al.*, *L- and M2-pyruvate kinase expression in renal cell carcinomas and their metastases*. Virchows Arch, 1994. **424**(2): p. 177-85.
148. Le Mellay, V., *et al.*, *Regulation of glycolysis by Raf protein serine/threonine kinases*. Adv Enzyme Regul, 2002. **42**: p. 317-32.
149. Eigenbrodt, E., *et al.*, *Pyruvate kinase and the interaction of amino acid and carbohydrate metabolism in solid tumors*. Anticancer Res, 1998. **18**(5A): p. 3267-74.
150. Yuryev, A., *et al.*, *Isoform-specific localization of A-RAF in mitochondria*. Mol Cell Biol, 2000. **20**(13): p. 4870-8.
151. Wiese, S., *et al.*, *Specific function of B-Raf in mediating survival of embryonic motoneurons and sensory neurons*. Nat Neurosci, 2001. **4**(2): p. 137-42.
152. Creedon, D.J., E.M. Johnson, and J.C. Lawrence, *Mitogen-activated protein kinase-independent pathways mediate the effects of nerve growth factor and cAMP on neuronal survival*. J Biol Chem, 1996. **271**(34): p. 20713-8.
153. Mazzoni, I.E., *et al.*, *Ras regulates sympathetic neuron survival by suppressing the p53-mediated cell death pathway*. J Neurosci, 1999. **19**(22): p. 9716-27.
154. Erhardt, P., E.J. Schremser, and G.M. Cooper, *B-Raf inhibits programmed cell death downstream of cytochrome c release from mitochondria by activating the MEK/Erk pathway*. Mol Cell Biol, 1999. **19**(8): p. 5308-15.
155. Wiese, S., *et al.*, *The anti-apoptotic protein ITA is essential for NGF-mediated survival of embryonic chick neurons*. Nat Neurosci, 1999. **2**(11): p. 978-83.
156. Yamauchi, N., A.A. Kiessling, and G.M. Cooper, *The Ras/Raf signaling pathway is required for progression of mouse embryos through the two-cell stage*. Mol Cell Biol, 1994. **14**(10): p. 6655-62.

157. Weber, C.K., *et al.*, *Active Ras induces heterodimerization of cRaf and BRaf*. *Cancer Res*, 2001. **61**(9): p. 3595-8.
158. Brummer, T., *et al.*, *Inducible gene deletion reveals different roles for B-Raf and Raf-1 in B-cell antigen receptor signalling*. *Embo J*, 2002. **21**(21): p. 5611-22.
159. Horbelt, D., *Diploma Thesis*. 2003.
160. Peyssonnaud, C. and A. Eychene, *The Raf/MEK/ERK pathway: new concepts of activation*. *Biol Cell*, 2001. **93**(1-2): p. 53-62.
161. Giroux, S., *et al.*, *Embryonic death of Mek1-deficient mice reveals a role for this kinase in angiogenesis in the labyrinthine region of the placenta*. *Curr Biol*, 1999. **9**(7): p. 369-72.
162. Woods, D., *et al.*, *Induction of beta3-integrin gene expression by sustained activation of the Ras-regulated Raf-MEK-extracellular signal-regulated kinase signaling pathway*. *Mol Cell Biol*, 2001. **21**(9): p. 3192-205.
163. Klemke, R.L., *et al.*, *Regulation of cell motility by mitogen-activated protein kinase*. *J Cell Biol*, 1997. **137**(2): p. 481-92.
164. Dugan, L.L., *et al.*, *Differential effects of cAMP in neurons and astrocytes. Role of B-raf*. *J Biol Chem*, 1999. **274**(36): p. 25842-8.
165. Frodin, M., P. Peraldi, and E. Van Obberghen, *Cyclic AMP activates the mitogen-activated protein kinase cascade in PC12 cells*. *J Biol Chem*, 1994. **269**(8): p. 6207-14.
166. Young, S.W., M. Dickens, and J.M. Tavaré, *Differentiation of PC12 cells in response to a cAMP analogue is accompanied by sustained activation of mitogen-activated protein kinase. Comparison with the effects of insulin, growth factors and phorbol esters*. *FEBS Lett*, 1994. **338**(2): p. 212-6.
167. Englaro, W., *et al.*, *Mitogen-activated protein kinase pathway and AP-1 are activated during cAMP-induced melanogenesis in B-16 melanoma cells*. *J Biol Chem*, 1995. **270**(41): p. 24315-20.
168. Busca, R., *et al.*, *Ras mediates the cAMP-dependent activation of extracellular signal-regulated kinases (ERKs) in melanocytes*. *Embo J*, 2000. **19**(12): p. 2900-10.
169. Marshall, C.J., *Specificity of receptor tyrosine kinase signaling: transient versus sustained extracellular signal-regulated kinase activation*. *Cell*, 1995. **80**(2): p. 179-85.
170. Dumont, D.J., *et al.*, *Dominant-negative and targeted null mutations in the endothelial receptor tyrosine kinase, tek, reveal a critical role in vasculogenesis of the embryo*. *Genes Dev*, 1994. **8**(16): p. 1897-909.
171. Fong, G.H., *et al.*, *Role of the Flt-1 receptor tyrosine kinase in regulating the assembly of vascular endothelium*. *Nature*, 1995. **376**(6535): p. 66-70.
172. Puri, M.C., *et al.*, *The receptor tyrosine kinase TIE is required for integrity and survival of vascular endothelial cells*. *Embo J*, 1995. **14**(23): p. 5884-91.
173. Hood, J.D., *et al.*, *Tumor regression by targeted gene delivery to the neovasculature*. *Science*, 2002. **296**(5577): p. 2404-7.
174. Eliceiri, B.P., *et al.*, *Integrin alphavbeta3 requirement for sustained mitogen-activated protein kinase activity during angiogenesis*. *J Cell Biol*, 1998. **140**(5): p. 1255-63.
175. Oda, N., M. Abe, and Y. Sato, *ETS-1 converts endothelial cells to the angiogenic phenotype by inducing the expression of matrix metalloproteinases and integrin beta3*. *J Cell Physiol*, 1999. **178**(2): p. 121-32.
176. Brooks, P.C., *et al.*, *Disruption of angiogenesis by PEX, a noncatalytic metalloproteinase fragment with integrin binding activity*. *Cell*, 1998. **92**(3): p. 391-400.
177. Temple, S., *The development of neural stem cells*. *Nature*, 2001. **414**(6859): p. 112-7.
178. Sanes, D.H., *Right place at the right time*. *Nat Neurosci*, 2002. **5**(3): p. 187-8.

179. Weiss, S., *et al.*, *Multipotent CNS stem cells are present in the adult mammalian spinal cord and ventricular neuroaxis*. J Neurosci, 1996. **16**(23): p. 7599-609.
180. Ciccolini, F. and C.N. Svendsen, *Fibroblast growth factor 2 (FGF-2) promotes acquisition of epidermal growth factor (EGF) responsiveness in mouse striatal precursor cells: identification of neural precursors responding to both EGF and FGF-2*. J Neurosci, 1998. **18**(19): p. 7869-80.
181. Represa, A., *et al.*, *EGF-responsive neural stem cells are a transient population in the developing mouse spinal cord*. Eur J Neurosci, 2001. **14**(3): p. 452-62.
182. Palmer, T.D., J. Takahashi, and F.H. Gage, *The adult rat hippocampus contains primordial neural stem cells*. Mol Cell Neurosci, 1997. **8**(6): p. 389-404.
183. Lillien, L. and H. Raphael, *BMP and FGF regulate the development of EGF-responsive neural progenitor cells*. Development, 2000. **127**(22): p. 4993-5005.
184. Bonni, A., *et al.*, *Cell survival promoted by the Ras-MAPK signaling pathway by transcription-dependent and -independent mechanisms*. Science, 1999. **286**(5443): p. 1358-62.
185. Kempermann, G., *et al.*, *Early determination and long-term persistence of adult-generated new neurons in the hippocampus of mice*. Development, 2003. **130**(2): p. 391-9.
186. Luskin, M.B., *Restricted proliferation and migration of postnatally generated neurons derived from the forebrain subventricular zone*. Neuron, 1993. **11**(1): p. 173-89.
187. Altman, J., *Autoradiographic and histological studies of postnatal neurogenesis. 3. Dating the time of production and onset of differentiation of cerebellar microneurons in rats*. J Comp Neurol, 1969. **136**(3): p. 269-93.
188. Lois, C. and A. Alvarez-Buylla, *Long-distance neuronal migration in the adult mammalian brain*. Science, 1994. **264**(5162): p. 1145-8.
189. Woods, D., *et al.*, *Raf-induced proliferation or cell cycle arrest is determined by the level of Raf activity with arrest mediated by p21Cip1*. Mol Cell Biol, 1997. **17**(9): p. 5598-611.
190. Kerkhoff, E. and U.R. Rapp, *Induction of cell proliferation in quiescent NIH 3T3 cells by oncogenic c-Raf-1*. Mol Cell Biol, 1997. **17**(5): p. 2576-86.
191. Morice, C., *et al.*, *Raf-1 and B-Raf proteins have similar regional distributions but differential subcellular localization in adult rat brain*. Eur J Neurosci, 1999. **11**(6): p. 1995-2006.
192. Hamilton, M. and A. Wolfman, *Ha-ras and N-ras regulate MAPK activity by distinct mechanisms in vivo*. Oncogene, 1998. **16**(11): p. 1417-28.
193. Brambilla, R., *et al.*, *A role for the Ras signalling pathway in synaptic transmission and long-term memory*. Nature, 1997. **390**(6657): p. 281-6.
194. Deutsch, P.J. and Y. Sun, *The 38-amino acid form of pituitary adenylate cyclase-activating polypeptide stimulates dual signaling cascades in PC12 cells and promotes neurite outgrowth*. J Biol Chem, 1992. **267**(8): p. 5108-13.
195. Tanaka, K., *et al.*, *Pituitary adenylate cyclase-activating polypeptide causes rapid Ca²⁺ release from intracellular stores and long lasting Ca²⁺ influx mediated by Na⁺ influx-dependent membrane depolarization in bovine adrenal chromaffin cells*. Endocrinology, 1996. **137**(3): p. 956-66.
196. Barrie, A.P., *et al.*, *Pituitary adenylyl cyclase-activating peptide stimulates extracellular signal-regulated kinase 1 or 2 (ERK1/2) activity in a Ras-independent, mitogen-activated protein Kinase/ERK kinase 1 or 2-dependent manner in PC12 cells*. J Biol Chem, 1997. **272**(32): p. 19666-71.
197. Vaudry, D., *et al.*, *Signaling pathways for PC12 cell differentiation: making the right connections*. Science, 2002. **296**(5573): p. 1648-9.

198. Rueda, D., *et al.*, *The endocannabinoid anandamide inhibits neuronal progenitor cell differentiation through attenuation of the Rap1/B-Raf/ERK pathway*. J Biol Chem, 2002. **277**(48): p. 46645-50.
199. Doetsch, F., *et al.*, *Subventricular zone astrocytes are neural stem cells in the adult mammalian brain*. Cell, 1999. **97**(6): p. 703-16.
200. Morshead, C.M., *et al.*, *Neural stem cells in the adult mammalian forebrain: a relatively quiescent subpopulation of subependymal cells*. Neuron, 1994. **13**(5): p. 1071-82.
201. Hartfuss, E., *et al.*, *Characterization of CNS precursor subtypes and radial glia*. Dev Biol, 2001. **229**(1): p. 15-30.
202. Franke, T.F., D.R. Kaplan, and L.C. Cantley, *PI3K: downstream AKTion blocks apoptosis*. Cell, 1997. **88**(4): p. 435-7.
203. Alessi, D.R., *et al.*, *Mechanism of activation of protein kinase B by insulin and IGF-1*. Embo J, 1996. **15**(23): p. 6541-51.
204. Lawlor, M.A. and D.R. Alessi, *PKB/Akt: a key mediator of cell proliferation, survival and insulin responses?* J Cell Sci, 2001. **114**(Pt 16): p. 2903-10.
205. von Gise, A., *et al.*, *Apoptosis suppression by Raf-1 and MEK1 requires MEK- and phosphatidylinositol 3-kinase-dependent signals*. Mol Cell Biol, 2001. **21**(7): p. 2324-36.
206. Majewski, M., *et al.*, *Activation of mitochondrial Raf-1 is involved in the antiapoptotic effects of Akt*. Cancer Res, 1999. **59**(12): p. 2815-9.
207. M. Hekmann, U.R., U. R. Rapp, manuscript in preparation.
208. Guan, K.L., *et al.*, *Negative regulation of the serine/threonine kinase B-Raf by Akt*. J Biol Chem, 2000. **275**(35): p. 27354-9.
209. Shelton, J.G., *et al.*, *Effects of the RAF/MEK/ERK and PI3K/AKT signal transduction pathways on the abrogation of cytokine-dependence and prevention of apoptosis in hematopoietic cells*. Oncogene, 2003. **22**(16): p. 2478-92.
210. Blalock, W.L., *et al.*, *Requirement for the PI3K/Akt pathway in MEK1-mediated growth and prevention of apoptosis: identification of an Achilles heel in leukemia*. Leukemia, 2003. **17**(6): p. 1058-67.
211. Peretto, P., *et al.*, *The subependymal layer in rodents: a site of structural plasticity and cell migration in the adult mammalian brain*. Brain Res Bull, 1999. **49**(4): p. 221-43.
212. Altman, J., *Autoradiographic and histological studies of postnatal neurogenesis. 3. Dating the time of production and onset of differentiation of cerebellar microneurons in rats*. J Comp Neurol, 1969. **136**(3): p. 269-93.
213. Taupin, P. and F.H. Gage, *Adult neurogenesis and neural stem cells of the central nervous system in mammals*. J Neurosci Res, 2002. **69**(6): p. 745-9.
214. Igney, F.H. and P.H. Krammer, *Death and anti-death: tumour resistance to apoptosis*. Nat Rev Cancer, 2002. **2**(4): p. 277-88.

APPENDIX

Abbreviations

β-Gal	β-Galactosidase
αα	Amino acid
Amp	Ampicillin
ASK1	Apoptosis signal-regulated kinase
APS	Ammoniumpersulphate
Arg	Arginine
Asp	Aspartic acid
ATP	Adenosine 5'-triphosphate
bFGF	Basic fibroblast growth factor
BLAST	Basic local allignment tool
BMP	Bone morphogenic protein
bzw	beziehungsweise
ca.	circa
CA1-3	Cornu ammonis regions 1-3
cAMP	cyclic Adenosine monophosphate
cfu	colony forming unit
chim	chimeric
Chol	Cholesterol
CIP	Calf Intestinal Phosphatase
CK2	Casein kinase 2
CNS	Central nervous system
CR1,2,3	Conservative region 1,2,3
CRD	Cysteine-rich domain
CREB	cAMP response element-binding protein
DAG	Diacylglycerin
DG	Dentate gyrus
(d)dNTP	(Di)Desoxynucleotide triphosphate
DMEM	Dulbecco's Modified Eagle Medium
DMF	Dimethylformamide
DMSO	Dimethylsulphoxide
DTT	Dithiothreitol
EC	Endothelial cell
E. coli	Escherichia coli
ECL	Enhanced Chemoluminescence
EDTA	Ethylendiamintetra acetic acid
e.g.	exempli gratia
EGF	Epidermal growth factor
EGFR	Epidermal growth factor receptor
EGL	External granular layer
ERK	Extracellular signal regulated kinase
ESC	Embryonic stem cell
et al.	et alii
Ex	Exon
FACS	Flow Cytometry and Fluorescence-Activated Cell Sorting
FADD	Fas-associated protein with death domain
FasL	Fas Ligand

FCS	Foetal calf serum
FGF	Fibroblast growth factor
FV	Fourth ventricle
GAP	GTPase-activating protein
GANC	Gancyclovir
GCL	Granular cell layer
GDP	Guanosine 5'-diphosphate
GEF	Guanine nucleotide exchange factor
GFAP	Glial fibrillary acidic protein
Glu	Glutamic acid
GPCR	G protein coupled receptor
Grb	Growth factor receptor bound protein
GTP	Guanosine 5'-triphosphate
GST	Guanidine-S-transferase
HA	Haemagglutinin
hGH	Human growth hormone
HSC	Haematopoietic stem cell
Hsp70,90	Hit shock protein 70,90
hu	Human
I κ B	Inhibitor of κ B
IAP	Inhibitor of apoptosis protein
IGF	Insulin-like growth factor
IKK	I κ B kinase
IL	Interleukin
IP	Immunoprecipitation
JAK	Janus kinase
JNK	c-Jun N-terminal kinase
JNKK	JNK kinase
bp	Basepairs
kb	Kilobasepairs
kD	Kilo Dalton
KIN	Knock-in
KO	Knock-out
KSR	Kinase suppressor of Ras
Leu	Leucine
LiAc	Lithium acetate
Lys	Lysine
M2-PK	Type M2 pyruvate kinase
MAPK	Mitogen activated protein kinase
MAP2K	MAPK kinase
MAP3K	MAP2K kinase
MEF	Mouse embryonic fibroblast
MEK	MAPK/ERK activating kinase
MEKK	MAPK/ERK activating kinase kinase
MHC	Major histocompatibility complex
MKK	MAP kinase kinase
ML	Molecular layer
MP1	MEK1 partner 1
MSZ	Institut für Medizinische Strahlenkunde und Zellforschung
NADH	Nicotinamide adenine dinucleotide, reduced
NADPH	Nicotinamide adenine dinucleotide phoshate, reduced

NCBI	National Center for Biotechnology Information
NEO	Neomycin resistance cassette
NF- κ B	Nuclear factor κ B
NGF	Nerve growth factor
NP40	Nonidet 40
NPC	Neuronal precursor/progenitor cell
NSC	Neuronal stem cell
OB	Olfactory bulb
OD	Optical density
ON	Overnight
ORF	Open reading frame
pA, polyA	Polyadenylation signal
PAK1,3	P21 activated kinase 1,3
PAGE	Polyacrylamide-Gel electrophoresis
PARP	Poly (ADP-ribose) polymerase
PBS	Phosphate buffered saline
PC12	Phaeochromocytoma cell 12
PCD	Programmed cell death
PCNA	Proliferating cell nuclear antigen
PCR	polymerase chain reaction
PDGF	Platelet derived growth factor
Phe	Phenylalanine
PI3K	Phosphatidyl inositide 3-kinase
PIP3	Phosphatidylinositol (3,4,5) trisphosphate
PKA	Protein kinase A
PKB	Protein kinase B
PKC	Protein kinase C
PP1, 2A	Protein phosphatase1, 2A
pSer	Phosphoserine
PTK	Protein tyrosine kinase
PTP	Permeability transition pore
pTyr	Phosphotyrosine
RBD	Ras binding domain
RKIP	C-Raf kinase inhibitor protein
RMS	Rostromigratory stream
rpm	revolutions per minute
Rsk	Ribosomal S6 kinase
RTK	Receptor protein tyrosine kinase
RT	Room temperature
Sc	Saccharomyces cerevisiae
Sp	Schizosaccharomyces pombe
SAPK	Stress-activated protein kinase
Ser	Serine
SGZ	Subgranular zone
SH	Src Homology
SHC	Src Homology domain containing
Sos	Son of sevenless
STAT	Signal transducers and activators of transcription
SVZ	Subventricular zone
TGF	Transforming growth factor
Thr	Threonine

TK	Tymidine kinase
tm	Transmission
TNF	Tumour necrosis factor
TRADD	TNF-R1 associated death domain protein
TRAF	TNFR associated factor
TNFR	TNF receptor
TPR	Tetratricopeptide repeat
Trp	Tryptophan
TUNEL	TdT-mediated dUTP nick end labelling
Thr	Threonine
Tyr	Tyrosine
Ub	Ubiquitin
v	Volume
V	Volt
Val	Valine
VDAC	Voltage-dependent anion channel
VEGF	Vascular endothelial growth factor
VEGFR1,2	Vascular endothelial growth factor receptor 1,2
VZ	Ventricular zone
W	Weight
Wb	Western blot
WT	Wilde type
XIAP	X-linked IAP

CURRICULUM VITAE

PERSONAL INFORMATION:

Tyrsin Oleg Yurievich (Tyrsin Oleg)

Sex: male

Date and place of birth: December 29, 1973, USSR, Moscow

Marital status: Married, 1999

Citizenship: Russian Federation

EDUCATION :

June 1991: Graduated from Moscow gymnasium Nr. 1251

June 1996: Graduated from Moscow State University, Faculty of Biology, Department of Bioorganic Chemistry. Speciality: biochemist. MSc equivalent.

September 1996 -1998: postgraduate student at V. A. Engelhardt Institute of Molecular Biology, Russian Academy of Sciences.

EMPLOYMENT RECORD:

1994 - 1996: graduate student, Laboratory of Human Genes Structure and Function , Shemyakin-Ovchinnikov Institute of Bioorganic Chemistry, Russian Academy of Sciences.

1996 - 1999: postgraduate student, Laboratory of Molecular Bases of Differentiation and Development, V.A. Engelhardt Institute of Molecular Biology, Russian Academy of Sciences.

1999 - present time: postgraduate student, Institute of Medical Radiation and Cell Research, Julius-Maximilians University.

Versbacher-Str.5, 97078 Wuerzburg, Germany

tel. (+49)0931-201-45847, fax. (+49)0931-201-45835

e-mail:tyrsin@hotmail.com, tyrsine.oleg@mail.uni-wuerzburg.de

PROFESSIONAL SOCIETIES:

Biochemical society, physical-chemical biology division, RAS.

LANGUAGE SKILLS :

fluent English

good French

good German

FIELD OF STUDY:

Neurogenetics, Molecular Neurobiology, Signal Transduction Pathways, Mouse Genetic

AREAS OF EXPERTISE

BASIC TECHNIQUES :

Molecular cloning (in plasmid and phage vectors)

Gel electrophoresis of nucleic acids
Nucleic acids isolation from animal cells and tissues
Nucleic acids analysis: Northern and Southern hybridization, restriction mapping, DNA sequencing
Polymerase chain reaction
In situ hybridization (mostly whole mounts)
Immunohistochemistry, TUNEL assay
Western blot
EMSA
Nuclear matrix & nuclear extract isolation
PCR fragments binding to the nuclear matrix in vitro
ES cells culturing, targeting, ES cells/morulae aggregation, blastocyst injection, production of chimeric germ line transmitting mice, embryo manipulation

MAJOR APPLICATIONS:

cDNA library construction (conventional)
Construction of PCR-amplified cDNA library at the level of a few cells
Library screening and clones isolation, subcloning.
RACE cloning
RT-PCR and RT-PCR with degenerated oligos (to isolate homologous genes and family members)
Knock-in mice production

LIST OF PUBLICATIONS:

1. S. B. Akopov, L. G. Nikolaev, **O. Yu. Tyrsin**, A. S. Ruzov, and E. D. Sverdlov. (1997) Identification and characterization of 14 sequences from the Chinese hamster genome preferentially binding to the nuclear matrix. *Bioorg. Khim.* **23**, (9)727-31
2. L. M. Fedorov, **O. Yu. Tyrsin**, V. Krenn, E. V. Chernigovskaya, and U. R. Rapp. (2001) Tet-system for the regulation of gene expression during embryonic development. *Transgenic Research.* **10**, (3)247-58
3. L. M. Fedorov*, **O. Yu. Tyrsin***, O. Sakk, A. Ganscher and, U. R. Rapp. (2001) Generation dependent reduction of tTA expression in double transgenic NZL-2/tTA(CMV) mice. *Genesis.* **31**, (2)78-84

* equal contribution

4. Fedorov L.M., Papadopoulos T., **Tyrsin O. Yu.**, Chernigovskaya E. V., and Rapp U.R. (2001) Bcl-2 is required for lung tumor development in the SP-C-c-Raf-1-BxB transgenic mice. *J. of Cancer Res. and Clin. Oncology.* Suppl. to **v.127**, S62

5. Fedorov LM, **Tyrsin OY**, Papadopoulos T, Camarero G, Goetz R, Rapp UR. (2002) Bcl-2 determines susceptibility to induction of lung cancer by oncogenic CRAf. *Cancer Res.* **62**, (21)6297-303
6. Fedorov LM, Papadopoulos T, **Tyrsin OY**, Twardzik T, Goetz R, Rapp UR. (2003) Loss of p53 in craf-induced transgenic lung adenoma leads to tumor acceleration and phenotypic switch. *Cancer Res.* **63**, (9)2268-77
7. **Tyrsin OY**, Camarero G, Fedorov LM, Goetz R, Rapp UR. B-Raf deficient embryos rescued from endothelial apoptosis in midgestation by A-Raf activity display some developmental defects. *In preparation*

OTHER MERITS

1. P.Balaban, D.Poteryev, I.Zakharov, **O.Tyrsin**, A.Belyavsky. (1998) Regulation of HSC2 gene expression in behaviorally identified snail neurons. *Proc. 28th Ann.Meeting Soc. Neuroscince.* p. 1702
2. *International Summer School Spetses 2000 „Molecular Mechanisms of Development and Disease“*. Spetses (Greece), September 5-14, 2000.
3. L. M. Fedorov, **O. Y. Tyrsin**, T. Papadopoulos, T. Twardzik, R. Goetz, and U. R. Rapp. Loss of p53 in CRAF induced transgenic lung adenoma leads to tumor acceleration and phenotypic switch. Cold Spring Harbor Laboratory, *Mouse Molecular Genetics Meeting 2002*. August 28-September 1. *Abstract book* p.53
4. **Tyrsin OY**, Camarero G, Fedorov LM, Horbelt D, Goetz R, Rapp UR. A-Raf only partially rescue B-Raf deficient embryos. The 5th EMBL *Mouse Molecular Genetics Meeting 2003*. 3-7 September, Heidelberg, Germany. *Abstract book* p.169

DECLARATION

I hereby declare that the submitted dissertation was completed by myself and no other. I have not used any sources or materials other than those enclosed.

Moreover I declare that the following dissertation has not been submitted further in this form or any other form, and has not been used for obtaining any other equivalent qualifications at any other organization/institution.

Additionally, I have not applied for, nor will I attempt to apply for any other degree of qualification in relation to this work.

Würzburg, den

Oleg Tyrsin